[redacted] ~~CONFIDENTIAL~~

ADVANCED WEAPON SYSTEMS STUDY

PART III - ADVANCED MILITARY SATELLITES

VOLUME III

EXCLUDED FROM
DECLASSIFICATION IAW E.O. 12958
REFER
TO: ST Labs

[redacted] CONFIDENTIAL

Copy 5 of 25

ADVANCED WEAPON SYSTEMS STUDY

PART III - ADVANCED MILITARY SATELLITES

VOLUME III

TR-59-0000-00604

DOWNGRADED AT 12 YEAR INTERVALS; NOT AUTOMATICALLY DECLASSIFIED. DOD DIR 5200.10

1 March 1959

Work Completed
10 September 1958

SPACE TECHNOLOGY LABORATORIES
P.O. Box 95001
Los Angeles 45, California

[redacted] CONFIDENTIAL

CONTENTS

CONTENTS (Continued)

CHAPTER 1

ASCENT TRAJECTORIES

1.1 INTRODUCTION

In Volume II of this report, a number of applications of advanced satellites were considered. Out of those considerations came recommendations for two types of satellite orbits--the 24-hour circular equatorial orbit and the 24-hour circular polar orbit*. The purpose of this chapter is to describe the means of ascent into these recommended orbits. Before describing the optimum ascent trajectories, we first describe some of the general features of ascent trajectories in order to give motivation for the final choice.

1.2 GENERAL CHARACTERISTICS OF ASCENT TRAJECTORIES

It is well known that the most efficient way, from the standpoint of propellant conservation, of establishing a large-radius circular orbit is to burn propellants near the surface of the earth so as to establish a horizontal (or nearly horizontal) velocity vector at burnout just sufficient in magnitude to cause the rocket to coast in an ellipse to the desired altitude of the circular orbit, and then, upon reaching the desired altitude, to add an additional velocity impulse to bring the rocket's speed up to that required for a circular orbit. The ellipse followed during ascent is called a Hohmann transfer ellipse. Its perigee is at the burnout point and its apogee at the altitude of the circular orbit. The rocket, as seen by an observer in space, coasts halfway around the earth during its ascent. (Earth's rotation must be taken into account in determining its position relative to the surface of the earth.)

Figure 1-1 shows the velocities associated with ascent to a circular orbit as a function of the altitude of that orbit. In computing these curves it was assumed that the injection into the Hohmann transfer orbit, i.e., the location of the low-altitude burnout point, takes place at an altitude of

*We use "24-hour orbits" for brevity. Actually the orbits recommended would have a period of one siderial day, or 23 hours, 56 minutes, 4.09 seconds, the period of rotation of the earth.

[redacted]

CONFIDENTIAL

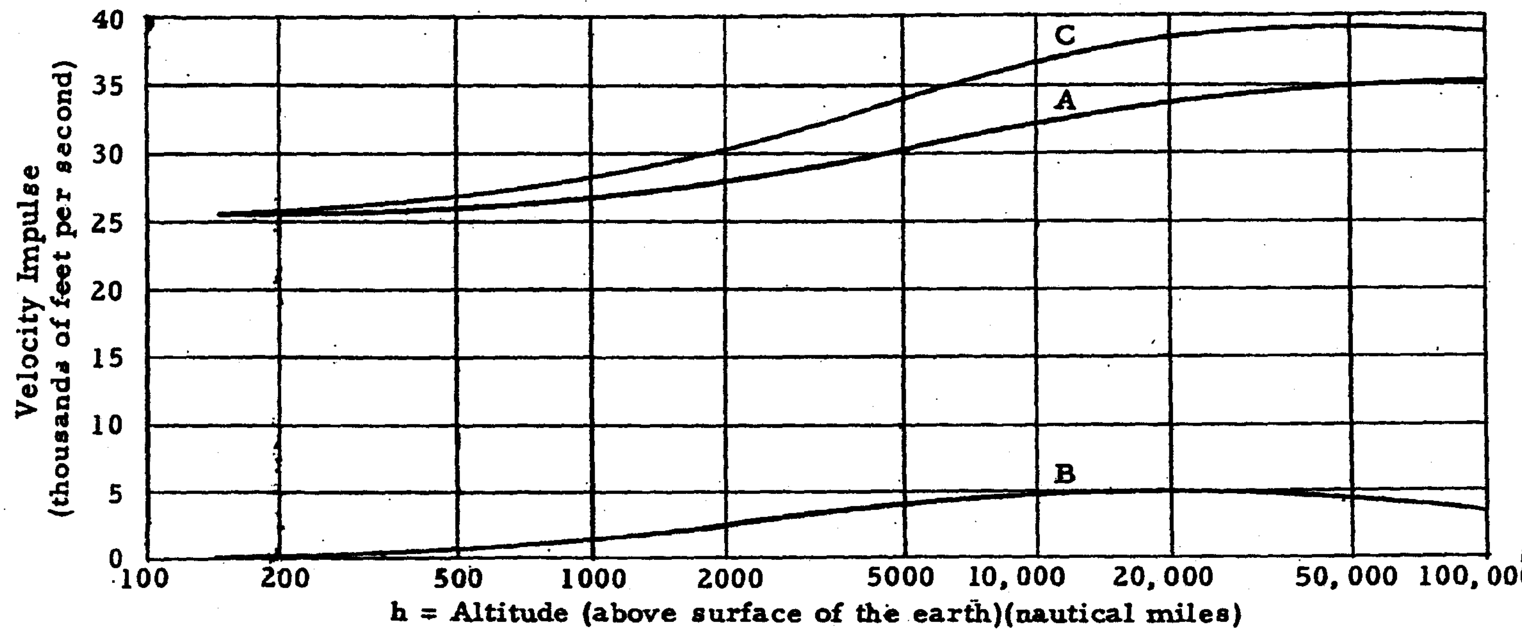

A. Burnout velocity at 140 nautical mile altitude required to coast to an altitude h in a Hohmann transfer ellipse.

B. Velocity increment required at apogee of Hohmann ellipse to establish circular orbit of altitude h.

C. A + B = total velocity impulse required to establish circular orbit.

Figure 1-1. Velocity Impulses Required for Establishing Circular Orbits.

CONFIDENTIAL

[redacted]

140 nautical miles. Curve A shows the velocity required at burnout and Curve B shows the additional velocity impulse which must be added at the apogee of the Hohmann transfer ellipse to establish the circular orbit. Curve C is the sum of the velocities in Curve A and Curve B. It represents the total velocity impulse which must be provided to the rocket, and consequently gives a good indication of the payload ratios which can be established in any orbit. These payload ratios are discussed in Chapter 4 of this volume.

It will be noted that Curve B reaches a maximum at an altitude of about 20,000 nautical miles, but approaches zero at both ends of the curve. This causes Curve C to have a maximum at about 50,000 nautical miles, and consequently it is more difficult, from the standpoint of propulsion, to establish a satellite at this altitude than at any other. In Volume II we argued that payload was relatively insensitive to altitude for altitudes above 10,000 nautical miles. This observation follows from the relative flatness of Curve C above this altitude.

The velocity indicated in Curve A is the required burnout velocity with respect to an inertial frame of reference. A portion of this velocity may be attained by firing in an easterly direction and taking advantage of the earth's rotation. For example, an easterly firing from an equatorial launching site provides about 1526 feet per second toward the velocity requirement shown in Curve A. An easterly launching from Cape Canaveral, Florida, will provide about 1341 feet per second.

There is a useful variation from the above method of ascent which costs nothing in the way of additional velocity impulse. In this variation the rocket is flown from the launch site and, as before, establishes a horizontal burnout velocity vector at an altitude of 140 nautical miles. But the speed at burnout is only sufficient to establish a circular orbit at 140 nautical miles. After coasting for some distance in the low-altitude circular orbit, a second burning period accelerates the rocket up to the speed indicated on Curve A. After engine shutdown, the rocket coasts as before in a Hohmann transfer ellipse, arriving at the desired altitude at the apogee of the ellipse. There the additional velocity shown in Curve B is applied and the high-altitude circular orbit is established. In this method of ascent, the speed shown in Curve A is gained in two burning periods rather than one, but the total velocity impulse required has undergone no change. The low-altitude coast has the effect of changing the point of entry into the high-altitude circular orbit. Such coast periods play an important part in the trajectories recommended for establishing the 24-hour orbits.

In the above example we have used 140 nautical miles as the burnout altitude for entry into the Hohmann transfer ellipse. Had a higher altitude been chosen, the velocity impulse both on entering and leaving the Hohmann transfer ellipse would have been less. But this is more than offset by the additional velocity impulse required in attaining the initially higher altitude. The net velocity impulse penalty is shown in Figure 1-2 as a function of the altitude of injection into the Hohmann transfer ellipse required for establishing a 24-hour orbit. As can be seen from this figure, the higher the altitude the greater the penalty. Altitudes lower than 140 nautical miles have not been recommended because they might lead to some difficulties with atmospheric drag during the initial burning period and during the low-altitude coast period. If, for the weight-to-drag ratios of the final vehicle design, the drag is found to be negligible over the coast periods required for the ascent methods described in this chapter, then it will be possible to assume a somewhat lower point of injection.

1.3 ESTABLISHING A 24-HOUR EQUATORIAL ORBIT

The 24-hour circular equatorial orbit with which we are concerned involves an eastward motion of the satellite in order that the satellite can remain stationary with respect to the surface of the earth. An efficient launching requires that the launching take place in a generally easterly direction. This suggests that Cape Canaveral, Florida, be used as the launch site. Before discussing the specific trajectories recommended for a Cape Canaveral launch, it is valuable to consider a more ideal launch site, namely, a hypothetical site located at the equator. By comparing the total velocity impulse required when using Cape Canaveral with that required when using the equatorial launch site, we shall determine the velocity penalty associated with Cape Canaveral.

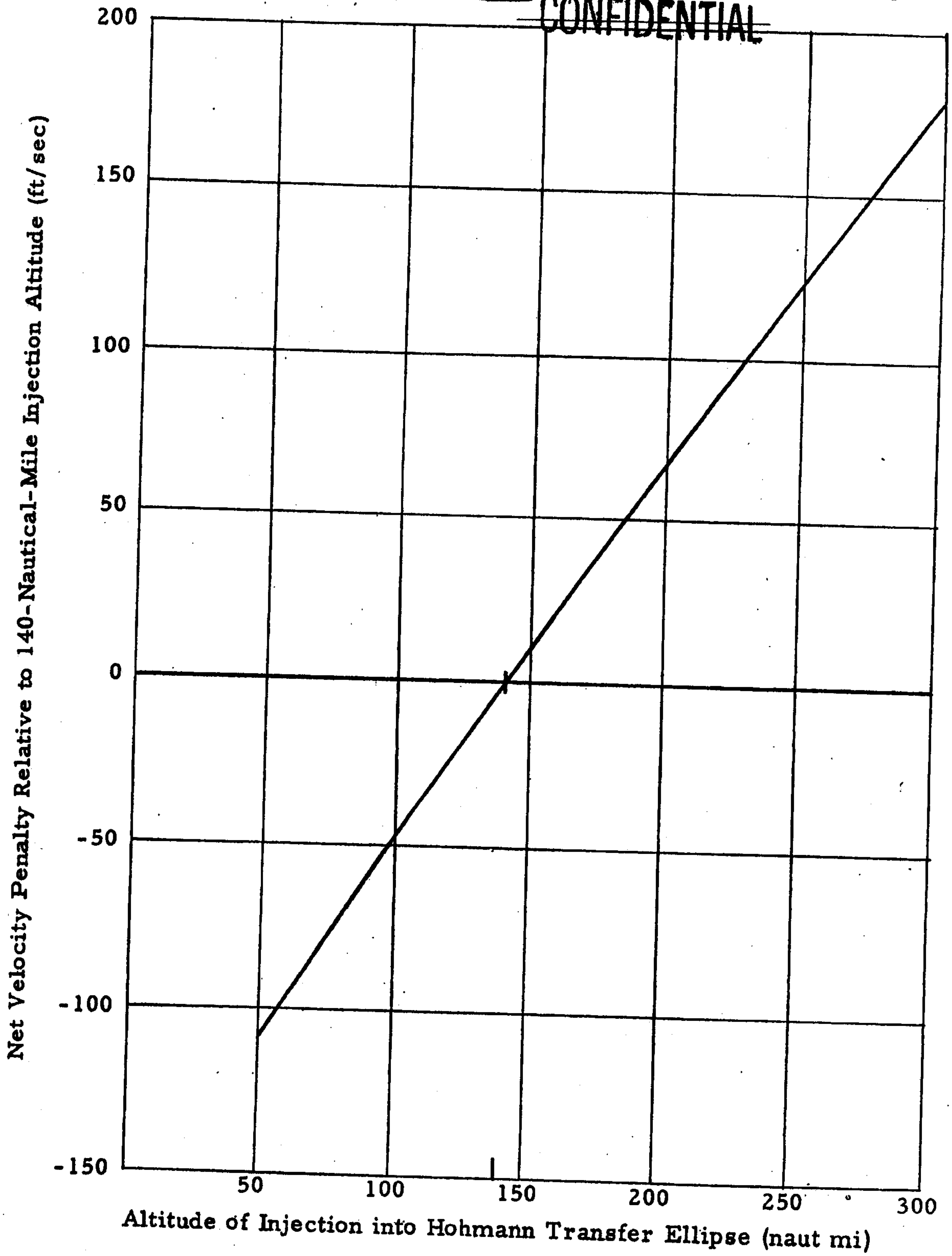

Figure 1-2. Velocity Penalty in Establishing a 24-Hour Circular Orbit as a Function of Altitude of Injection into the Hohmann Transfer Ellipse.

1.3.1 Equatorial Launch Site

Figure 1-3 is a schematic drawing of the ascent orbit which would be used if an equatorial launch site were available. The flight consists of three powered portions, one in the vicinity of the launch site which ends when the missile has attained a circular orbit satellite velocity of 25,424.0 feet per second at an altitude of 140 nautical miles. This is followed by a coast period, the purpose of which is to ensure that the second burning period of the 24-hour satellite will be initiated at the proper time so that when in orbit the satellite shall "hover" over the particular longitude selected for the military application to be performed. The low-altitude coast is followed by the second or perigee burning period which adds an additional 7996.4 feet per second so that a horizontal burnout velocity of 33,420.4 feet per second is achieved. The missile now coasts in a Hohmann transfer ellipse, proceeding halfway around the earth during its ascent. A period of 5 hours, 16 minutes, 6.7 seconds is required for the second coast period. The speed at apogee has been reduced to only 5261.3 feet per second. As apogee is reached (or, more exactly, a minute or two before apogee is reached), the third and final burning period begins. During this period an additional velocity of 4826.2 feet per second is added, resulting in a total velocity of 10,087.5 feet per second, which is just adequate to ensure that a circular orbit is followed.

There will, of course, be errors in guidance and control during ascent and consequently the satellite will not follow precisely the prescribed 24-hour orbit. The deviations from this orbit can be considerably reduced by observing and correcting the motion of the satellite over a period of a day or more, an interval which we shall call the vernier correction period.

During the period from missile lift-off to the establishment of the final 24-hour orbit (a period of 5.4 to 6.8 hours, depending on the length of the low-altitude coast), the earth has been rotating and the launch site longitude is some 81 to 102 degrees east of its initial position. This must be taken into account in trying to establish the desired longitude for the stationary satellite.

There is a direct and simple relationship between the weight of fuel consumed, the specific impulse of the engine, and the velocity gained during

[redacted] CONFIDENTIAL

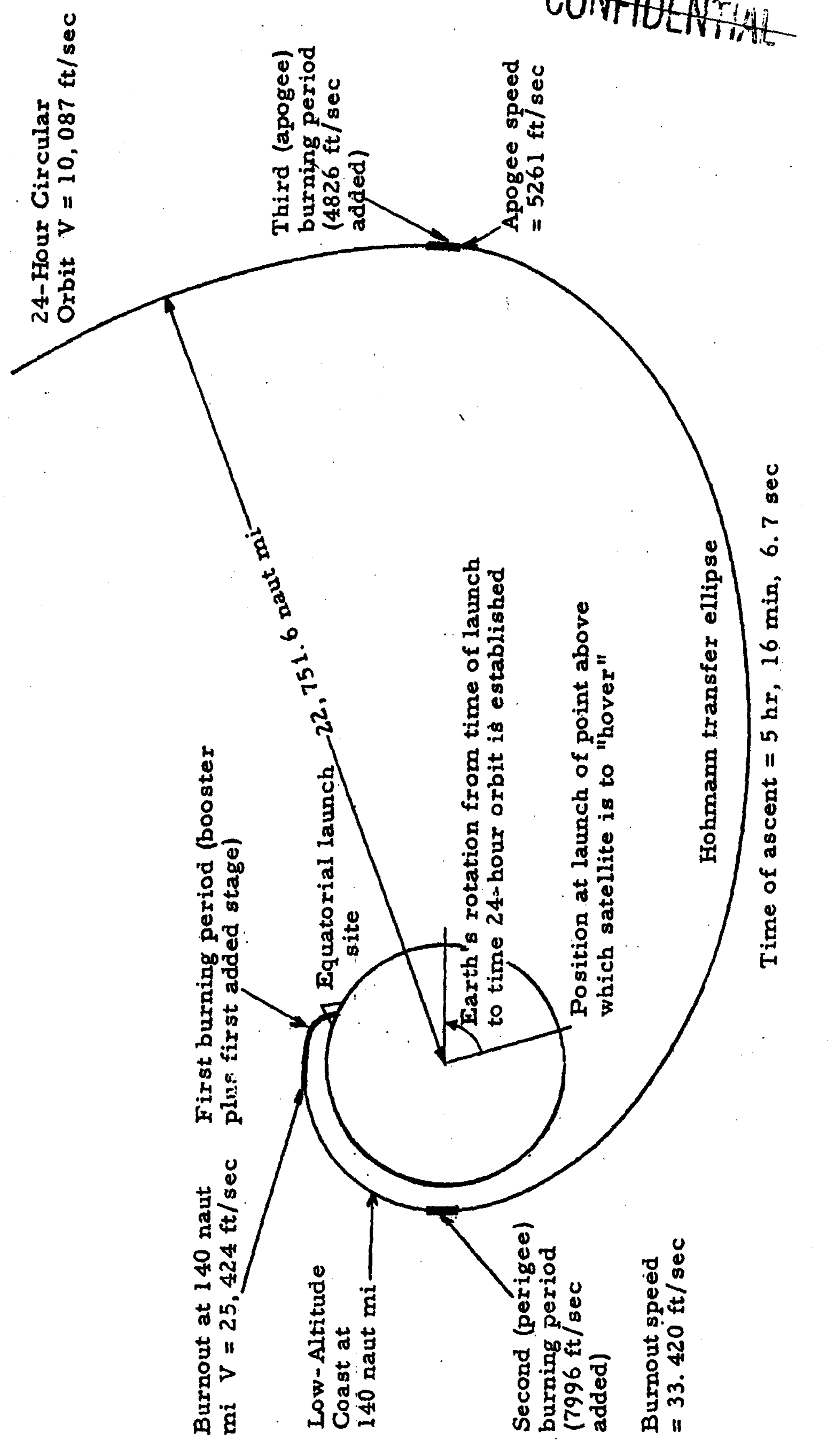

Figure 1-3. Total Trajectory for Satellite Launched on Equator.

[redacted] CONFIDENTIAL

the second and third burning periods. During these periods the drag forces acting on the missile are completely negligible, and, since the missile is burning in a horizontal path, gravity has no effect in reducing the velocity gained. The velocity gained is given by the simple expression

$$\Delta V = g \, I_{sp} \, \ln \frac{M_o}{M_1}$$

where g is the standard acceleration of gravity, I_{sp} is the vacuum specific impulse, M_o is the mass at the beginning of the burning period, and M_1 is the mass at the end of the burning period.

The speed gained during the first burning period is far more complicated to compute. During this time there are drag effects, effects of atmospheric pressure in reducing specific impulse, "gravity losses" due to the effect of gravity acting back along the path, and, finally, Coriolis "forces" associated with the rotation of the earth. In Chapter 2, Volume IV, use is made of machine computations to obtain the performance of various boosters during the first burning period. What is important here is a consideration of the effect of geographical location of the launch site on the velocity gained. The effects of gravity, atmospheric pressure, and drag are relatively independent of the geographic location of the launch site. We are more concerned here with the effects of earth rotation and the influence of the location of the launch site on the velocity gained from the earth's rotation. To a first approximation, the velocity gained due to the rotation of the earth is merely the surface speed of the earth at the latitude of the launch site. At the equator this is 1526 feet per second.

1.3.2 Cape Canaveral Launch

The problem of establishing an equatorial satellite from Cape Canaveral, which is at a latitude of 28.475°N, is considerably more complex than when an equatorial launch site is used. If the launch were eastward from Cape Canaveral directly into a Hohmann transfer ellipse, the plane of the orbit would be inclined to the equatorial plane by 28.475 degrees and the apogee of the ascent ellipse would be reached at a latitude of 28.475°S. At apogee, 4826.2 feet per second would have to be added to obtain a circular 24-hour orbit (see Section 1.3.1), but the orbit would not be an equatorial one. As the satellite crosses the equatorial plane, an additional velocity would have to be added to convert the orbit into an equatorial one, as illustrated in the following vector velocity diagram, as viewed from above:

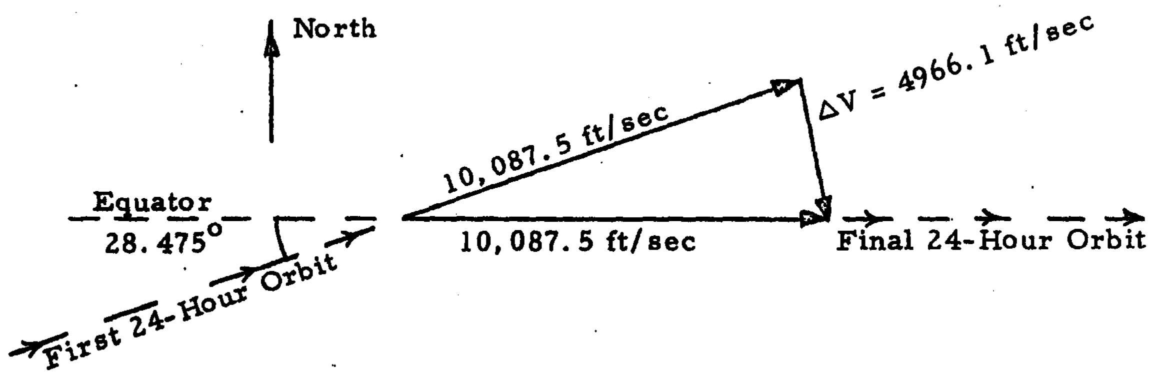

The additional velocity increment of 4966.1 feet per second is very costly in terms of payload, and consequently it is important to think of an alternative scheme.

Fortunately, by using a low-altitude coast of the proper length, it is possible to reduce considerably the penalty associated with not using an equatorial launch site. Launching eastward from Cape Canaveral, the missile is brought to an altitude of 140 nautical miles and a speed of 25,424.0 feet per second, the speed required to establish a circular orbit at the burnout altitude. The missile is then allowed to coast until it crosses the equator, where it enters a second burning period. During the second burning period a velocity increment of 7996.4 feet per second injects the missile into the Hohmann transfer ellipse. Since the perigee of the Hohmann ellipse is at the equator, its apogee will be at the equator also. At apogee a velocity increment is added of such magnitude and in such a direction that the speed is brought up to 10,087.5 feet per second (the 24-hour orbit speed), and the final direction of motion is corrected to be in the equatorial plane, as illustrated in the following diagram:

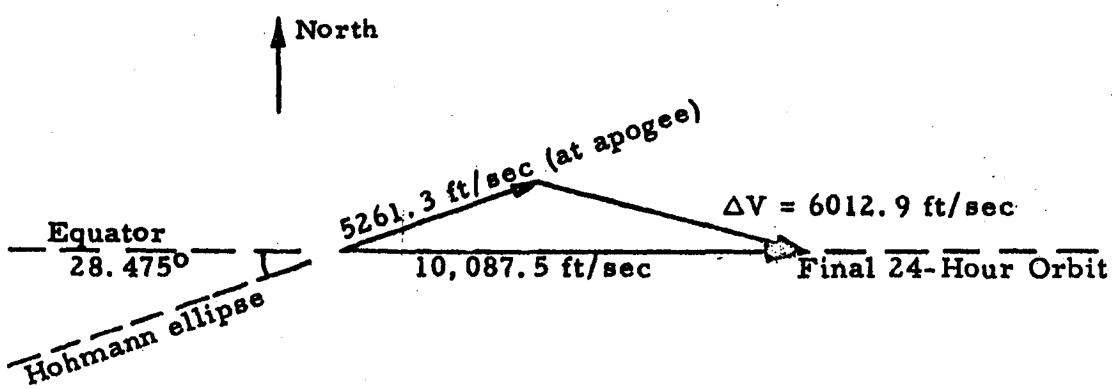

It is seen that by combining the operations of increasing the speed and adjusting its direction into a single operation, the total velocity increment is only 6012.9 feet per second instead of the 9792.3 feet per second described earlier (4826.2 feet per second to obtain orbital speed and 4966.1 feet per second to correct the plane of the orbit). The 6012.9 feet per second is only 1186.7 feet per second more than the 4826.2 feet per second which was required for an equatorial launch site. In addition, there is a penalty paid during the first burning period because the speed of rotation of the earth at

Cape Canaveral is only 1341.4 feet per second instead of the 1526.0 feet per second of an equatorial launch site. This penalty of 184.6 feet per second added to the 1186.7 feet per second makes a total penalty of 1371.3 feet per second (or about a 15 per cent decrease in gross payload) associated with the use of Cape Canaveral.

If the rocket is fired due east from Cape Canaveral, and if its motion is constrained to the plane which passes through the center of the earth and through Cape Canaveral in an easterly direction, then it will cross the equator at a longitude of 90 degrees east of Cape Canaveral for a nonrotating earth. The longitude of Cape Canaveral is 80.55°W; consequently, the missile would cross the equator at 9.45°E if the earth were not rotating. Actually, it will pass the equator west of this point by the angle through which the earth rotates during the time of flight. The burning period to reach circular satellite velocity at an altitude of 140 nautical miles is approximately 5.4 minutes,[*] and during this time the missile will have moved downrange approximately 450 nautical miles,[*] which is 7.5 degrees of arc from Cape Canaveral. The time required to cover the remaining 82.5 degrees of arc in the low-altitude orbit is 82.5/360 of the period of the satellite. The satellite period at an altitude of 140 nautical miles is 88.56 minutes, and consequently the coast time is 20.3 minutes. The total time of flight, therefore, is 25.7 minutes (5.4 plus 20.3), and during this time the earth will have rotated through 6.44 degrees. Consequently, the actual point at which the missile reaches the equator is at a longitude of 3.01°E.

During the ascent in the Hohmann transfer ellipse, the satellite covers an arc of 180 degrees. Consequently, if the earth were not rotating during this period, the satellite would reach apogee at 176.99°W (3.01°E of the International Date Line). However, since the time of ascent is 5 hours, 16 minutes, 6.7 seconds, the earth will have rotated through 79.24 degrees

[*] The burning time and downrange distance depend on the details of the missile design and the powered-flight dynamics. The numbers quoted are approximate, but the results of the arguments given here are relatively insensitive to these quantities.

during the ascent period, and the apogee is actually attained at a longitude of 103.77°E, which will be just above Singapore. It is at this point* that the 24-hour orbit is established, and consequently the satellite would remain over Singapore.

The question now arises as to what scheme can be used for launching a 24-hour equatorial satellite which is to achieve a final longitude not equal to that of Singapore, but still launching from Cape Canaveral. This may be achieved by using a longer coast period in the circular orbit at 140 nautical miles and by entering the Hohmann transfer ellipse at some subsequent crossing of the equator. During the low-altitude coast period the rotation of the earth will bring the desired longitude of injection into the Hohmann transfer ellipse close to the plane of the 140-nautical-mile orbit. The injection into the Hohmann transfer ellipse may be introduced at any of the equatorial crossings, whether they be in a southerly or northerly direction, and since these crossings occur at time intervals of 44.28 minutes apart, the earth will have rotated through 11.1 degrees between subsequent crossings. We shall let N be the number of complete half-revolutions included in the low-altitude coast. Therefore, the crossing at 3.01°E described above will be referred to as the "zeroth crossing." The next crossing, which will be in the northerly direction, will be referred to as the "first crossing," the next southerly crossing as the "second crossing," etc. Table 1-1 shows the longitudes of the successive crossings, the time from lift-off to the crossing in question, the corresponding longitudes of the 24-hour equatorial satellite, and the total time to establish the satellite (obtained by adding 5 hours, 16.11 minutes for the ascent time in the Hohmann transfer ellipse). It will be noted that a satellite can be put up over any point on the earth (to within 11.1 degrees) by using a low-altitude coast period no longer than 12 hours, 14.2 minutes and a total time of no longer than 17 hours, 30.3 minutes.

*For purposes of this computation we have assumed that perigee and apogee burning are performed impulsively (with zero burning time). The figures given here will need refinement when the actual burning programs have been specified.

[redacted]

~~CONFIDENTIAL~~

Table 1-1. Low-Altitude Coasts Needed to Establish Various Longitudes for 24-Hour Circular Equatorial Orbits Launched from Cape Canaveral.

Number of Complete Half-Revolutions at 140 Nautical Miles (N) (southerly crossings)	(northerly crossings)	Longitude of Crossing (Point of Entry into Hohmann Ellipse)	Time of Crossing from Lift-Off	Longitude of 24-Hour Equatorial Satellite	Total Time to Establish Satellite
0		3.01°E	25.7 min	103.77°E	5 hr 41.8 min
	1	171.91°E	1 hr 10.0 min	87.33°W	6 hr 26.1 min
2		19.19°W	1 hr 54.3 min	81.57°E	7 hr 10.4 min
	3	149.71°E	2 hr 38.5 min	109.53°W	7 hr 54.7 min
4		41.39°W	3 hr 22.8 min	59.37°E	8 hr 38.9 min
	5	127.51°E	4 hr 07.1 min	131.73°W	9 hr 23.2 min
6		63.59°W	4 hr 51.4 min	37.17°E	10 hr 07.5 min
	7	105.31°E	5 hr 35.7 min	153.93°W	10 hr 51.8 min
8		85.79°W	6 hr 19.9 min	14.97°E	11 hr 36.1 min
	9	83.11°E	7 hr 04.2 min	176.13°W	12 hr 20.3 min
10		107.99°W	7 hr 48.5 min	7.23°W	13 hr 04.6 min
	11	60.91°E	8 hr 32.8 min	161.67°E	13 hr 48.9 min
12		130.19°W	9 hr 17.1 min	29.43°W	14 hr 33.2 min
	13	38.71°E	10 hr 01.3 min	139.47°E	15 hr 17.5 min
14		152.39°W	10 hr 45.6 min	51.63°W	16 hr 01.7 min
	15	16.51°E	11 hr 29.9 min	117.27°E	16 hr 46.0 min
16		174.59°W	12 hr 14.2 min	73.83°W	17 hr 30.3 min

~~CONFIDENTIAL~~

[redacted]

The above scheme provides only a discrete set of final longitudes for the 24-hour satellite unless allowance is made for a coast period longer than 12 hours, 14.2 minutes in the low-altitude orbit. These longitudes could be shifted somewhat by using an altitude other than 140 nautical miles for the low-altitude coasting orbit. However, there is another simple scheme for obtaining any intermediate location with a very small additional velocity penalty. Instead of firing due east from Cape Canaveral, one could fire slightly north of east or slightly south of east. For example, if one fires 6.0 degrees north of east,* the plane of the 140-nautical-mile orbit will cross the equator about 11.6 degrees east of the crossing for a due east launch. Moreover, the length of the great circle arc from the launching point to the zeroth crossing of the equator will be about 10.2 degrees greater than 90 degrees. During the extra 2.5 minutes required for the satellite to transverse this 10.2 degrees, the earth will have rotated through 0.6 degree. When this is subtracted from the 11.6 degrees, one sees that the zeroth crossing point will be 11.0 degrees east of 3.01°E, the crossing point for a due east launch. If one launches 6.0 degrees to the south of due east, then the zeroth crossing will take place 11 degrees west of 3.01°E. Since the period of the low-altitude satellite is the same as before, all subsequent crossings are shifted by precisely the same increment of longitude.

Figure 1-4 is a plot of the longitude shift given as a function of the angle between the launching direction and due east. This longitude shift may be used to adjust the longitudes shown in Table 1-1, both the longitudes of the equatorial crossing (point of injection into the Hohmann ellipse) and of the point of establishment of the equatorial satellite.

Figure 1-5 shows the velocity penalty associated with not launching due east. One of the penalties, shown in Curve A, is associated with not

---

* As seen by observing the path relative to the earth. When the earth's rotational speed at Cape Canaveral, 1341 feet per second, is added in the eastward direction, the total velocity is only 5.7 degrees from east as viewed from a nonrotating frame of reference.

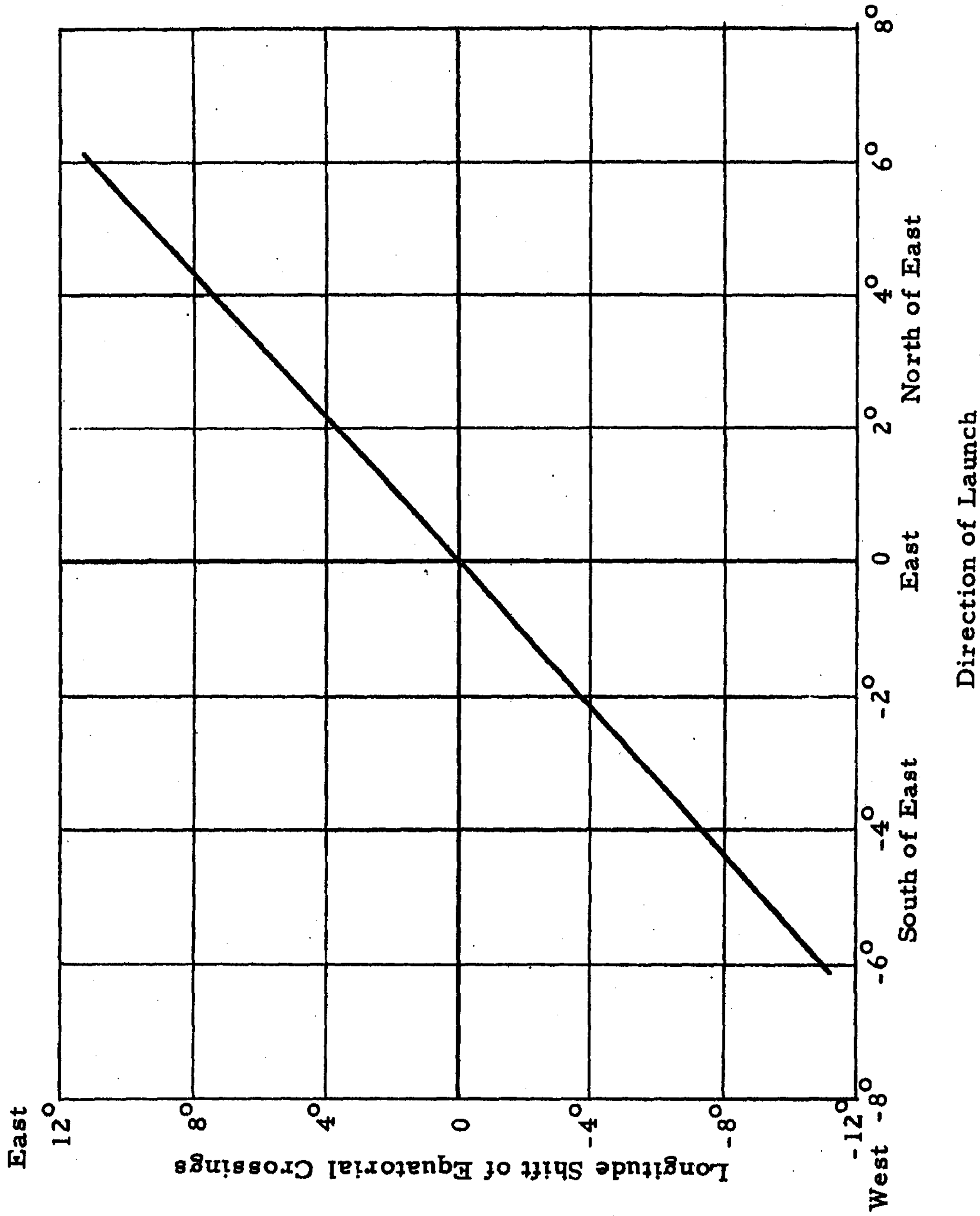

Figure 1-4. Effect of Non-Easterly Launch from Cape Canaveral on Longitude Shift of Equatorial Crossings.

~~CONFIDENTIAL~~

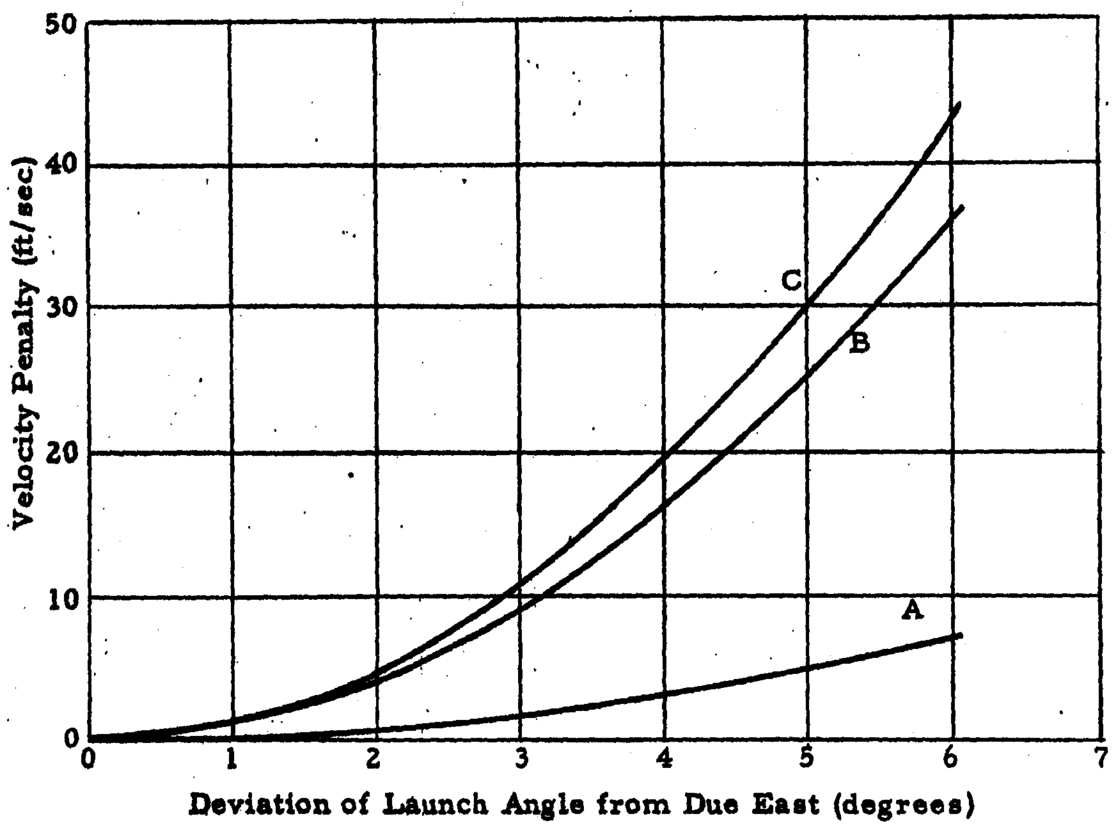

A. Velocity penalty due to not fully utilizing earth's rotation.

B. Velocity penalty incurred during apogee burning because of increased inclination angle.

C. = A + B = Total velocity penalty.

Figure 1-5. Velocity Penalty Associated With Not Launching Due East.

~~CONFIDENTIAL~~

utilizing fully the earth's rotational velocity, since only the component of the surface velocity in the direction of launch is effective. Curve B illustrates the additional penalty incurred at the point of entry into the 24-hour orbit. This velocity penalty is associated with the fact that when a missile is not launched due east from Cape Canaveral, the inclination angle, measured from the equator, of the plane of the orbit is more than 28.475 degrees. Curve C is the sum of the two penalties. It will be noted that the maximum penalty which need be tolerated is when a 6.05-degree northerly (or southerly) launching is used, and this penalty is only 44 feet per second.

There is one refinement which should be mentioned before leaving the discussion of the 24-hour equatorial orbits launched from Cape Canaveral. We have assumed heretofore that there was no change in the orbital plane during the second burning period--that is, at the point of injection into the Hohmann transfer ellipse. Actually, the velocity added there should be oriented slightly in the direction to decrease the inclination angle of the plane of the orbit. This is illustrated in Figure 1-6. Decreasing the inclination angle requires a somewhat greater incremental velocity during the perigee burning period (Curve B), but it has the effect of reducing the incremental velocity which must be added at the apogee of the Hohmann transfer ellipse (Curve A). The net velocity impulse saved is shown by Curve C. In the case of due easterly launch from Cape Canaveral, the optimum plan is to decrease the inclination angle by about 2.2 degrees. This requires an additional 77 feet per second during the perigee burning period but decreases the velocity increment to be added during the apogee burning by 162 feet per second, with a net saving of 85 feet per second.

Table 1-2 gives pertinent trajectory information for establishing equatorial satellites at the particular locations recommended in Volume I of this report.

[redacted]

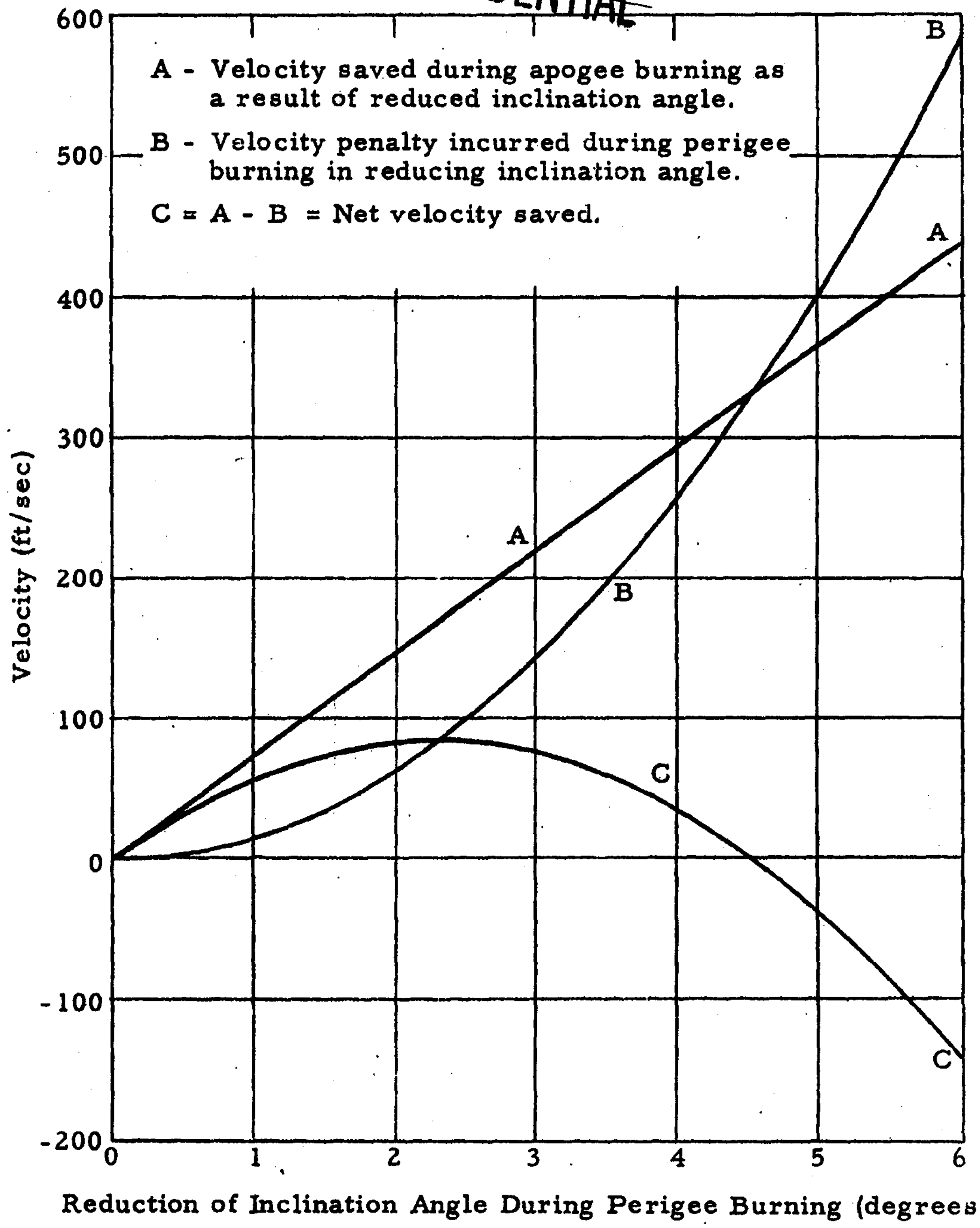

Figure 1-6. Velocity Saved by Reducing Inclination Angle During Perigee Burning (Based on East Launch from Cape Canaveral).

[redacted]

Table 1-2

Communication Relay Coverage of 24-Hour Satellite	Desired Longitude of Satellite	Deviation of Launch Angle from Due East	Number of Complete Half Revolutions	Time of Injection Into Hohmann Ellipse	Longitude at Injection into Hohmann Ellipse
U.S. to Europe	30°W	0.3°S	12	9 hr 17.0 min	130.76°W
U.S. to Asia	170°W	3.3°N	9	7 hr 05.6 min	89.24°E
U.S. interior	45°W to 130°W	*	1, 3, 5, 12, 14, or 16	*	*
Asia, Africa, Indian Ocean (Low-Density Traffic)	65°E	3.1°N	4	3 hr 24.1 min	35.76°W
Relay for Low-Altitude Reconnaissance from Western USSR to Central USA	25°W	2.4°N	12	9 hr 18.1 min	125.76°W
Relay for Low-Altitude Reconnaissance from Eastern USSR to Central USA	175°W	0.6°N	9	7 hr 04.5 min	84.24°E

*Varies according to desired longitude of satellite; see Table 1-1.

1.4 ESTABLISHING A 24-HOUR POLAR ORBIT

Cape Canaveral is not well suited for the launching of a polar satellite because firing either to the north or south would involve passage over land during the initial powered flight. On the other hand, Cooke AFB is quite ideally situated for the launching of a polar satellite by firing to the south.

In Volume II of this report, it was pointed out that three 24-hour polar satellites are required to give continuous communications coverage of the north polar region of the earth. It was there recommended that the polar satellites be placed in circular orbits which would cross the equator at a longitude 60°W, and that the satellites be so phased that their northward (or southward) equatorial crossings would be separated by 8 hours. It will be noted that in launching the first of the three polar satellites, care need only be taken that the orbit established for this satellite cross the equatorial plane at 60°W. On the other hand, for the second and third satellites we have not only the above requirement, but also the requirement that the equatorial crossing take place 8 or 16 hours after the crossing of the first satellite. Therefore, in launching the second and third polar satellites, it is necessary to time the countdown so that missile lift-off will take place at a particular time of the day.

The method of ascent which is here recommended bears a considerable resemblance to the equatorial launch of an equatorial satellite described in Section 1.3.1. First, we will describe an ascent path which is always applicable to the first polar satellite launched, but which is applicable to the second and third satellites only when they are launched on schedule. In the event that the second or third satellite is launched early or late, a variation of this ascent method must be used. This variation will be described later.

The " on time" scheme consists of launching due south from Cooke AFB which is located at longitude 120.58°W and latitude 34.75°N. Again we launch into a circular orbit at an altitude of 140 nautical miles, and, as in the equatorial case, we assume a burning period of 5.4 minutes and a point of injection into the circular orbit 450 nautical miles downrange from the launching site, that is, at a latitude of 27.25°N. The vehicle is allowed to continue in the low-altitude orbit until it completes a little more than one revolution and arrives at a latitude of 14.86°N. Thus, it traverses 372.39 degrees in the 140-nautical-mile orbit. Since the period of the circular orbit is 88.56 minutes, the time required in this orbit is 91.6 minutes. When this is added to the 5.4 minutes required for the burning program, we see that the total time from lift-off is 97.0 minutes, and during this time the earth rotates through 24.32 degrees. Consequently, the point of injection into the Hohmann transfer ellipse is at a longitude of 144.90°W and a latitude of 14.86°N. If the earth did not rotate during the ascent in the Hohmann trajectory, the apogee point would be at a latitude of 14.86°S and a longitude of 35.10°E. However, since the earth does rotate through 79.24 degrees during the 5 hours, 16.11 minutes of ascent*, the apogee actually will occur at longitude 45.14°W, latitude 14.86°S. It is at this point* that the additional velocity is added as required to inject the satellite into a circular orbit. As the satellite, now moving north, traverses the remaining 14.86 degrees to reach the equatorial plane, the earth also rotates through 14.86 degrees, and when this is added to the longitude of 45.14°W, we see that the first equatorial crossing of the satellite takes place at 60°W, as required.

It will be noted that the entire flight path takes place in one plane in space. Consequently, we see the similarity to the launching of an equatorial satellite from an equatorial launch site, but in this case we gain no advantage from earth's rotation in establishing the low-altitude orbit. The velocity of an orbit at 140 nautical miles is 25,424.0 feet per second. As in the equatorial launch of the equatorial satellite, the velocity which must be added to the low-altitude orbital velocity in order to establish the Hohmann transfer ellipse is

---

* For purposes of this computation we have assumed that perigee and apogee burning are performed impulsively (with zero burning time). The figures given here will need refinement when the actual burning programs have been specified.

[redacted]

CONFIDENTIAL

7996.4 feet per second, and the velocity which must be added at the apogee of the Hohmann transfer ellipse in order to establish the 24-hour circular orbit is 4826.2 feet per second.

Clearly this scheme can be used to establish the first polar satellite. If this scheme is also used to establish the second and third polar satellites, then they too will have their equatorial crossings at 60°W. But if lift-off does not occur at precisely the right time of day, the crossings will not be spaced 8 hours apart. Necessarily, two of the three satellites will then be spaced more than 8 hours apart in their successive northward crossings of the equator. When these two satellites are in the Northern Hemisphere (and the third satellite in the Southern Hemisphere), there will be a time when their latitudes are equal. Nominally, this latitude should be 30°N, but since they are more than 8 hours apart, they will find themselves at the same latitude when they are somewhat south of 30°N, and consequently the polar communications coverage, especially that in the Eastern Hemisphere, is decreased. For example, if the satellites are 8 hours and 40 minutes apart, instead of 8 hours apart, then they will find themselves at the same latitude when they are at latitude 25°N. This would have the effect of decreasing communications coverage in Siberia by approximately 5 degrees of latitude.

Rather than accept this decrease in communications coverage, it is possible to utilize a late (or early) firing and still establish a pattern of coverage very close to that attained when a precise schedule is maintained. This is done by establishing an orbit (for the second or third satellite) which crosses the equator at the right time, though not at the right longitude. For example, assume that the second satellite is launched an hour late. Instead of starting the perigee burning when the rocket has coasted to the nominal latitude of 14.86°N, one should allow it to coast another 16.03 degrees until it reaches latitude 1.17°S. During the extra 3.94 minutes added to the coast period, the earth will have rotated through 0.99 degree. Consequently, instead of reaching apogee at a longitude of 45.14°W and a latitude of 14.86°S, as in the

CONFIDENTIAL

[redacted]

nominal case for "on-time" firing, the missile would reach apogee at longitude 46.13°W and latitude 1.17°N. It is at this point that the 24-hour orbit commences. On the nominal firings it takes 63.94 minutes to traverse the 16.03 degrees between 14.86°S and 1.17°N. But it will be recalled that 3.94 minutes were used up by lengthening the coast period. Consequently, exactly 1 hour has been gained, as required. It will be noted, however, that the equatorial crossings will now take place at 44.96°W (1.17 degrees east of apogee longitude). Therefore the longitude of the figure eight traced by the late satellite is displaced from its correct position by approximately 15 degrees for each hour of lateness (or earliness). A shift of 15 degrees in longitude has only a very minor effect on the area covered by the polar communications system. The guidance system discussed in Chapter 2 of this volume utilizes a measurement of coast time in the low-altitude orbit. In order to effect the correction which we have just illustrated, it is only necessary to reset the desired coast time as a function of the actual time of launch.

There is a means of ascent for polar satellites quite analogous to the scheme suggested in Section 1.3.2 for equatorial satellites launched from non-equatorial bases. This scheme, in principle, is capable of launching a polar satellite into precisely the correct orbit (correct both in longitude and timing) regardless of the time of launch. The missile is launched in a generally southerly direction into a low-altitude circular orbit. Twice each period of this low-altitude orbit it threads through the plane (in space) which contains the desired 24-hour polar orbit. At one of the crossings the missile is injected into a Hohmann transfer ellipse which, consequently, has its apogee at the next point of crossing. It is at this point that the orbital plane is changed, simultaneously with adding the additional speed to establish the 24-hour circular orbit. By adjusting the coast time, that is, the number of half-revolutions in the low-altitude orbit, one can make a gross adjustment of the time of equatorial crossing of the final 24-hour orbit. As in the equatorial case, this adjustment allows placement of the satellite in its correct orbit with an angular error of less than 11 degrees. A fine correction is introduced by choosing the direction of launch so as to slightly change the dihedral angle between the plane of the original low-altitude orbit and the plane of the desired polar 24-hour orbit.

Although the method just introduced would seem ideal from the standpoint of always establishing the optimum polar coverage, it suffers from several practical disadvantages. First, unless the firing time is within an hour or so of nominal firing time, the dihedral angle is a large one, and it is very costly from the standpoint of propulsion to turn through the dihedral angle at apogee. Second, the location of the apogee point is not necessarily within the line-of-sight of conveniently located radio tracking systems, and consequently the guidance scheme suggested in Chapter 2 might be difficult to apply. Third, the velocity to be gained by the first stage depends upon the direction of fire. Because of the rotation of the earth and, unless the fuel level in the first stage were changed as a function of the time of firing, it would be necessary to carry enough fuel to achieve the low-altitude orbit under the most unfavorable firing direction. This would penalize the performance unnecessarily. Fourth, a similar argument holds for the amount of fuel which would have to be carried in the stage which performs apogee burning, inasmuch as the dihedral angle, and consequently the velocity increment, would vary as a function of time of firing. Because of these reasons we do not recommend this method of ascent.

1.5 TRAJECTORY PHASES (AND STAGING)

It is important to draw the distinction between burning periods and vehicle staging. Consider the "first burning period", that which takes the vehicle from launch up to injection into the low-altitude orbit. In practice it will be necessary to use several rocket stages during this period, but in spite of the several stages involved, this will be regarded as one "burning period" or one "trajectory phase" because the coast periods between burnout of one stage and ignition of the next can be made as small as practical considerations (e.g., adequate time for stage separation) will allow. In Chapter 2, Volume IV, it is shown that one stage added to the Thor, Atlas, or Titan is capable of achieving injection into the 140-nautical-mile orbit.

Next, although the perigee burning period on entering the Hohmann orbital transfer ellipse and the apogee burning period on leaving the Hohmann ellipse may utilize the same rocket stage ignited twice, these are two distinct burning periods separated by a 5.3-hour coasting period.

Table 1-3 gives a listing of the trajectory phases, applicable to both equatorial and polar orbits, together with the staging which is recommended in Chapter 2, Volume IV. The recommended plan is to climb to the low-altitude orbit using a modification of an existing booster (single-stage Thor, 1-1/2-stage Atlas, or 2-stage Titan) plus a first added stage. Shortly after this orbit is established, the first added stage is jettisoned. The final stage

Table 1-3

Staging	Guidance Phases	Time
Booster (1 or 2 stages) First Added Stage	Injection into Low Altitude Orbit	~5 min
Final Stage	Low Altitude Coasting	Max 10 hr
	Perigee Burning	~4 min
	Ascent Coasting	5.3 hr
	Apogee Burning	~3 min
	Orbit Correction	24 or 48 hr
	Attitude Stabilization	6 mo to 1 yr

now coasts in orbit for a period ranging from about 1-1/2 hours for polar orbits up to as much as about 10 hours for equatorial satellites. The final stage engine is then ignited for perigee burning. When this burning is completed, the final stage coasts to apogee where an engine (either the same one that was used at perigee or a different engine, see Chapter 2, Volume IV) is ignited for apogee burning. When apogee burning is completed, the vehicle is reoriented so as to direct its nose downwards. There is no jettisoning of tanks or other structure. During the next 24 to 48 hours a series of small orbital corrections (see next chapter) is effected using gas jets as the means of obtaining the small impulses needed. Thereafter, for the life of the satellite, the only working components are the communications (or other payload) equipment, the auxiliary power supply, the cooling equipment, and the attitude stabilization equipment. The attitude stabilization problems are discussed in Chapter 3 of this volume, and electric power and cooling are discussed in Chapter 1 of Volume IV.

CHAPTER 2

GUIDANCE SYSTEMS

2.1 GUIDANCE FUNCTIONS AND ACCURACY

The guidance system for satellites of the type described in this report is more complex than the systems designed for the ICBM or for the IGY satellites. The system to be described in the following pages must be capable of putting a satellite in an orbit of very slight eccentricity and of extremely accurate known period. In addition to being in the proper orbit with the proper period, the satellite must be placed in a particular position in that orbit. When one couples this required precision with the difficulties of launching from nonideal locations such as Cape Canaveral, it becomes evident that system complexity is apt to be greater than in other more well-known guidance systems.

The central problem for the guidance system is to establish and keep the satellite in the correct orbit. If the satellite, once established in orbit, has an error in its period, then it will drift off "station" to the east or west and therefore the earth's horizon, as seen by the satellite, will shift (see Figure 2-1). Since both the high-density communication system and the infrared early-warning system discussed in Volume II view areas near the horizon, this shift would mean loss of coverage. It is probably desirable to restrict the drift, say, to about ±2 degrees* during the operational life of the satellite. This would restrict the shift of the boundary of the "covered area" to 120 nautical miles at the equator, and to only 85 nautical miles at Longitude 45°N. A drift of ±2 degrees

*If, on establishing the orbit, the eccentricity is limited such that the apogee radius is no more than 200 nautical miles greater than the perigee radius, then the diurnal oscillation in the east-west direction caused by this eccentricity will be only ±1/2 degree. It is relatively easy to establish an orbit with this eccentricity. Likewise, the error in establishing the inclination of the orbital plane is likely to be quite small compared with 2 degrees. The narrow beamwidth (0.1 degree) ground antennas can track this 2-degree drift by moving the antenna feed. It is not necessary to move the dish unless considerably larger drifts are to be accommodated. It is also assumed that as the satellite drifts, its altitude relative to the earth is maintained. The problems of maintaining altitude are discussed in Chapter 3.

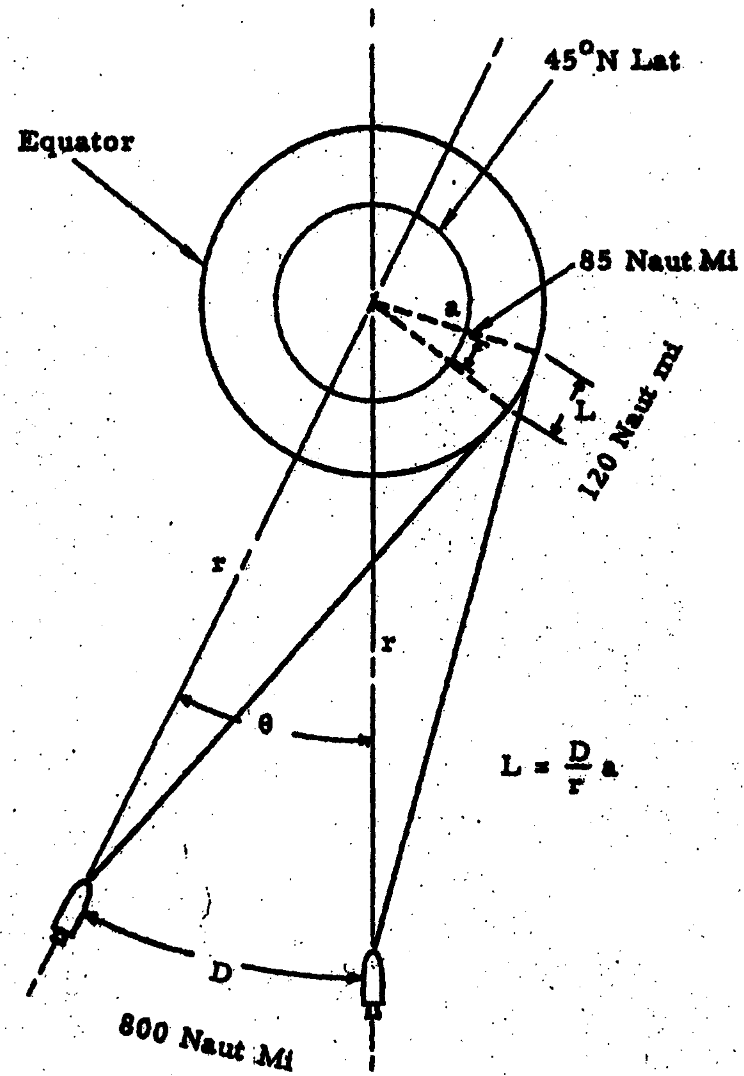

Figure 2-1. Loss of Ground Coverage if Satellite Changes Orbital Position by 800 Nautical Miles.

corresponds to an east-west drift in orbit of about ±800 nautical miles.* Taking the operational life between 6 months and 1 year, say 9 months to be definite, this permits an average drift rate of 0.2 foot per second.

It is beyond the present state-of-the-art to achieve this accuracy when the satellite is first placed in the high-altitude circular orbit. To achieve such accuracy it will be necessary to track the satellite in orbit and then to apply appropriate small impulses over the next 24 (or at most 48 hours) to correct the orbit. By such correction schemes the above drift-rate requirement can be met, and it is even quite likely that the drift rate can be brought down to 0.03 foot per second thus permitting 5-year operational periods if and when communications, power supply, and attitude subsystem shall have reached a status of reliable operations over such periods.

It is, of course, possible to relax the orbital drift requirements if orbital correcting impulses are applied every few weeks or months, but this would demand repeated operation of the orbital correction guidance and control subsystem which would introduce additional possible sources of system failure. However, the repeated corrections will probably be unnecessary since it appears quite feasible to correct the orbit in 1 or 2 days to the requisite accuracy for "holding" station for the operational life of the satellite. Thus, some 24 or 48 hours after the orbit is first established, the guidance system will no longer be required to operate.

The question now arises as to the accuracy required of that portion of the guidance system which first places the satellite in orbit, the "ascent guidance." Since any errors which accumulate prior to establishing the 24-hour orbit will be wiped out during the orbital correction period, it would

*Therefore such diurnal oscillators east-west or north-south are in any event less critical than the steady east-west drift. They too, can be traced by moving the feed on the ground antenna. They would require, however, a continuing correction of satellite attitude to compensate the duirnal satellite displacement. Consequently, it is probably desirable to reduce these oscillators by the orbital correction methods described on the following pages, thereby simplifying the ground tracking and particularly the attitude stabilization.

appear that quite crude guidance equipment can be used. By using a crude guidance system, guidance equipment weight can be saved. However, if the initial errors in the orbit are very large, large correcting impulses are required, and the weight of gas expended in these impulses can exceed the weight saved by using the crude guidance equipment. No attempt will be made in this report to arrive at the optimum point in the trade-off between ascent guidance weight and ascent guidance accuracy. Rather, we have here assumed the use of ascent guidance equipment based on small additions to and modifications of equipment which is being developed in any event for ballistic missile systems. Appendix A is an analysis of how the errors in ascent guidance affect the accuracy of injection into the 24-hour orbit. When the accuracies of the ascent guidance equipment are substituted into the error transformation equations developed in Appendix A, one finds that the sum of the velocity impulses required of the orbital correcting gas jets is only about 100 feet per second.

The guidance functions during the various trajectory phases listed in Table 1-3 are described in Sections 2.1.1 through 2.1.6. However, before getting into the phase-by-phase description, there are certain general features of the guidance problem which require mention here inasmuch as they determine the over-all character of the system.

As mentioned earlier, it is necessary to track the satellite over a period of 1 or 2 days after it has reached the 24-hour orbit. This tracking provides an accurate determination of the orbital errors, and therefore provides the information which is required for orbital correction. Radio tracking means are probably the most dependable means of performing this tracking inasmuch as optical tracking at such large distances is likely to be quite difficult and is, moreover, dependent on good weather conditions. A radio transponder beacon must, therefore, be carried by the satellite in order to provide a sufficiently strong signal for radio tracking.

Unfortunately, it is not possible to use the same radio command guidance during all of the guidance phases. In particular, it could not always be used during perigee burning because perigee burning may take place over open ocean area which is not within line-of-sight of friendly land areas. For example, as shown in Table 1-2, Chapter 1, the perigee burning for the U. S.-to-Asia communication satellite, which is to be established at Longitude 170°W takes place over the Indian Ocean (at 89°E Longitude). For this reason, a self-contained all-inertial guidance system has been selected for use during the perigee burning period. An all-inertial system is also well adapted to the guidance problems encountered in establishing the low-altitude orbit. Modifications of the current Arma system or certain other systems under development will give satisfactory performance for the climb to the low-altitude orbit and for perigee burning.

In principle, the inertial system can also be used to carry out guidance during apogee burning, but this would lead to quite large errors in orbit due, primarily, to the cumulative effect of the errors introduced in earlier guidance phases. However, since apogee is always within line-of-sight of friendly territory (it must be in order to establish communications to the U. S.), the vehicle can be tracked prior to reaching apogee, and the tracking information may be used to command the apogee burning, thereby wiping out many of the errors which accumulated during the earlier blind operation. It turns out, however, that the smoothing time associated with angular rate tracking at the extreme ranges of the 24-hour satellite is so long that the inertial guidance system must be depended upon to carry out the command. Consequently, both radio and inertial systems are used in the suggested scheme for apogee burning.

2.1.1 Booster-Powered Flight

Guidance during the booster-powered flight is accomplished with a gyro-stabilized inertial platform mounting three orthogonal accelerometers. This platform works in conjunction with a primary guidance digital computer. During the first-stage booster burning period, the vehicle follows a programmed pitch attitude and is stabilized in roll and yaw using the platform as a reference. The primary guidance computer calculates position and velocity throughout this period. Attitude control and steering instructions are provided for subsequent stages in the climb to the low-altitude orbit by the primary computer, which also issues engine start and cutoff signals.*

---

*If the Titan is used, the first stage cutoff signal is derived from level sensing devices in the first stage fuel and lox tanks.

A relatively heavy primary computer is required for the preorbital period because of the complexity of the computations associated with the trajectory during this period. During perigee and apogee burning periods, however, the computations are sufficiently simple to be carried out by a rudimentary digital computer, called here the steering and shutoff computer. Therefore, the primary guidance computer is located in the first added stage and is jettisoned before perigee burning in order to reduce the guidance weight in the critical final stage.

2.1.2 Low-Altitude Coasting

The inertial guidance system is capable of measuring the velocity and position of burnout (latitude, longitude, and altitude) with greater accuracy than it can control these quantities. The resultant control in altitude and speed errors at the point of injection into the low-altitude orbit effects the low-altitude coast period and this leads, together with the downrange error at injection into the low-altitude orbit, to an error in the downrange position of the satellite at the nominal time of perigee burning. The resulting error, however, in downrange position at perigee burning can be compensated by adjusting the initiation time for perigee burning. Velocity and altitude errors at the actual time of perigee burning can also be compensated by adjusting the vector velocity increment to be added at perigee. Computations of the perigee correction biases are made in the primary guidance computer, and before the first added stage is separated from the vehicle, the biases are transferred to and stored in the smaller digital steering and shutoff computer housed in the final stage. This simple transfer can be avoided if an additional impulse of approximately 30 feet per second is provided at apogee burning to steer out the velocity errors which result from not biasing the perigee burning program with the transferred data.

The vehicle or final stage is reoriented to the attitude required for perigee burning after separation of the first added stage. The vehicle is held at a constant attitude by reference to the stable platform during the coast in the 140-nautical-mile circular orbit. A simple analog computer commands the attitude control jets by converting platform gimbal angles into on-off signals for the jets.

2.1.3 Perigee Burning

Perigee burning adds approximately 8000 feet per second to the speed. This nominal desired impulse is somewhat modified by the perigee impulse correction stored in the steering and shutoff computer. Steering and shutoff commands are provided by the computer on the basis of accelerometer readings. Steering commands during this period are fed to the perigee-apogee autopilot which also make use of platform gimbal angle measurements and angular rate data platform from rate gyros.

2.1.4 Ascent Coasting

The guidance system must stabilize the vehicle attitude throughout ascent in the Hohmann transfer ellipse and the vehilce must be tracked from a ground station during the final 2 or 3 hours of ascent. By observing a transponding beacon, it will be possible to measure the vehicle's position during ascent coasting with an angular tracking radar and the vehicle's velocity with a radio interferometer. The tracking data are then fed into a ground digital computer, and apogee burning correction biases are sent to the vehicle as modulations on the tracking waves. These are stored in the steering and shutoff computer.

Attitude stabilization during ascent coasting is provided by the platform. During ascent the vehicle must be rotated about 127 degrees to accomplish apogee burning with the same motor.

2.1.5 Apogee Burning

Apogee burning must add about 4800 feet per second for polar satellites. On the other hand, for equatorial satellites launched from Cape Canaveral, since the plane of motion must be turned through approximately 28.5 degrees about 6000 feet per second are required. The nominal values are adjusted according to information derived from ground tracking.

Apogee burning is initiated when the vehicle reaches the correct angle relative to the earth (the correct latitude for the polar satellite and the correct longitude for the equatorial satellite). The engine start signal is commanded from the ground on the basis of the angular position tracking information.

Because burning is initiated on the basis of the correct angle, prior measurement and control errors will prevent the burning from occurring precisely at apogee. Thus, just before the burning period there will be radial component of velocity which can be cancelled out by correctly orienting the velocity increment added during "apogee" burning. Thus, the desired burnout velocity is horizontal, and this horizontal burnout velocity should be controlled as a function of altitude to be that which leads to a satellite period of one sidereal day. It will not be that of the circular one-sidereal-day orbit unless the altitude at apogee burning is, by chance, exactly the nominal one. Thus, if the altitude at apogee burning is in error, the satellite is purposely put into an elliptical (not circular) orbit with a period of one sidereal day (except, of course, for errors in the command caused by errors in radio tracking and errors in apogee burning control caused by platform drift and accelerometer errors). The advantages of having a period of very nearly one sidereal day are that secular drift is very nearly elimintated (at the cost of introducing daily oscillations) and the orbital correction scheme, discussed in the next section, is simplified.

As in the perigee burning period, cutoff commands are issued by the steering and shutoff computer on the basis of acceleration measurements obtained from the platform-mounted accelerometers. Since, at this point in flight, none of the accelerometer axes will lie along the direction of the desired velocity increment, some simple computations must be performed in the computer to resolve the measured velocity increment into a suitable coordinate system.

The vehicle is reoriented by 90 degrees after apogee burning to point the nose-mounted antennas toward the ground stations. It is thus oriented with its long axis radial. This is accomplished with gas jets using data from the inertial platform to control the orientation.

After rough orientation based on platform information, a more precise attitude is achieved and unwanted angular rates are eliminated by the attitude control system described in the next chapter. This attitude control system must work throughout the life of the satellite to maintain correct orientation.

2.1.6 Orbital Correction Period

Assume for the moment that apogee burning is so timed that on the completion of that burning the satellite is precisely at the correct longitude in the case of an equatorial satellite (or precisely at the correct latitude in the case of the polar satellite). Next, assume that the burning is so controlled that after apogee burning there is no radial component of velocity. Finally, assume that the horizontal velocity, chosen as a function of the actual observed altitude at apogee burning, is that which is required to establish the satellite in an elliptical orbit with a period of precisely one sidereal day. Under these assumptions, the satellite is, at the completion of "apogee burning," either at the apogee or the perigee of an elliptical orbit. There still would remain the problem of eliminating the eccentricity of this orbit and adjusting the inclination of the orbital plane.

As an example, let us first consider a satellite which is injected into an orbit which lies precisely in the equatorial plane, and consider the case where the actual altitude at apogee burning is greater than the nominal altitude. In this case the satellite is at the apogee of an ellipse whose period is one sidereal day. Since the angular rate of the satellite eastward around the earth is slowest when it is at apogee, and since its average angular rate is the same as that of the earth, the satellite recedes slowly to the west as viewed by an observer on the rotating surface of the earth. As the altitude decreases, the apparent angular regression slows up and 6 hours after apogee, as the satellite crosses the altitude of the nominal circular orbit, the westward regression is converted into an apparent eastward progression. The eastward rate of progression reaches a maximum when the satellite is at perigee. Thus, as illustrated in Figure 2-2, the motion of the satellite relative to an observer on a rotating earth is, to a first approximation, a small ellipse. An analysis shows that the satellite traverses this ellipse with harmonic motion, and it can also be shown that the major axis of the ellipse is horizontal and is always twice the dimension of the minor axis. In the figure the point C lies on the desired meridian at the altitude of a circular orbit having a period of one sidereal day. The point A is the position of the satellite at the end of apogee burning; it lies

[redacted]

CONFIDENTIAL

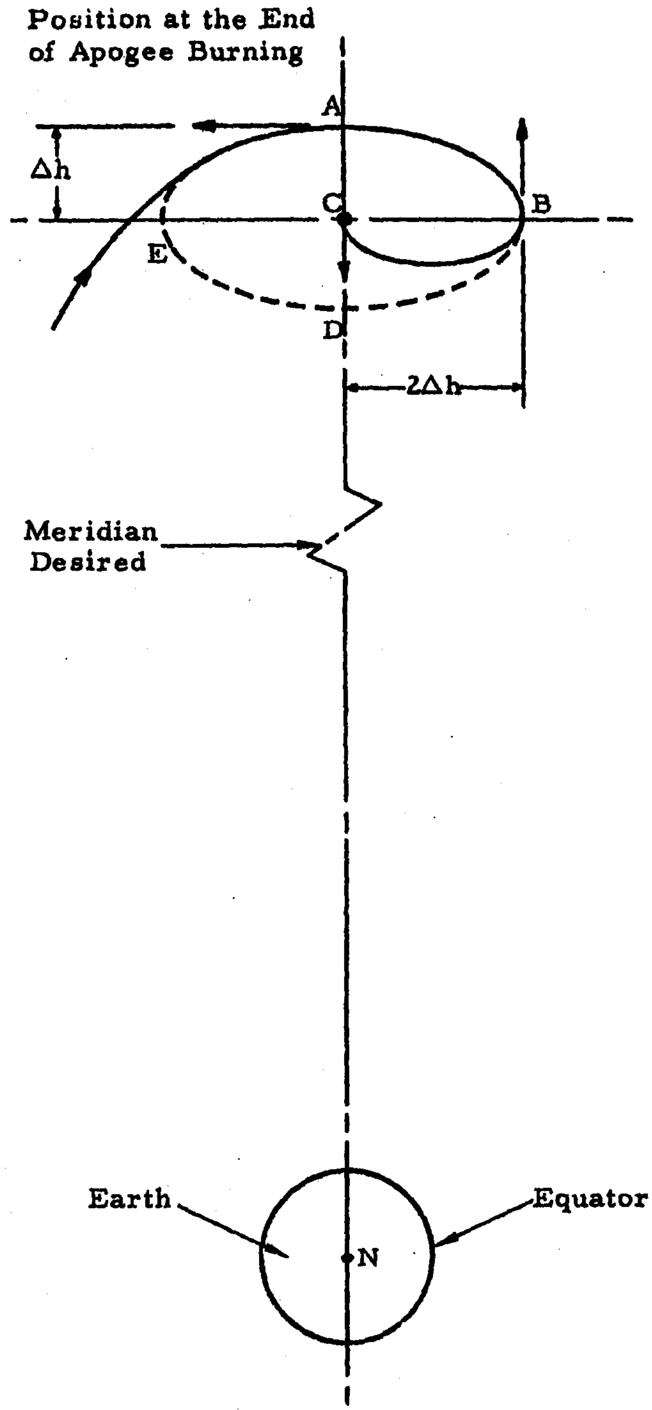

Figure 2-2. Apparent Path of Satellite as Viewed from the Rotating Earth.

CONFIDENTIAL

[redacted]

on the same meridian but at an altitude Δh too high. Six hours after apogee burning the satellite is at the point B; its apparent motion has been to the west a distance $2\Delta h$. If no orbital correction were made at the point B, the satellite in its apparent motion would continue around through the points D and E. However, at point B, an outward radial impulse is applied which halves the inward radial velocity component. This has the effect of halving the eccentricity and consequently halving the dimensions of the harmonic ellipse which represents the path as viewed from the rotating earth. Thus, during the next 12 hours the apparent motion of the satellite is along the elliptical arc BC represented by the dotted curve in the figure. When the satellite arrives at the point C, a second impulse is applied equal and opposite to that applied at point B. This impulse completely arrests all relative motion. From this time on the satellite is in the desired circular orbit.

In the above correction scheme it was assumed that certain conditions held at the end of apogee burning. In reality, apogee burning will not be completed at the correct meridian (in the case of the equatorial satellite) nor will the radial component of velocity be precisely zero, nor will the period of the elliptical orbit be precisely one sidereal day. This situation is brought about because of the unavoidable measurement errors in the tracking radar, which lead to errors in the apogee burning command, and because of measurement and control errors in satisfying this command (for example, errors in the direction of the velocity increment added at apogee caused by platform drift, and errors in the magnitude of the velocity increment caused by accelerometer errors). As a result it will be necessary to use the ground radar for tracking the satellite during the orbital correction period. The point B (Figure 2-2) should be taken as the point where the satellite crosses the altitude of the nominal circularorbit. Because of errors in apogee burning, the satellite will not pass through B precisely 6 hours after apogee burning. At point B the nominal correction, which was described earlier, must be modified to cancel out any apparent horizontal component of velocity, and the vertical component must be chosen to adjust the eccentricity that the satellite will pass through the point C. Based on further tracking data collected between B and C, modifications are made to the nominal correction program at the point C.

The magnitudes of the impulses which must be added at B and C depend, of course, on Δh, and this, in turn, depends upon the accumulated guidance errors from launch to apogee. (There is no way to eliminate Δh during apogee burning.) Although it now appears that accelerometers under development will be able to measure the velocity increment to better than the required 0.2 feet per second, should it develop that lower drift rates are desirable, to provide larger life times without significant departure from station, there it would be necessary to go through a second correction cycle. Since the impulses of the second correction cycle will be very small -- of the order of 0.1 feet per second -- the required increased accuracy could be established. It should also be noted that any effect of the uncertainty in the value of GM, the product of the universal gravitational constant and the mass of the earth, can be wiped out during the one- or two-day orbital correction period.

To this point only corrections in the equatorial plane have been discussed. If at the end of apogee burning the plane of the orbit is not precisely equatorial, then it may be desirable to adjust the inclination of the orbital plane. A nonequatorial plane can come about through apogee burning not being precisely over the equator, or it can come about due to errors in the north-south component of velocity at apogee burnout. An error analysis indicates that the total excursion of the north-south oscillation caused by having the orbital plane inclined to the equatorial plane may not be large enough to warrant correction. However, if it is necessary to reduce this oscillation, this can easily be accomplished by applying an impulse to the satellite in the north-south direction as it crosses the equatorial plane.

The above paragraphs discuss primarily the problem of correcting equatorial orbits. The polar orbital correction problem is somewhat different. Here it is not necessary to closely control either eccentricity or orbital inclination. The period can be measured by noting the time between two successive passes over a given point. A horizontal correcting impulse (or one each on two successive days to give a vernier control) can then be applied in much the same way as described above for the equatorial satellite.

[redacted]

Appendix B is a study of solar and lunar perturbations of a 24-hour circular orbit. The effect of these perturbations is to cause small oscillations of the order of three miles or so, and also small steady drifts. The perturbations can be accurately calculated theoretically, and, consequently, the nominal altitude of the satellite may be so chosen as to compensate for the slow steady drift rates. It can be concluded, therefore, that lunar and solar perturbations are of negligible importance so far as their effects on the 24-hour satellite are concerned.

Orbital correcting impulses can be supplied by a system of gas jets controlled by orders stored in the steering and shutoff computer which receives commands through a decoder from the ground tracker and computer. Such a data link and decoder, associated with the transponder beacon, is currently used on the Atlas missile. Since the jets cannot be calibrated precisely, a vernier acceleration sensing system must be used to control the velocity impulses by a feedback loop through the steering and shutoff computer. The sensitive accelerometers used for the correction period may remain caged prior to the completion of apogee burning.

Throughout the one- or two-day correction period and during the life of the satellite, attitude control is maintained by the system described in the next chapter. The attitude correcting torques can be produced by the same gas jets which provide orbital correction impulses. This jet system and the gas supply for it is described in Chapter 3.

2.1.7 Equipment Needed

The following guidance components need to be carried in the vehicle:

In the booster stage or stages:

1. Booster autopilots

In the first added stage:

2. Autopilot of first added stage
3. Primary guidance computer (digital)

[redacted]

In the final stage:

4. Gyro-stabilized inertial platform
5. Steering and shutoff computer (digital)
6. Perigee-apogee autopilot
7. Attitude stabilization computer* (analog)
8. Tracking beacon with data link and decoder
9. Vernier acceleration-sensing system
10. Clock for timing various operations aboard the vehicle (can be part of the steering and shutoff computer).

In addition to these airborne components, the guidance system also relies upon an accurate tracking radar and radio interferometer and upon a digital computer on the ground. Determinations of vehicle position are made by this ground system and impulse commands are transmitted to the vehicle over the data link.

Figure 2-3 relates the function of the guidance components to the six phases of the trajectory.

2.2 SYSTEM OPERATION AND COMPONENTS

2.2.1 Climb to Low-Altitude Orbit

a. Guidance Scheme

Guidance during climb to low-altitude orbit (except for the programmed guidance of Stage I) is performed by an inertial system consisting of a gyro-stabilized platform with three accelerometers and an associated primary digital guidance computer. This computer controls the powered flight of the vehicle up to the time of injection into the low-altitude orbit; it is jettisoned prior to the perigee burning period. Figure 2-4 shows a block diagram of the guidance scheme.

*This computer works with inputs from the inertial platform, rate feedback from the "perigee-apogee autopilot," and controls the vehicle attitude from launch until the 24-hour orbit is established. Thereafter attitude control is taken over by the monopulse system working in conjunction with attitude computer and other components; the system of attitude control after the 24-hour orbit is reached is the subject of the next chapter.

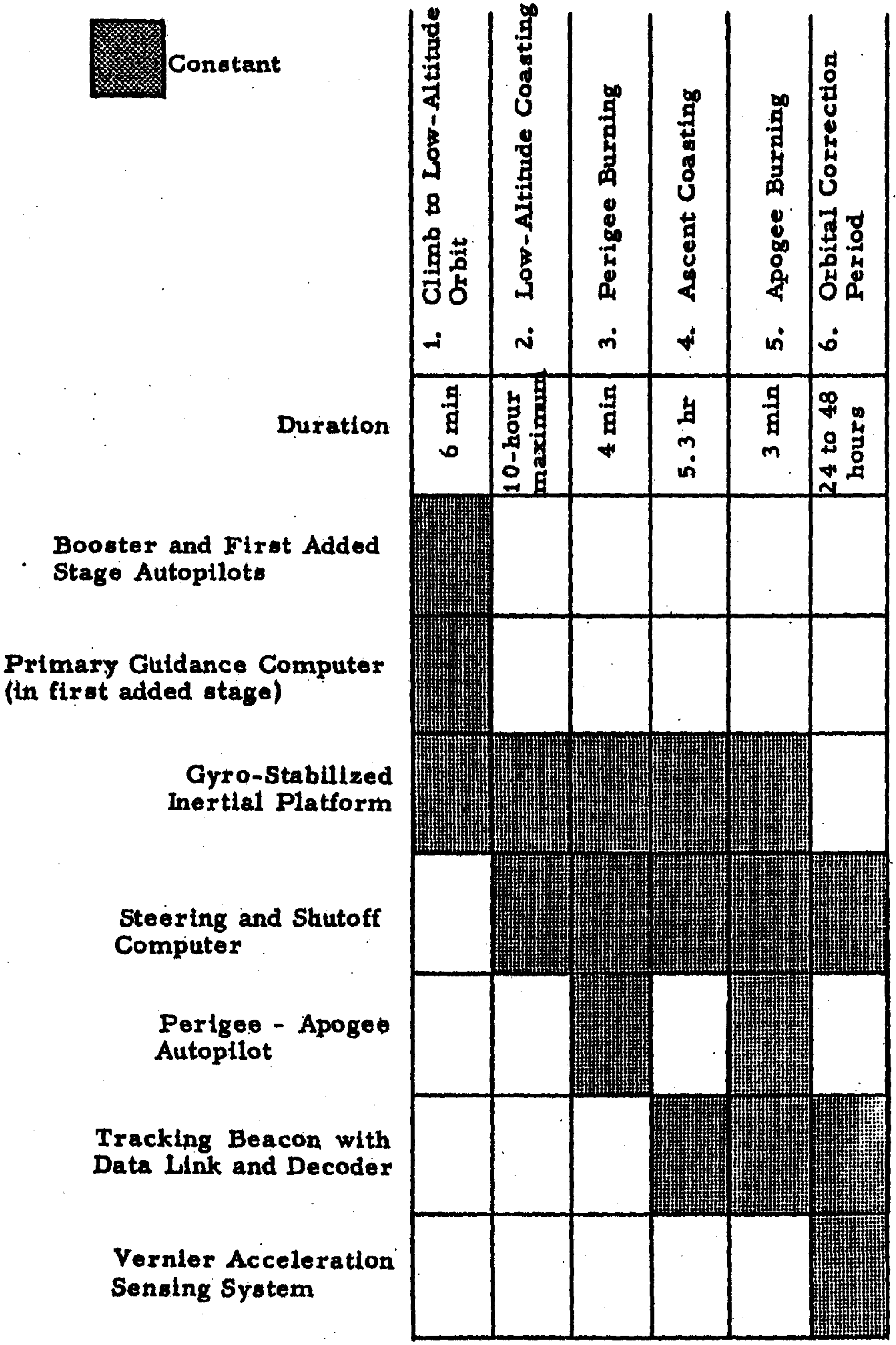

Figure 2-3. Airborne Component Operation Timetable.

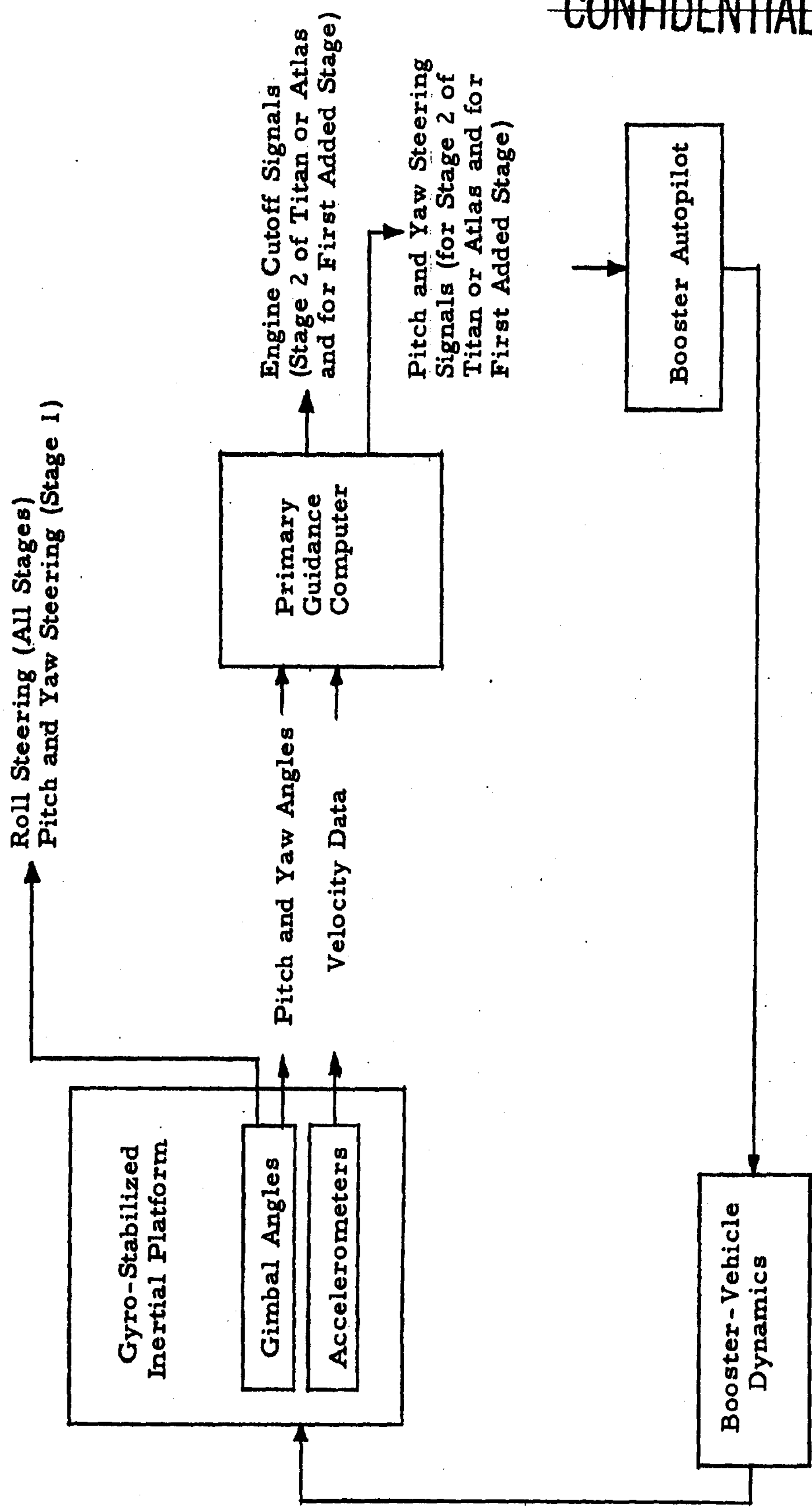

Figure 2-4. Guidance System Proposed for Climb to Low-Altitude Orbit

The stabilization gyros maintain the inner element (on which the accelerometers are mounted) fixed in an inertial frame. The orthogonally mounted accelerometers define a rectangular coordinate system in which the guidance computations are carried out. For reasons of accuracy and ease of system alignment, one axis (z) is aligned parallel to the local vertical at the launch point (see Figure 2-5). The y-axis is aligned normal to the powered-flight pitch plane.*

For an eastward firing, the powered-flight pitch plane coincides with the desired low-altitude orbital plane, that is, the x and z axes of the computing coordinate system lie in the desired plane of the low-altitude orbit. The lateral steering during booster-powered flight is then extremely simple, since it is merely necessary to control and y and $\dot{y}$ errors to zero by the time the booster engines are cut off.

For firing azimuths other than due east, the earth's velocity has a component along the y axis at launch, and hence the x-z plane does not coincide with the desired low-altitude orbital plane. It is necessary, then to compute lateral position and velocity errors with respect to the desired orbital plane and control these errors to zero. If the azimuth of the computing coordinate system is chosen so that the velocity vector at the final booster cutoff point for a <u>standard</u> missile (nominal performance parameters, no disturbances such as winds) lies in the desired low-altitude orbital plane, then a standard missile is required to do no yaw maneuvering to compensate for the earth's rotation. Corrections need be applied only for in-flight disturbances.

Control of the pitch motion of the vehicle is somewhat more complicated. Ideally, it would be desirable to control the pitch motion of the vehicle and terminate the booster thrust at a time such that the vehicle is established in a circular orbit at a predetermined altitude with the injection occurring over a predetermined point on the earth. However, it is impossible to satisfy these constraints simultaneously without thrust control, although it is possible to control the booster flight so that a circular orbit at some altitude h is established. It is necessary to control the powered flight by means of controlled

---

* This is an inertially fixed plane. For a nominal missile executing no yaw motion, the vector remains parallel to this plane during the booster-powered flight. Because of the earth's rotation, the missile does not fly in this plane except in special cases.

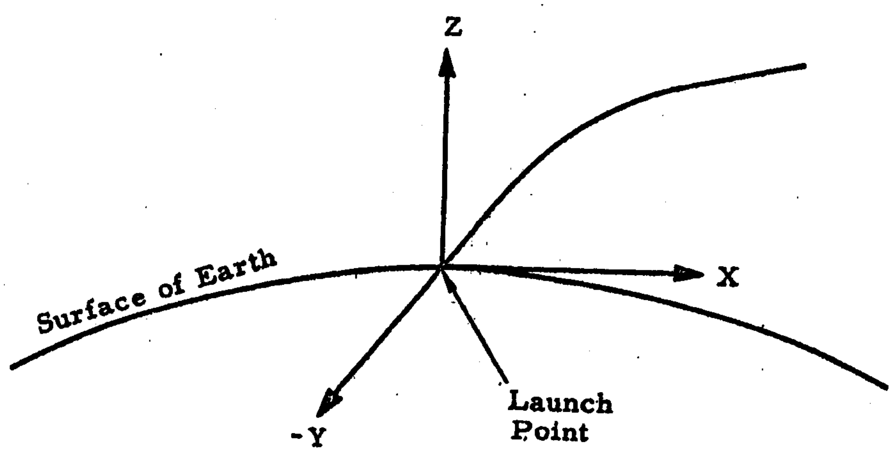

Figure 2-5. Inertial Computing Coordinate System.

thrust termination and pitch steering so that the actual altitude and velocity of the vehicle is made to approach the required altitude and velocity.

This guidance scheme, using velocity vector control, will lead to altitude errors as well as latitude, longitude, and time errors at the injection point if the missile is nonstandard. At most, altitude errors will amount to a mile or two. It is possible with the inertial system to measure the position and time errors at the injection point to about ±600 feet in each direction. Subsequent corrections can be made during later burning periods, so these errors are of no great consequence. The correction scheme will be described in detail in Section 2.2.3 and Section 2.2.5.

b. <u>Guidance Accuracy</u>

Based on the inertial components described later in this section, the estimated rms guidance <u>measurement</u> errors at injection into the low-altitude orbit may be stated as follows:

Error in velocity magnitude	±2 feet per second
Error in direction of the velocity vector	
(a) in orbital plane	2×10^{-4} radian
(b) normal to orbital plane	1×10^{-4} radian
Position errors (all directions)	±600 feet

The <u>control</u> of the actual position and velocity coordinates at the end of the preorbital burning period will not be as accurate as the measurement accuracy, but the <u>control</u> errors can be cancelled by subsequent corrections at perigee burning. It appears that position coordinates will be controlled to about 6000 feet, normal to the flight path and to about 20,000 feet along the flight path. With no vernier burning period at injection into the low-altitude orbit, the velocity magnitude can probably be controlled to about 5 feet per second, and the velocity direction to about 2×10^{-4} radian. The measurement errors specified above are comparable with those required for an ICBM guidance system with a one- to two-nautical mile cep.

c. Computer Requirements

In order to accomplish the control functions described above, the primary guidance digital computer must be capable of:

(1) Accepting acceleration data (integrated once) from the stabilized accelerometers, computing the acceleration due to gravity (from position data), integrating this once to obtain the velocity due to gravity, and combining this with the accelerometer inputs to obtain the total velocity.

(2) Performing another integration to obtain position data.

(3) Computing pitch and yaw steering commands and engine cutoff commands based on position, velocity, and time data.

At the low-altitude orbital injection point, the computer must also calculate corrections to the low-altitude coast time and to the desired velocity increment to be added during the perigee burning period (see Section 2.2.3). It is proposed that the desired corrections be calculated shortly after injection and transmitted to a second (simpler) digital computer, which governs the flight during all subsequent burning periods. After computing and transmitting the desired corrections, the primary computer is jettisoned. The transfer of this data is optional and could be dispensed with if the resultant apogee control errors ±600 feet per second can be economically eliminated by judicious steering during apogee burning, but this study will proceed as though the perigee corrections are to be made.

In order to provide the necessary computing functions with minimum weight, size, and power requirements, the primary guidance computer must be specially designed for the task. Such a computer would be of the fixed program type and would be similar to the airborne computer being built by Arma for the WS 107A-2. If building blocks similar to the Arma Computer (diode matrices for constant storage and magnetostrictive delay lines for dynamic storage) are used, such a computer would weight about 90 pounds and draw about 250 watts. Such a computer could be designed and manufactured on a model shop basis and would be available for flight test about one year after the detailed guidance equations are frozen. The earliest possible flight test date for this subsystem would be the middle of 1960.

A computer having a lighter weight (perhaps 40 to 50 pounds) and drawing less power could be developed using a magnetic drum as the storage element. Development of a suitable drum to withstand the missile environment would take a minimum of two years; the advantages gained by such a computer do not appear to be very great for this application.

d. Inertial Measurement Unit

Table 2-1 indicates some of the major sources of error and approximately the accuracies which can probably be obtained by suitable inertial components within the next two or three years. It is expected that the Arma 10×10^6 gyros currently in development will meet the 0.02 degree per hour drift specification. It is also likely that one of the gyros now under development at the MIT Instrumentation Laboratory would be suitable for this application.

The precision accelerometers assumed in Table 2-1 are about a factor of two better than early models of the Arma vibrating-string accelerometer used in the inertial guidance system for the WS 107A-1, but it is expected that these accelerometers will meet the listed accuracy by the end of the present development program.

Although it is expected that the component accuracies listed in Table 2-1 will be met by 1960 or 1961, it should be emphasized that the success of the ascent guidance system is by no means dependent on such accuracies. Greater errors will only mean the consumption of slightly greater quantities of propellant during apogee burning and during the subsequent orbital correction period.

Table 2-2 summarizes the weight and power requirements of the inertial measurement unit (platform, accelerometers, and electronic packages) for two systems, one available in 1960, and the other available in 1961. System I would use the Arma 4×10^6 gyros and the less accurate accelerometers. System II would use 10×10^6 gyros and improved accelerometers. Dimensions of the stable platform assembly (the largest single unit) and the shock mounts are about 37 x 32 x 23 inches with a volume of about 5 cubic feet. Total system volume* including the computer would be about 12 cubic feet.

*Volume of the early Arma systems used in the WS 107A-1 is about 17 cubic feet.

CONFIDENTIAL

Table 2-1. Inertial Measurement Unit Component Accuracies.

Source of Error	Magnitude of Error (rms)
Gyros	
Drifts Independent of Acceleration	0.02 deg/hr
Drifts Proportional to Acceleration*	0.08 deg/hr/g
Drifts Proportional to Square of Acceleration (due to vibration)**	0.06 deg/hr/g^2
Accelerometers	
Linearity	2×10^{-5} g/g
Cross Coupling	2×10^{-5} g/g
Zero Offset	1×10^{-5} g
Orthogonality	6 sec of arc
Platform Rigidity	2 sec of arc/g
Platform Alignment (all axes)	6 sec of arc

*It is assumed that an optimum gyro orientation is used.

**For the optimum gyro orientation, anisoelastic drifts due to steady accelerations are neglible.

Table 2-2. Inertial Measurement Unit (Stable Platform and Accelerometer System)--Weight and Power Summary.

System	Earliest Availability Date	Weight	Power 3 φ ac	Power dc
I	Jan 1960	200	350	50
II	Jan 1961	160	280	20

CONFIDENTIAL

[redacted]

e. Tie-in with the Booster Autopilot

Figure 2-6 and 2-7 show functional block diagrams of the guidance control system for the climb to low-altitude orbit. During Stage I the vehicle follows a programmed pitch attitude and is stabilized in roll and yaw with the platform as a reference. The primary guidance computer is inactive except for computing vehicle position and velocity at the appropriate time. If a Titan booster is used, the first stage cutoff signal is generated by low-level sensors in fuel and lox tanks. At the beginning of Stage II burning, control of the vehicle is switched to the primary guidance computer, which issues all subsequent engine start and cutoff signals, and also issues pitch and yaw steering signals to control the flight path.

As will be noted from the block diagrams (Figures 2-6 and 2-7) the autopilot (excluding engine actuators and their power supply) is comprised of the following elements:

(1) Pitch attitude programmer (Stage I)

(2) Three rate gyros

(3) Associated electronic amplifiers and compensation networks.

Weights and power requirements for these components are summarized in Section 2.2.7.

2.2.2 Low-Altitude Coasting

The vehicle moves in a low-altitude (140-nautical-mile) circular satellite orbit following booster burnout until perigee burning is initiated. The duration of this orbital coasting is fixed in advance according to the desired longitude of the vehicle in its high-altitude orbit according to the scheme described in Chapter 1. Small variations of this coasting time can be exploited to minimize the control errors accrued at injection into the low-altitude orbit because of the inability of the vehicle to follow the guidance system commands exactly and particularly due to the lack of thrust control. Because burnout position can be measured by the more accurately than the position can be controlled, the position control errors may be in large part compensated by adjusting the coasting time. Velocity control errors at burnout can also be reduced by appropriate adjustement of the perigee burning and steering program.

[redacted]

CONFIDENTIAL

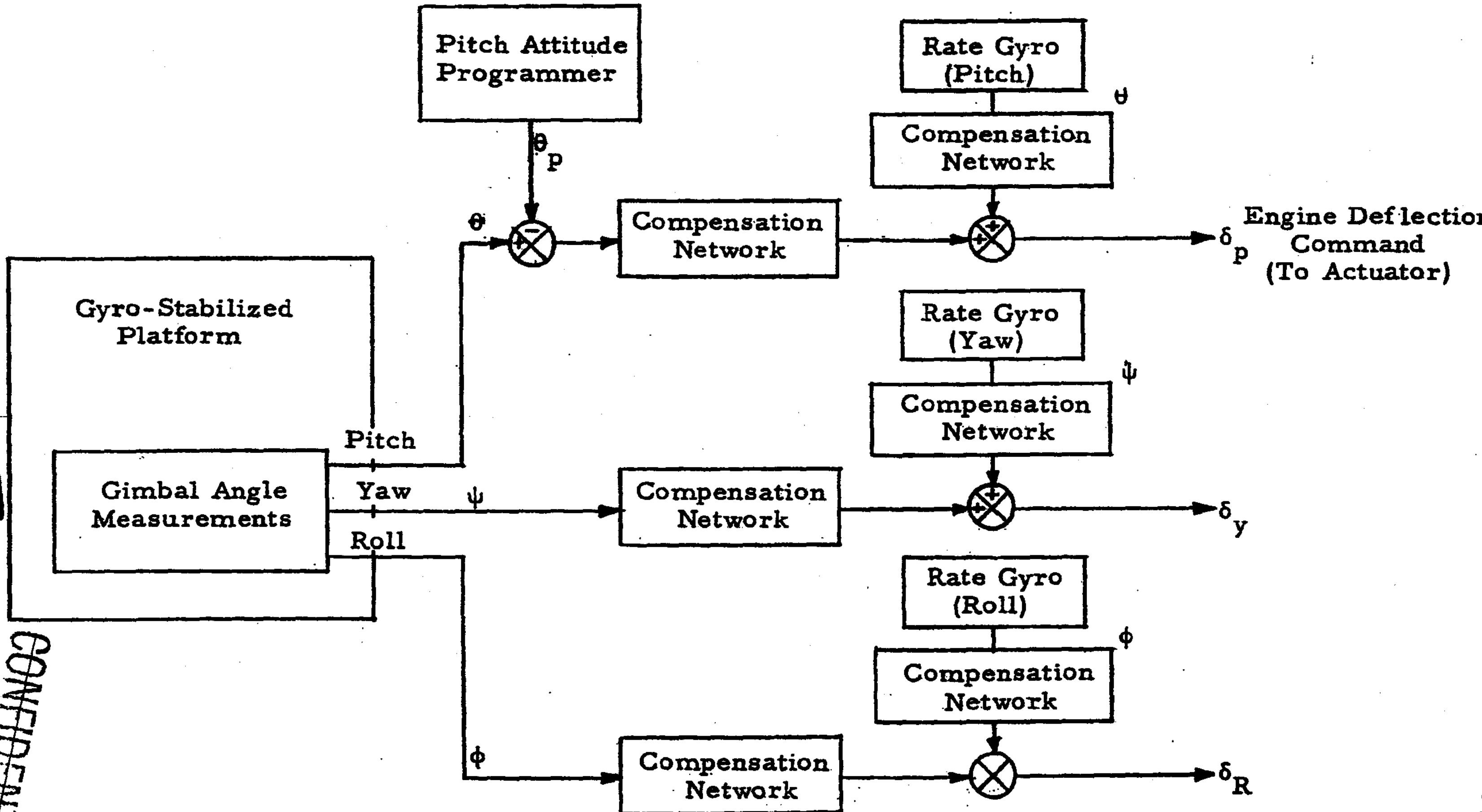

Figure 2-6. First Stage Booster (Thor, Atlas Booster, or Titan First Stage) Programmed Flight Control

CONFIDENTIAL

[redacted]

CONFIDENTIAL

[redacted]

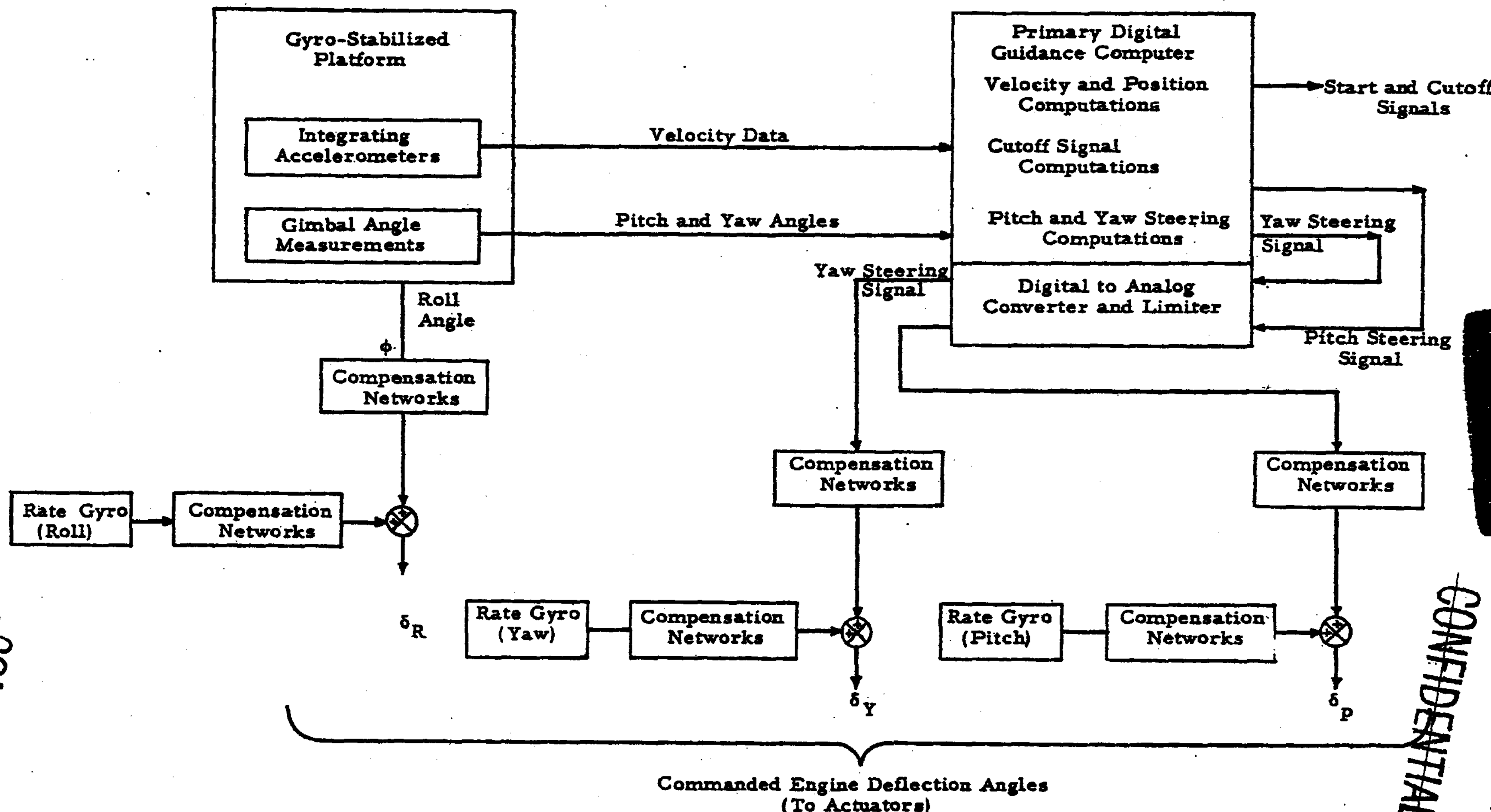

Figure 2-7. Guidance and Control System for Titan or Atlas Second Stage and for First Added Stage (all vehicles).

CONFIDENTIAL

[redacted]

Referring to Table 1-2, Chapter 1, it can be seen that the low-altitude coasting may last as long as 10 hours in order to position certain equatorial satellites. There are two primary functions to perform during this time.

(1) Attitude stabilization of the vehicle

(2) Computation of the coasting duration adjustment and the perigee velocity impulse adjustment to remove control errors imparted at injection into the low-altitude orbit.

Attitude stabilization is required during the coasting phase to prevent the gyro-stabilized inertial platform from going into gimbal lock and to orient the vehicle so that it is aligned approximately in the direction of perigee thrusting. It is proposed that the vehicle be attitude-stabilized during the coasting trajectory by measuring vehicle attitude with the stable platform and computing with a special analog computer control commands for a gas system. Details of the atttitude stabilization system are discussed in Chapter 3, Section 3.2.

The bias computations would be performed with the primary digital guidance computer, using the guidance system measurements of burnout control errors. (See Section 2.2.3 for details of this computation.) Since the computer is placed in orbit together with the first added stage in which it is housed, its utilization during this time requires only that the necessary power be supplied during the time required to calculate the corrections.

2.2.3 Perigee Burning

The proposed control scheme for perigee burning is shown in Figure 2-8. This burning period must add approximately 8000 feet per second to the low-altitude circular satellite orbit speed of 25,424 feet per second in order to start the vehicle on its ascent trajectory along the Hohmann transfer ellipse. The nominal direction for this impulse is tangent to the local earth surface and in the original plane of motion.* The computation of coasting duration and velocity bias corrections by the primary guidance computer for this period is discussed at the end of this section.

*It may be desirable to reorient the flight plane by a small angle at this point for propulsion efficiency. (See Chapter 1, Figure 1-6) such maneuvers do not affect the guidance systems significantly.

[redacted]

CONFIDENTIAL

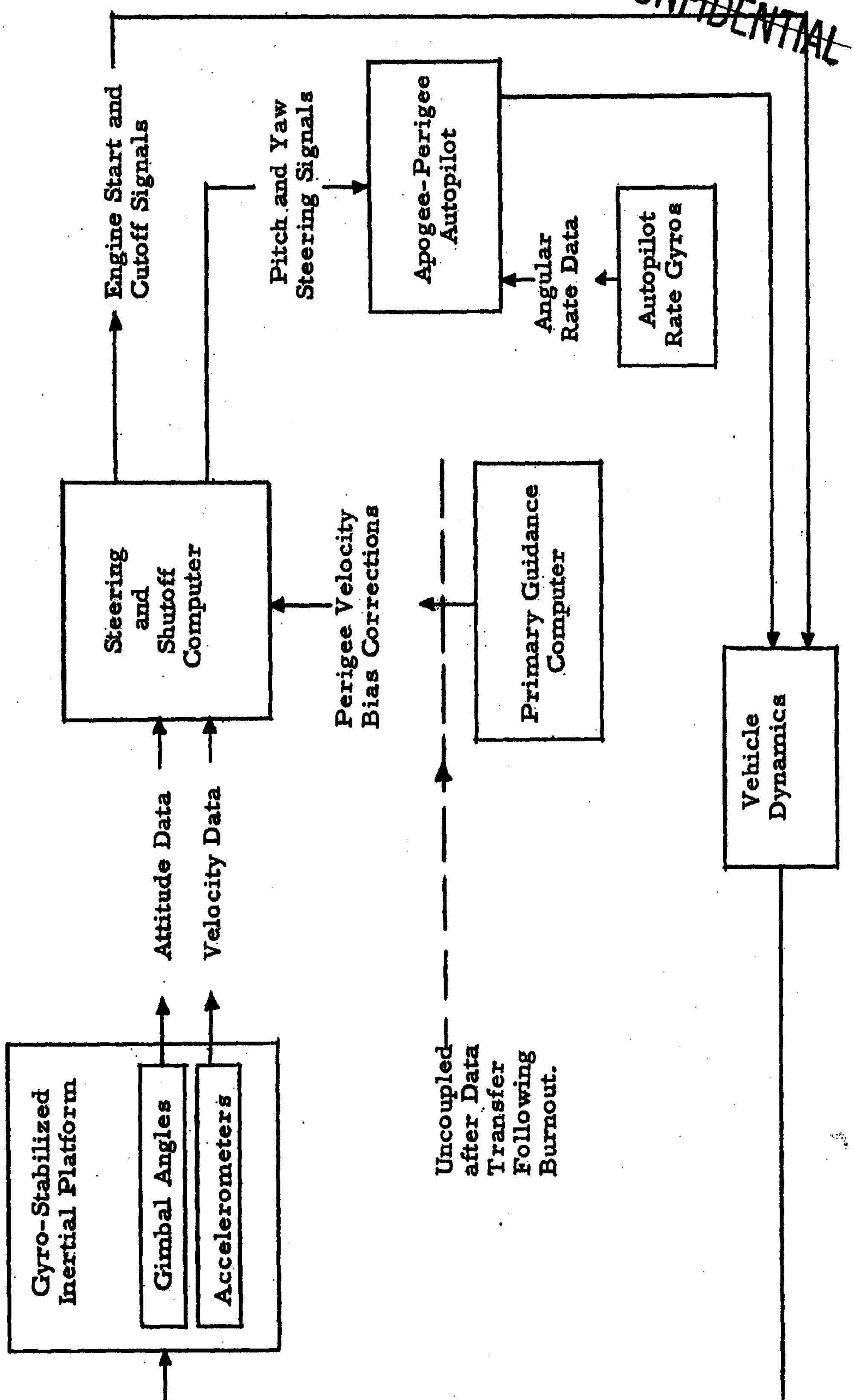

Figure 2-8. Guidance Scheme Proposed for Perigee Burning Control.

CONFIDENTIAL

[redacted]

The bias corrections are stored in a smaller digital steering and shutoff computer that remains in the vehicle. This computer controls both the perigee and apogee burning programs and also regulates the vernier velocity corrections during the orbital correction phase. It is estimated that such a computer could be specially designed for a total weight of 20 pounds, and would probably draw 20 watts of 400-cycles per second ac and 20 watts of 20-volt dc power. The computer would be operated only during the burning and orbital correction periods.

Readings from the accelerometers on the inertial platform would be fed into this computer as velocity data. These measurements would be compared with incremental velocity required as adjusted from nominal according to computations made by the primary guidance computer at injection into the low-altitude orbit. The steering and shutoff computer would compute pitch and yaw steering signals for the autopilot, and command the engine start and cutoff signals.

The same autopilot would be used for both perigee and apogee burning. It is estimated that the entire autopilot, including rate gyros, would weigh less than 15 pounds and need not draw more than 25 watts of 400-cycles per second ac power and 10 watts of 20-volt dc power. The rate gyros should be good to 10^{-4} radian per second over fractions of a second, and would control high-frequency vehicle vibrations and flexures during perigee burning. The inertial platform accelerometers would control velocity impulse, since they are attitude-stabilized and quite accurate ($\delta a/a = 2 \times 10^{-5}$). Motor shutdown control errors will probably limit the speed control to about one foot per second. Since perigee burning is characterized by low acceleration levels, the g and g^2 platform errors are neglected and the total velocity orientation control error at the end of perigee burning is equated to the platform drift. The perigee burning errors are thus

$$\delta \gamma = \delta \epsilon = \pm 0.2 \text{ degree} = 3.5 \text{ milliradians}$$

$$\delta (\Delta V) = \pm 1 \text{ foot per second,}$$

where γ is azimuth and ϵ is elevation of the applied velocity increment and ΔV is the magnitude of the velocity increment. Since 8000 feet per second is added, the angular errors each introduce an unwanted cross component of velocity equal to 28 feet per second.

The guidance system is not able to control the missile position and velocity vectors as accurately it can measure them. This is due primarily to lack of precise thrust control but also to smoothing, response lags, and motor shutdown errors. Estimated control and measurement accuracies at the time of injection into the low-altitude orbit (t_o) are compared in Section 2.2.1b. The error analysis of Appendix A shows that these control errors are transformed into position and velocity errors at the end of the low-altitude coasting (t_1) according to Equations (2.1) through (2.6). First, however, we define the symbols used, assuming an equatorial satellite is being launched.

U = circumferential velocity

V = total magnitude of velocity

ϕ = transit angle in plane of motion

r = distance from vehicle to center of earth

α = climb angle of vehicle above local horizontal

μ = GM, gravitational constant multiplied by mass of earth

W = radial velocity = $\dot{r}$

σ = inclination, i.e., dihedral angle between plane of motion and equatorial plane

Φ = transit angle from initial burnout to "zeroth" crossing of equatorial plane

λ = latitude

$\mathrm{sgn}\lambda_o$ = +1 for northern latitudes, -1 for southern

β = azimuth of velocity vector

N = number of half revolutions from "zeroth" crossing in low-altitude coast

θ = longitude difference between burnout and "zeroth" crossing of equator

ρ = longitude

Ω = angular rate of rotation of earth.

and subscripts indicate the period of occurrence.

Velocity Errors at t_1 (end of low-altitude coast)

$$\frac{\delta U_1}{V_o} = -(1-\cos\phi_1)\frac{\delta r_o}{r_o} + (2\cos\phi_1 - 1)\frac{\delta V_o}{V_o} - \sin\phi_1\,\delta a_o + (1-\cos\phi_1)\frac{\delta\mu}{\mu}, \qquad (2.1)$$

$$\frac{\delta W_1}{V_o} = \sin\phi_1\frac{\delta r_o}{r_o} + 2\sin\phi_1\frac{\delta V_o}{V_o} + \cos\phi_1\,\delta a_o - \sin\phi_1\frac{\delta\mu}{\mu}, \qquad (2.2)$$

$$\delta\sigma_1 = -\cos\Phi(\mathrm{sgn}\,\lambda_o)\,\delta\beta_o + \sin\theta(\mathrm{sgn}\,\lambda_o)\,\delta\lambda_o, \qquad (2.3)$$

Position Errors at t_1

$$\frac{\delta r_1}{V_o} = (2-\cos\phi_1)\frac{\delta r_o}{r_o} + 2(1-\cos\phi_1)\frac{\delta V_o}{V_o} + \sin\phi_1\,\delta a_o - (1-\cos\phi_1)\frac{\delta\mu}{\mu} \qquad (2.4)$$

$$\begin{aligned}\delta\lambda_1 = {} & \left[(-1)^N\cos\lambda_o\sin\theta\right]\delta\beta_o + \left[(-1)^N\cos\theta\right]\delta\lambda_o \\ & + \left[(-1)^{N+1}\sin\sigma_1(\mathrm{sgn}\,\lambda_o)\right]\left[(2\sin\phi_1 - 3\phi_1)\frac{\delta r_o}{r_o}\right. \\ & + (4\sin\phi_1 - 3\phi_1)\frac{\delta V_o}{V_o} + 2(\cos\phi_1 - 1)\,\delta a_o \\ & \left. + (2\phi_1 - 2\sin\phi_1)\frac{\delta\mu}{\mu} + \frac{U_o}{r_o}\,\delta t_1\right] \qquad (2.5)\end{aligned}$$

CONFIDENTIAL

$$\delta \rho_1 = \sin \lambda_o \, \delta \beta_o + \delta \rho_o + \Omega \, \delta t_1 + \cos \sigma_1 \Big[(2 \sin \phi_1 - 3 \phi_1) \frac{\delta r_o}{r_o}$$
$$+ (4 \sin \phi_1 - 3 \phi_1) \frac{\delta V_o}{V_o} + 2 (\cos \phi_1 - 1) \, \delta a_o$$
$$+ (2 \phi_1 - 2 \sin \phi_1) \frac{\delta \mu}{\mu} + \frac{U_o}{r_o} \delta t_1 \Big] \tag{2.6}$$

The above equations hold equally well for polar orbits, but the quantities appearing therein must be redefined: σ is the angle between the plane of the orbit and the desired plane; ρ is the azimuthal angle measured in the final desired plane of the orbit; λ is the angle from the satellite to the desired plane; and so on, with the final desired plane replacing the equatorial plane in the definitions. Of course, in the case of a polar orbit, the term containing Ω in Equation (2.6) does not occur, but a similar term would occur in the counterpart of Equation (2.5).

If the actual position and velocity could be measured with infinite precision, the control errors could be computed as the difference between these and the nominal values stored in the primary guidance computer. The above equations would allow one to predict the corresponding control variations in position and velocity which would result at the end of the coasting phase. The transverse velocity errors [Equations (2.2) and (2.3)] can be compensated by judicious steering during perigee burning. The speed impulse added during perigee burning can be altered so as to compensate for too little or too much speed (δU_1) at t_1. The altitude error at perigee burning can be corrected simultaneously with the speed error, since there is an appropriate speed impulse for transfer takeoff from any altitude. The simultaneous correction of δr_1 and δU_1 does not depend upon fixing the coasting time.

The latitude and longitude errors at perigee burning can be minimized by choosing the coasting time on the basis of the burnout measurements. This may be seen from Equations (2.5) and (2.6), since if all of the burnout control errors are measured with infinite precision, the variation of coasting time, δt_1, can be chosen so as to minimize one or the other, or perhaps both. For a vehicle fired due east from Cape Canaveral with a maximum transit of seven

CONFIDENTIAL

[redacted]

full revolutions in the low-altitude orbit after the first equatorial crossing, these last two error expressions assumed the following numerical forms:

$$\delta \lambda_1 = 0.88\, \delta \beta_o + 64.3 \frac{\delta r_o}{r_o} + 63.3 \frac{\delta V_o}{V_o} + 0.95\, \delta \alpha_o - 42.5 \frac{\delta \mu}{\mu} - 0.56 \times 10^{-3}\, \delta t_1 ,$$

$$\delta \rho_1 = 0.48\, \delta \beta_o + \delta \rho_o + 118 \frac{\delta r_o}{r_o} - 116 \frac{\delta V_o}{V_o} - 1.76\, \delta \alpha_o + 78.2 \frac{\delta \mu}{\mu} + 0.95 \times 10^{-3}\, \delta t_1 .$$

Subject to the basic uncertainty in the gravitational product $\mu = GM$, one may solve for the δt_1, and eliminate either $\delta \lambda_1$ or $\delta \rho_1$. An optimum strategy seems to be to choose δt_1 so that the same bracketed quantity in Equations (2.5) and (2.6) vanishes. Actually, the measurements are not infinitely accurate, so that the propagation of the burnout measurement errors must be reckoned as control errors when the vehicle arrives at apogee. Correction of a 2-foot-per-second speed-control error at burnout requires that the coasting time be changed by 9.2 seconds to correct the latitude at perigee burning, and by 5.4 seconds to correct the longitude. The error coefficients are not changed significantly during such times, so that the computations are linear and constant for a fixed nominal trajectory.

Velocity and coasting duration corrections are simply a matter of transforming the difference between measured and control quantities at burnout via the above constant matrix. This could be performed quite easily in the primary guidance digital computer, which is also brought into the low-altitude coasting orbit with the vehicle. To take advantage of this computer, however, it is necessary to postpone separation until the computation is completed and the correction signals are fed to the steering and shutoff computer which controls perigee burning. The additional power requirements for this computation are negligible since it is estimated that the constant-coefficient six-by-six matrix multiplication could be performed in the computer in less than 1 second.

2.2.4 Ascent Coasting

Perigee burning ends with a total vehicle speed of approximately 33,420 feet per second. This speed is gradually lost as the vehicle exchanges kinetic energy for potential energy during the slow rise along the elliptical path to apogee. The combined effect of perigee-burning control errors and extrapolated booster burnout errors is to prevent precise control of position and velocity vectors at apogee. There are two primary functions to perform during this phase:

(1) Attitude stabilization of the vehicle during ascent

(2) Tracking by ground stations to determine the actual position and velocity vector of the vehicle as it nears apogee.

In the case of an equatorial satellite which enters perigee burning on a southward crossing of the equator, the angle between the longitudinal axis of the vehicle and the equatorial plane during perigee burning is about 28.5 degrees. (If the plane of the orbit is to be reduced by 2.2 degrees, as suggested in Chapter 1 for propulsion efficiency, then the angle between the longitudinal axis and the equator is about 9 degrees less.) Just before apogee burning the vehicle is again approaching the equatorial plane at an angle of 28.5 degrees from the south. During apogee burning the longitudinal axis of the vehicle must be pointed south from the equatorial plane by an angle of about 24.5 degrees in order to cancel the northerly motion of the vehicle as it approaches the equatorial plane. The angle between initial and final orientation is about 127 degrees (180 degrees - 28.5 degrees - 24.5 degrees). If the equatorial crossing at perigee burning is toward the north, a similar reorientation is required. In addition, it is necessary to control attitude during the final hours of ascent so that an appropriately designed transponder antenna pattern will cover the ground tracking station.

The same attitude stabilization system is used during the ascent coasting trajectory as for the low-altitude coasting phase. Torqueing commands for the gas jets are generated in the analog attitude stabilization computer using vehicle orientation as read from gimbal angles on the inertial platform (see Chapter 3, Section 3.2).

Although the position and velocity at apogee cannot be controlled with great precision because of blind navigation errors, it is possible to measure the vehicle's position and velocity with considerable accuracy after it rises above the radar horizon of a ground tracker, presumably the same tracker as would be used for the orbital correction phase. The position of a vehicle launched from an equatorial launch site as a function of time during the ascent trajectory is shown in Figure 2-9 in a coordinate system which rotates with the earth. The vehicle spends over 4 of the 5.27 hours of coasting time within 17 degrees of its final meridian and provides a very good target for position and velocity determination. As can be seen from the figure, there is a good deal of flexibility in the allowable location of the ground station.

Preferably, for accuracy of tracking during the orbital correction phase (to avoid foreshortening of the base line of the radio interferometer), it should be close to the nadir point below the satellite. But for logistic simplicity, it may be desirable to place the tracker at one of the communication stations which are, of course, within line-of-sight of the satellite's terminal position.

Tracking accuracy requirements during ascent coasting are far less severe than tracking requirements during the orbital correction phase. Consequently, it is the latter phase which sets the specifications and determines the design of the tracking system.

Since the most critical specification on orbit accuracy is that of meeting the 0.2-foot per second drift rate, the most critical measurement is angular rate. The Maui propagation experiments show that at 10,000 megacycle, 1 microradian per second can be achieved with a 20-second smoothing time. (At X-band, it is probable that the influence of ionospheric diffraction will be less than the influence of the tropospheric effects.)

Since rate errors are improved in proportion to the three-halves power of the smoothing time, a smoothing time of 1 hour would provide angular rate accuracies of 0.0004 microradians per second. This would determine horizontal velocity to better than 0.06 foot per second. However, there is some question about the physical possibility of measuring this accurately over long

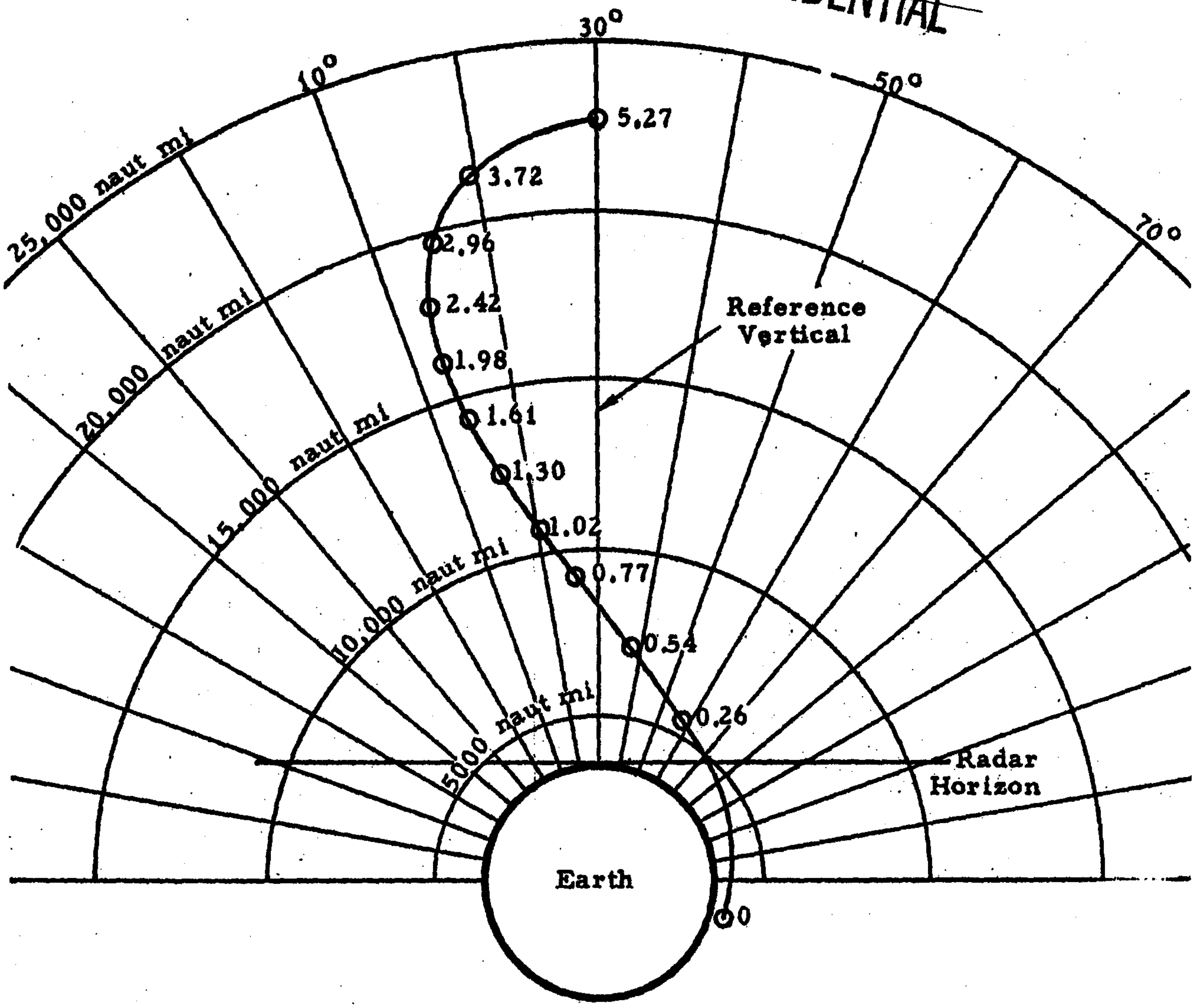

Figure 2-9. **Position of Vehicle in Equatorial Plane at Various Times During Ascent Relative to Rotating Earth.**

periods of time, since diurnal variations in the atmospheric refractive-index configuration must be recognized together with the random variations whose effects are being smoothed, and carefully devised experimental tests of long-term smoothing for tracking data should be initiated.

Equipment for making the above measurements would consist of a ground interferometer installation possessing three stations spaced approximately 2000 feet apart. Calculations show that adequate signal-to-noise ratio (approximately 40 db with a 10-cycle bandwidth) can be achieved using 6-foot diameter ground antennas, one of which is radiating 10 watts at X-band. The ground antennas must be capable of tracking the vehicle as it rises during the last few hours. This could be accomplished by slaving them to a single tracking antenna which tracks the beacon in the vehicle. The three ground antennas must be connected by phase-coherent links. These could be supplied either (1) by waveguide as in the Mod III General Electric Atlas rate system or (2) by air links.

It seems clear that the various accuracy requirements of the system (minimizing attitude control problems, easing ground tracking requirement, etc.) can be met if angular position is determined to about 1 milliradian. This requirement can be easily met by the position tracker of the GE system. If much higher accuracies should ever be required, an alternative for measuring angular position is to use noise modulation on the X-band radio interferometer signal sent to the missile transponder. By measuring the difference of transmission times to the several ground receivers, one determines angular position. A base line of 2000 feet in each (orthogonal) direction would give a tropospheric fluctuation accuracy of 10 microradians (rms), according to the Maui tracking simulation experiments, but boresighting will limit the absolute accuracy to a somewhat larger number.

Range rate to the vehicle could be measured by round-trip doppler techniques to 0.25 foot per second quite readily. The GE radio system has shown this accuracy in current tests. This measurement could be improved by a factor of 10 if it were necessary, since propagation noise is not an important factor.

Absolute range can be measured to an accuracy of 200 feet, which is limited by the uncertainty of one part in 10^6 for the velocity of light. Propagation effects give a range error of less than 1 foot. It should be noted that relative range can probably be measured to 10 feet at this distance.

The airborne transponder takes the signal from one of the ground stations, offsets it in frequency and transmits it. The airborne antenna could be a flush antenna or a fixed horn. The transponder can also be used to receive commands from the ground tracker. The command channel could be incorporated as modulation on the rate system signals. The decoder could be built into the transponder. The average power requirements for the transponder would be approximately 75 watts. It would radiate 100 milliwatts. The transponder, including power supply, but not including batteries, might weigh 15 pounds and occupy three-fourths of a cubic foot. These estimates are based on current design techniques, using a mixture of currently available vacuum tubes and transistors. It is very likely that the weights and powers of all vehicle-borne equipment could be reduced appreciably if a significant effort were made in this direction.

It should also be noted that continuous tracking is not required, since it is only the low-frequency noise which is critical for such long smoothing times. It is therefore proposed that the vehicle be tracked for approximately 2 seconds every 2 minutes to conserve transponder battery power in the vehicle. Since some of the airborne beacon equipment must remain in operation during the down times, this probably corresponds to 10 per cent of the nominal total power requirement.

The tracking data would be fed into a ground digital computer in the form of round-trip doppler shifts and doppler differences. The computer would smooth the high-frequency components of the radio tracking data and then compute the several invariants of a free-fall ellipse (e.g., eccentricity, major axis, inclination of orbital plane, etc.). These invariants can then be smoothed to eliminate low-frequency noise. The final results of the computations are commands transmitted to the vehicle via the transponder data link. Quantities transmitted are the time to commence apogee burning when the correct longitude is reached (for the equatorial satellites or the correct latitude for polar satellites) and adjustments to the incremental vector velocity (magnitude and direction) to be added during apogee burning.

2.2.5 Apogee Burning

For the equatorial satellite, the apogee burning period must add approximately 6000 feet per second to establish the vehicle in the 24-hour orbit, simultaneously changing the plane of motion by 28.5 degrees. The guidance scheme proposed for controlling the burning phase is shown in Figure 2-10, which indicates that the steering and shutoff computer is the central control. The ground-tracking system measures the actual trajectory during the ascent coasting phase and transmits velocity bias correction to the vehicle. These are stored in the steering and shutoff computer. Apogee burning is initiated when the vehicle reaches the correct position. The engine start signal is commanded from the ground on the basis of angular position tracking information which establishes the true longitude of the vehicle.

As mentioned in Section 2.1.5 the incremental velocity added during apogee burning is so chosen that the radial component of velocity and the north-south component of velocity are both brought to zero, and the eastward component of velocity is chosen to establish the satellite in an orbit having a period of one sidereal day. Consequently, the burnout velocity must be chosen as a function of the observed altitude at apogee burning. The commands to add the correct vector velocity increment are transmitted from the ground tracker and stored in the steering and shutoff computer.

The steering program during apogee burning is controlled by the digital steering and shutoff computer using the stored commands from the ground tracking station and using the platform-mounted accelerometers for sensing velocity changes of the vehicle. The ground tracker cannot be used for controlling the velocity increment added during apogee burning nor can it be used for controlled azimuth steering during apogee burning because the smoothing times in the angular rate circuits are too long to keep up with the velocity changes. In principle, the ground tracker could be used for controlling elevation steering since the dopper range rate circuit can have a

[redacted]

~~CONFIDENTIAL~~

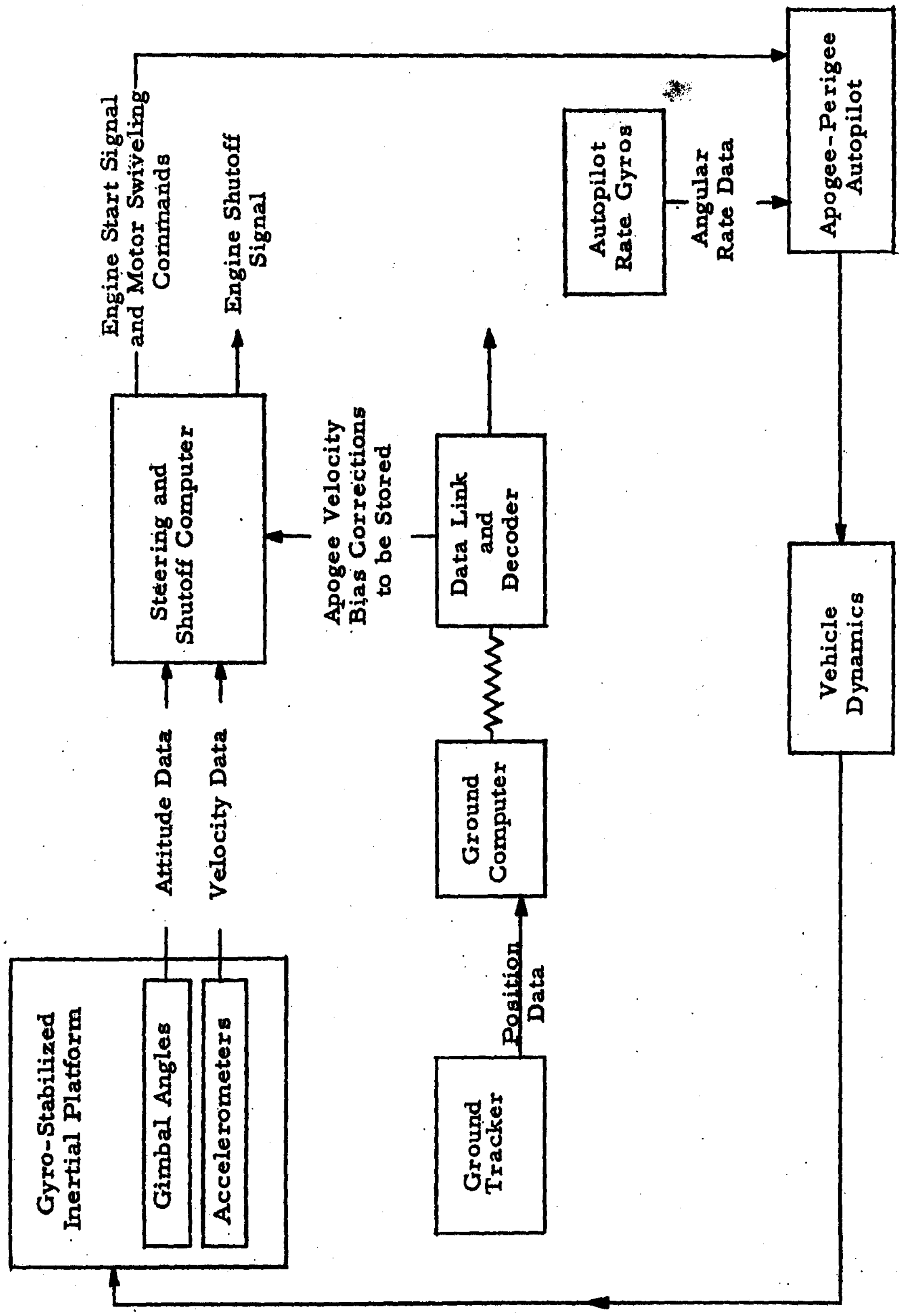

Figure 2-10. Guidance System Proposed for Apogee Burning Control.

[redacted] ~~CONFIDENTIAL~~

very short smoothing time. However, since the inertial platform must be used for controlling azimuth steering it is simpler to let it control elevation steering as well. Since the steering and shutoff computer and the inertial platform were used during perigee burning, no new components are introduced into the system for apogee burning. The incremental velocity vector should be controllable to 5 milliradians in angle and about 1 foot per second in magnitude, including uncertainties in engine shutdown characteristics.

2.2.6 Orbital Position Correction

During the orbital correction period, position and velocity data are derived from the ground tracker and are used to compute commands which are sent to the vehicle on the data link. The commands consist of orders to fire the appropriate orbital correction jets together with information on the incremental velocity to be added, the latter to be stored in the digital steering and shutoff computer. Since long smoothing times are needed to improve the latitude and longitude velocity measurements, the tracking can be intermittent. This will reduce the power consumption by the tracking beacon. It is expected that only 2 seconds of tracking every 2 minutes are needed during the 24 or 48 hours of vernier control, which calls for an average beacon power of only 7 watts. A block diagram of this system is shown in Figure 2-11.

The gas jets described in Chapter 3 are operated at intervals during the first 24 or 48 hours. A total velocity impulse of about 100 feet per second must be supplied for all of these corrections. Since the jets cannot be calibrated precisely, a vernier acceleration sensing system is used to control velocity impulses by a feedback loop through the computer. Three body-mounted accelerometers plus the associated electronics can probably be designed for 15 pounds and 30 watts of dc power. Since the impulses will be supplied at low acceleration levels, it is possible to use sensing schemes which are more accurate than those used for ICBM flights, where a dynamic range of 10 g's is required. There is considerable room for invention in this area of low-thrust accelerometers.

The gas jet system proposed in the next chapter would produce between 10 to 20 pounds of thrust. This leads to accelerations during the application of

[redacted]

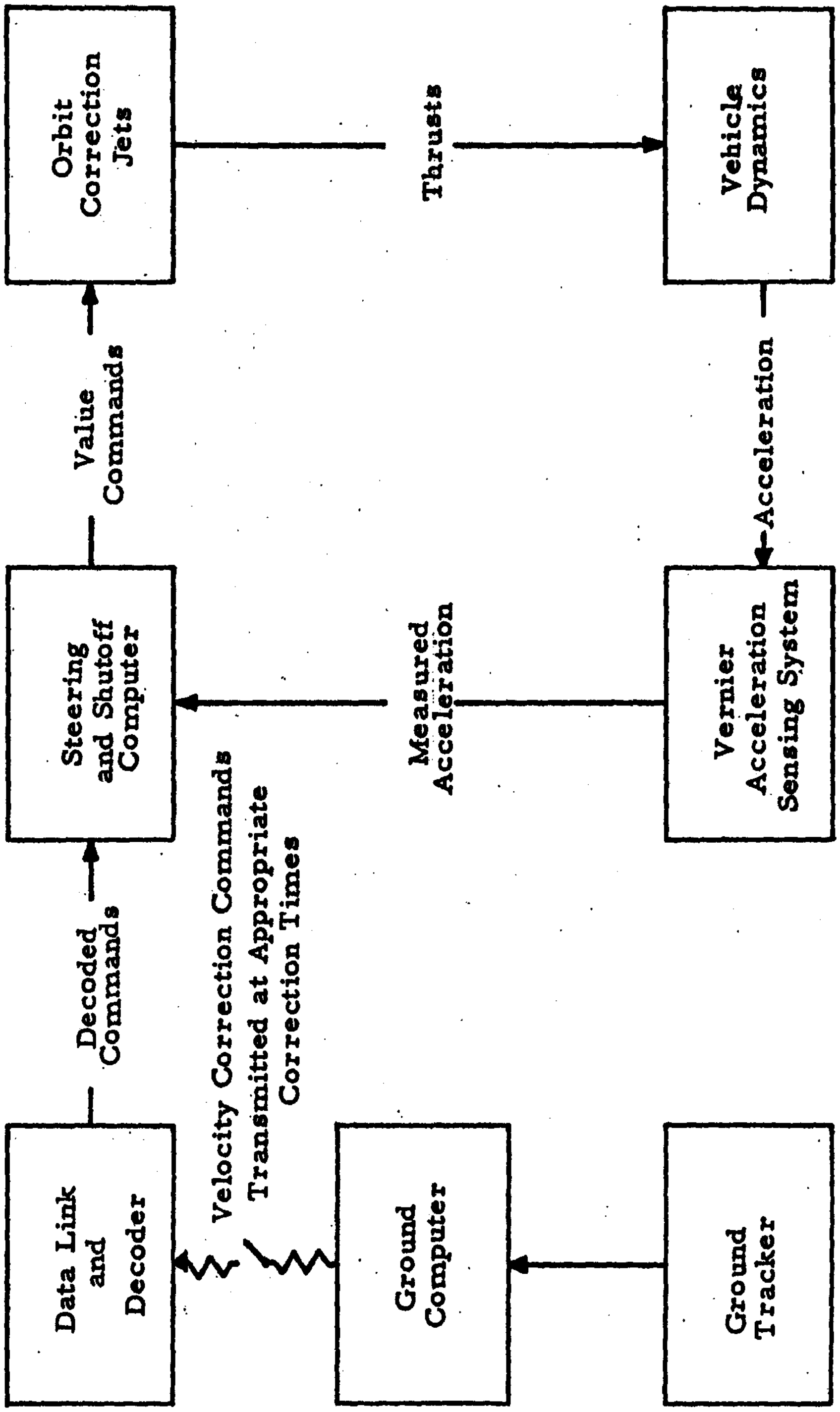

Figure 2-11. Proposed Guidance Scheme for Orbital Corrections.

[redacted]

correcting impulses of about 0.01 g. If we assume that accelerations can be measured to 10^{-5} g's (requiring a null error of 10^{-5} g's and a scale factor error of 10^{-3} of full scale), then the 100 feet per second or so which is added can be measured to 0.1 foot per second which meets the requirements set up earlier. If this specification can be met, then the total time required for corrections should not be greater than about 18 hours. On the other hand, if the accelerometers do not meet this specification, it may be necessary to go through a second cycle of corrections as described in Section 2.1.6.

2.2.7 Weight and Power Summaries

Estimates for subsystem design weights and power requirements are summarized in Table 2-3. The data in Table 2-3 is combined in Table 2-4 with the airborne component operation time table to produce the estimated weight and power requirements by component for each phase of the orbit-establishing trajectory. The total weight and power requirements for each phase of the trajectory is also given. However, the power consumption is quite uneven due to the intermittent use of the components. The primary guidance computer is turned off and jettisoned as part of the first added stage following the booster burning period to reduce the total weight and power required. A single crystal clock accurate to one part in 10^6, will also be necessary. However, it will weigh only about 1 pound including circuitry and will require neglible power.

The analysis of each phase of the guidance sequence given in Section 2.2 establishes the probable accuracy and the weight and power requirements. It is found that 370 pounds of airborne guidance in the last stage could localize the vehicle above any point on the equator accurately enough for all of the applications indicated in Volume II. The average power consumption during ascent is about 450 watts although this requirement varies considerably throughout the guidance phases.

Analysis of the accuracy of the system shows that the suggested combination of inertial and radio measurements at appropriate points on the ascent trajectory stabilizes for a period of 5 years or more for both the position and

Table 2-3. Airborne Guidance Components - Final Stage Weight and Power Requirements.

Component	Weight (pounds)	AC Power[b] 400 cps 3 ϕ (watts)	DC Power 20 volt (watts)
Gyro-stabilized inertial platform and electronics	235	350	50
Steering and Shutoff computer (digital)	20	20	20
Perigee - Apogee autopilot[a]	15	25	10
Tracking beacon with data link and decorder	50		50
Vernier acceleration-sensing system[c]	15		20
Cabling	25 (per stage)		
Total	360	395	150

[a] Only the weight and power of the measuring instruments and required computing functions are included. Hydraulic power requirements are not included. These are included in propulsion weights.

[b] DC inverters must be supplied at additional weight cost to provide alternating current, since only direct current is supplied by power supply.

[c] Makes use of the same computer as Item 5. A set of body-mounted accelerometers are used rather than the platform accelerometers.

[redacted]

Table 2-4. Power Breakdown for Each Phase of Orbit-Establishing Sequence.

Airborne Component	Preorbital Trajectory		Low-Altitude Coasting (10 hours)	Perigee Burning	Ascent Coasting (5.3 hours)	Apogee Burning	Vernier Correction (24 to 48 hours)
	Weight (pounds)	Power (watts)	Power (watts)	Power (watts)	Power (watts)	Power (watts)	Power (watts)
1. Primary guidance computer (digital)	90	250					
2. Booster autopilot[a]	15	35					
	110	285					
3. Gyro-stabilized inertial platform and electronics	235	400	400	400	400	400	
4. Steering and shutoff computer (digital)	20		40	40	40	40	40
5. Apogee and perigee autopilot[a]	10			35		35	
6. Tracking beacon with data link and decoder[b]	15				5[c]		5[c]
7. Vernier acceleration-sensing system	20						10
8. Clock	1						
9. Cabling	25						
Total	326	400	440	475	445	475	55

[a]Does not include actuators

[b]50 watts

[c]Tracking for 2 seconds every 2 minutes

[redacted]

altitude of the vehicle in the high orbit. The vernier velocity impulses required to stabilize the orbit are probably about 100 feet per second total.

The guidance system used to establish polar satellites varies slightly from that for the equatorial, since only broad-beam coverage is required, in contradistinction to the antenna-bearing problem associated with point-to-point relaying for equatorial satellites. In essence, this means that the polar satellite need not be stabilized in yaw after the initial velocity corrections are made.

CONFIDENTIAL

CHAPTER 3

ATTITUDE CONTROL

3.1 INTRODUCTION

This chapter is devoted to the problems of establishing and maintaining the final stage vehicle attitude both before and after the 24-hour orbit has been attained. The recommended method of attitude control prior to attaining the 24-hour orbit is to use the inertial platform to control a "coarse" gas jet system. Each jet should produce about 5 pounds of thrust for a Thor-boosted vehicle or 10 pounds for a Titan- or Atlas-boosted vehicle and when paired should produce a torque couple of about 25 or 50 foot pounds (assuming 2 jets each, 2-1/2 feet from the center of rotational inertial). This "coarse" gas jet system is used to reorient the vehicle during low-altitude coasting, ascent coasting, and to point the nose of the vehicle toward the earth after apogee burning. The same gas jet system, with the pairs oriented for adding thrust rather than for producing a couple, are used to add the small velocity increments needed for orbital correction (Sections 2.1.6 and 2.2.6).

Fine attitude control during low-altitude coasting and ascent coasting is achieved by again using the inertial platform to control a second set of gas jets, each jet producing only 0.005 or 0.01 pound of thrust and when paired producing torque couples of 0.025 or 0.05 foot pound. The same fine jet system is used to accurately establish attitude and reduce angular rates after the 24-hour orbit has been attained.

In the 24-hour orbit a 10-pound flywheel with its axis perpendicular to the plane of the orbit "pins" the vehicle, stabilizing it against rotations in roll and yaw.* The angular rate of the large wheel is held constant by means of an accurate electronic (for example, crystal controlled) clock. Although weak pitch stability might result from the combined effects of gravity and centrifugal force tending to align the long axis of the vehicle along the vertical, at the altitude of the 24-hour orbit this pitch stability is so weak that even a very small torque such

* To represent change in the angle between the long axis and the local vertical measured in the plane of the orbit. Roll represents rotation about the nominal velocity (horizontal). Yaw is rotation about the vertical.

as might result from a meteor impact or from a slight misalignment of the large flywheel would upset the balance. Consequently, a small variable speed wheel with axis perpendicular to the plane of the motion (parallel) to the axis of the large flywheel) is used to "absorb" small pitch angular momenta. If a number of meteors should have a cumulative effect causing the small wheel to exceed its design speed, then its motion can be stopped as the pitch gas jets are used to hold attitude; this would leave the pitch wheel free to absorb future disturbances in pitch. If the assumptions of Appendix F, Volume IV, on meteor frequency as a function of size are verified by future explorations in space, then it is quite likely that the small pitch wheel alone will be able to compensate for meteor impact and the fine gas jets need be used only during the orbital correction period (24 to 48 hours) when relatively large accidental torques may result from imbalance of the coarse jets used for producing the orbital corrections.

The purpose of attitude control for the communications satellite is to insure that the communications antennas remain pointed at the ground stations. For the "stationary" equatorial satellite two small monopulse receiving antennas with a relatively broad receiving pattern can be used as "finders" for the relatively narrow beam communications antennas. Error signals derived from the monopulse antenna system can be used to control the fine gas jet system and the pitch wheel. For the polar satellite it is only necessary to keep one 16-degree antenna pointed at the earth; there is no requirement for yaw control. Pitch and roll measurements of the polar satellite can be made by an infrared horizon scanner; these measurements are used to control the fine gas jet system and the variable speed pitch wheel. The attitude error signals from either the monopulse system (equatorial) or the horizon scanner (polar) are processed in analogue circuits (the vernier attitude control computer) to derive control signals.

3.2 ATTITUDE CONTROL PRIOR TO ATTAINING THE 24-HOUR ORBIT

3.2.1 Requirements

Attitude control of the booster and first added stage during the climb to the low-altitude orbit is similar to that for an ICBM and will not be treated here.*

---

*Attitude control during Hohmann accelerations will be regulated either by using two engines or by using the coarse gas jets. If the latter is used, a small additional amount of gas will have to be supplied.

This discussion is limited to the control of the final stage vehicle during coast periods.

The attitude-control system during the low-altitude coasting phase is required to:

(1) Prevent the gyro-stabilized inertial platform from going into gimbal lock, and

(2) Orient the vehicle so that the vehicle is aligned approximately in the direction of perigee thrusting.

There is no need to align the vehicle so as to direct the beacon transponder antenna toward the ground since radio tracking will not commence until the ascent coasting phase. Moreover, since it is recommended in Chapter 1, Volume IV, that solar surfaces not be deployed until the 24-hour orbit is reached, solar surfaces will not affect attitude requirement prior to establishing the 24-hour orbit.

The vehicle pitch altitude during the low-altitude coast is shown in Figure 3-1. Figures 3-1a and 3-1b show the low-altitude coast of equatorial satellites launched from Cape Canaveral. These figures show that approximately a 90-degree attitude reorientation is necessary to correctly align the vehicle for perigee burning* whether perigee burning takes place on a southerly or northerly crossing of the equator. Figure 3-1c shows that less than 20 degrees of attitude reorientation is required when a polar satellite is launched to the south from Cooke Air Force Base and enters perigee burning at 14.86°N (see Chapter 1, Section 1.4).

During ascent coasting, the attitude control system is required to

(1) Prevent the gyro-stabilized inertial platform from going into gimbal lock,

(2) Orient the vehicle so that the beacon transponder's antenna pattern illuminates the ground tracker during the final hours of ascent,

(3) Finally, orient the vehicle approximately in the direction of apogee thrusting.

---

*A net velocity impulse of 85 ft/sec (see Chapter 1, Figure 1-6) may be saved by reducing the inclination of the orbital plane by 2.2 degrees at perigee burning. This requires orienting the vehicle about 9 degrees out of its orbital plane (toward the equatorial plane).

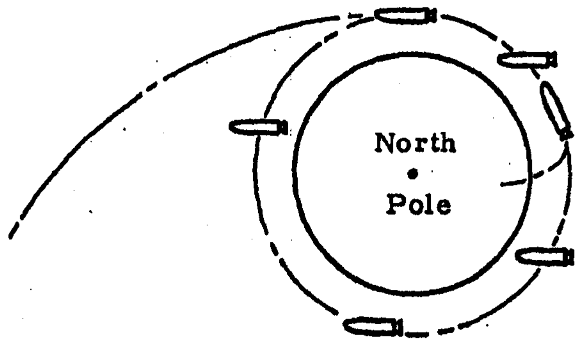

Figure 3-1a. Eastward Launch from Cape Canaveral Perigee Burning on Southerly Crossing of Equator.

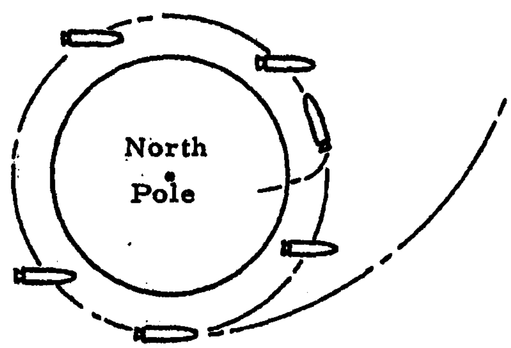

Figure 3-1b. Eastward Launch from Cape Canaveral Perigee Burning on Northerly Crossing of Equator.

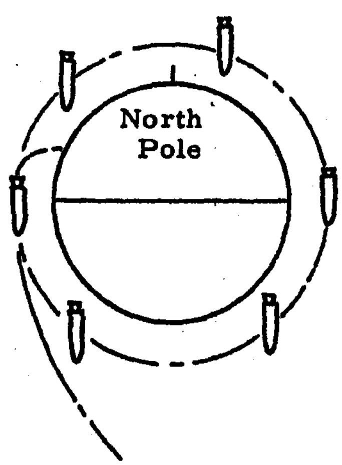

Figure 3-1c. Northward Launch from Cooke Air Force Base (34-3/4°N) Perigee Burning at 14-3/4°N.

CONFIDENTIAL

As seen in Figure 3-2, in which it is assumed that perigee burning takes place on a southward crossing of the equator, the vehicle is oriented at perigee parallel to the orbital plane, some 28.5 degrees from the equatorial plane. (If the inclination of the orbital plane is reduced by 2.2 degrees at perigee burning to save a net of 85 feet per second (see Chapter 1, Figure 1-6), then the vehicle attitude during perigee burning is about 9 degrees closer to the equatorial plane.) During apogee burning the thrust must have a southward component to arrest the northward motion; the vehicle attitude must be about 24.5 degrees from the equatorial plane (somewhat less if the plane has been oriented by 2.2 degrees). Altogether a reorientation of 127° (180°-28.5°-24.5° = 127°) is required. The figure shows this reorientation taking place just after perigee burning, but clearly it could take place any time during ascent coasting, so far as meeting the requirement for apogee burning is concerned.

Since the satellite must be tracked during the first 24 or 48 hours after the 24-hour orbit is reached and since the nose must point toward the earth during this time (to direct the communications antennas and monopulse attitude toward the ground stations), the transponder beacon must also have an antenna which is directed toward the earth from the nose. As seen from Figure 3-2, if the reorientation were to take place as shown, the nose would be pointed generally toward the south and nearly parallel to the surface of the earth during the last hours of ascent. Consequently, if the satellite is to be tracked during the final hours of ascent coasting, either the transponder antenna must rotate with respect to the vehicle frame, or the transponder must have a second antenna on the side of the vehicle, or the vehicle must be reoriented twice.

If the last alternative is chosen, then as shown in Figure 3-3, the first reorientation through an angle somewhat more than 90 degrees must take place after perigee burning. This would direct the single transponder antenna toward the ground during the last two or three hours of coasting. The precise orientation should be chosen so as to maximize the tracking time from a given tracking station. Just before (possibly one minute or so) the satellite arrives at the correct longitude (for equatorial satellites) or latitude (for polar satellites) the apogee burning commands are transmitted to the satellite via the data link and decoder, which are part of the transponder beacon equipment. This command would actuate the final reorientation through a little

[redacted]

~~CONFIDENTIAL~~

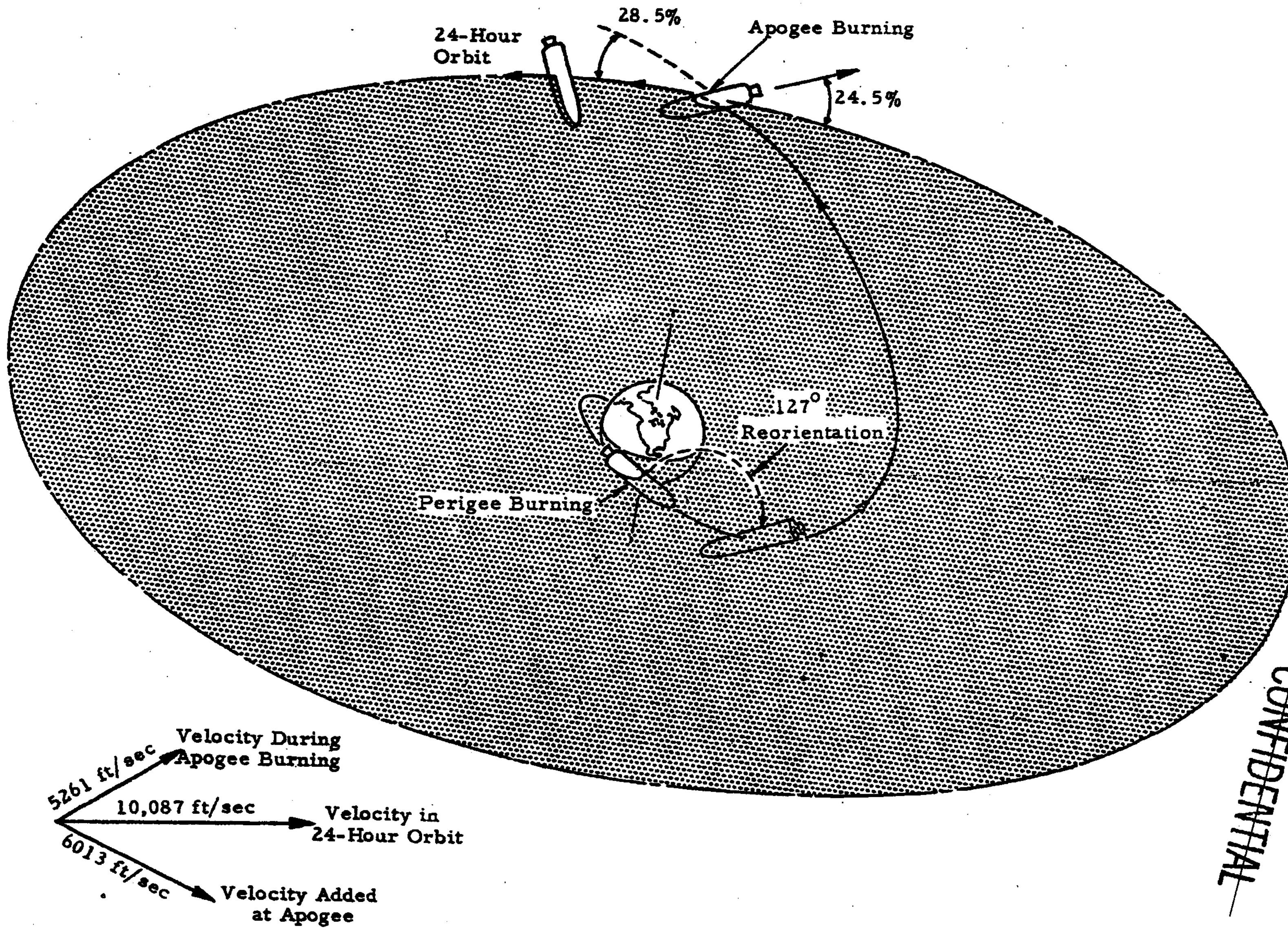

Figure 3-2. Flight Path and Attitude of Vehicle During Ascent Coasting, and Apogee Burning Conditions (Perigee Burning on Southerly Corssing of the Equator).

[redacted]

~~CONFIDENTIAL~~

CONFIDENTIAL

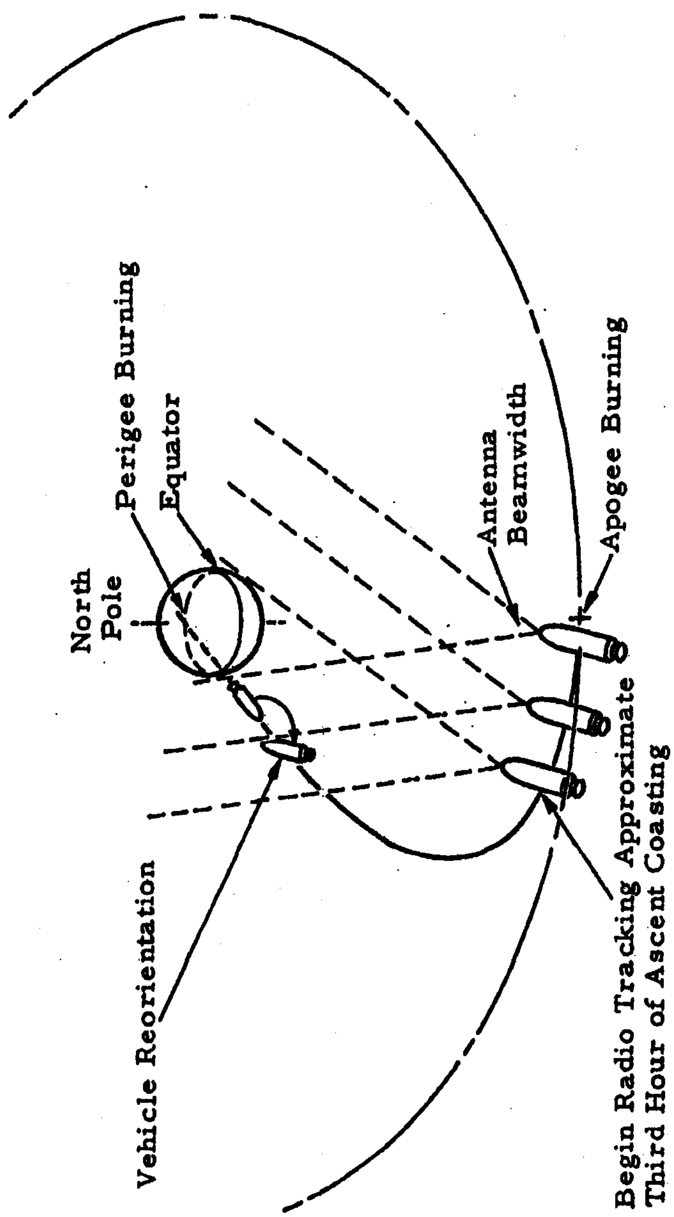

Figure 3-3. Orientation of Vehicle and Airborne Antenna Beamwidth for Radio Tracking During Ascent Coasting.

CONFIDENTIAL

[redacted]

CONFIDENTIAL

less than 90 degrees aligning the vehicle along the direction of thrust required for apogee burning. Then at a certain fixed interval after the instant in which the command was transmitted, apogee burning is initiated. If a rotatable antenna or multiple antennas are used, only a single reorientation is required during ascent coasting. Moreover, there need be no delay to act upon the command to initiate apogee burning.

After apogee burning a final reorientation through 90 degrees is required to align the vehicle along the vertical. What then becomes yaw, i.e., rotation about the long axis, must then be adjusted to point the antennas at the appropriate ground stations.

Although the attitude must be controlled during low-altitude and ascent coasting, there is no need to hold the programmed attitude with high precision. Certainly, avoiding gimbal lock imposes no precise attitude control, and providing transponder beacon coverage imposes an accuracy requirement of only a small fraction of the antenna beamwidth. Assuming an antenna beamwidth of 20 or 30 degrees, a reasonable attitude tolerance would be 2 or 3 degrees. Obviously, the orientation of the vehicle at perigee and apogee burning requires greater accuracy than avoiding gimbal lock and providing antenna coverage, but even for this case extreme accuracy is not necessary since residual angular errors can be corrected by the servoloop controlling the direction of thrust of the engines during the burnings.

However, at the end of each burning period (or weight jettisoning), the attitude control system must first arrest residual accidental angular rates imparted to the vehicle before carrying out any programmed reorientation. The servoloop used to steer the rocket engines during burning periods has an appreciable time lag. As a consequence, when the thrust of the rocket engine is terminated, a small random, residual angular momentum is imparted to the vehicle.

Based on the estimated characteristics of the rocket engine and the associated servocontrol loops in the final stage vehicle, it is estimated that the residual angular rate imparted to the vehicle at rocket engine cutoff will not exceed a value of 3 degrees per second.

CONFIDENTIAL

3.2.2 Mechanization

Figure 3-4 is a schematic of the "coarse" gas jets which can be used to control attitude and to make orbital corrections. Although a number of configurations are possible, the one which is illustrated is a simple configuration requiring only four gas jets, each of which has single axes of rotation. In this configuration, no jets are required at the nose or tail of the vehicle and thereby interference with antennas or the main engine (or engines) is avoided.

The top three sketches in Figure 3-4 show the jets oriented for producing a net thrust (but, in principle, no net torque) as required for adding a velocity increment during the orbital correction phase. It will be noted that, whereas only the top and bottom nozzles can be used for producing east-west thrusting and only the side nozzles for producing north-south thrusting, either or both pairs of nozzles may be used for radial thrust. If the required thrust direction is midway between radial and east-west, then by rotating the top and bottom nozzles to an intermediate angle they can be made to produce the required thrust in one operation. This saves gas when compared with a fixed jet system which would require thrusting by two sets of jets, one in the radial direction and the other in the east-west direction. Similarly, if the required thrust is midway between radial and north-south it can be produced by side jets at an intermediate angle. However, if the required thrust has both an east-west and a north-south component then both jets must be used.

During the orbital correction phase a Thor-boosted vehicle weighs about 900 pounds and a Titan- or Atlas-boosted vehicle weighs about 1900 pounds (see Volume IV, Section 2.4). A 10-pound thrust (five from each jet) for a Thor-boosted vehicle or a 20-pound thrust for a Titan- or Atlas-boosted vehicle will give accelerations of about 0.01 g's. With such an acceleration, accelerometers currently under development can measure the velocity increments (totaling approximately 100 feet per second) to about 0.1 foot per second. Moreover, assuming the gas jets can be cut off in 0.05 seconds, the velocity cutoff error is only 0.016 foot per second.

Assuming the gas jets have an exit velocity of 2000 feet per second (corresponding to a vacuum specific impulse of 62 pounds-second per pound)

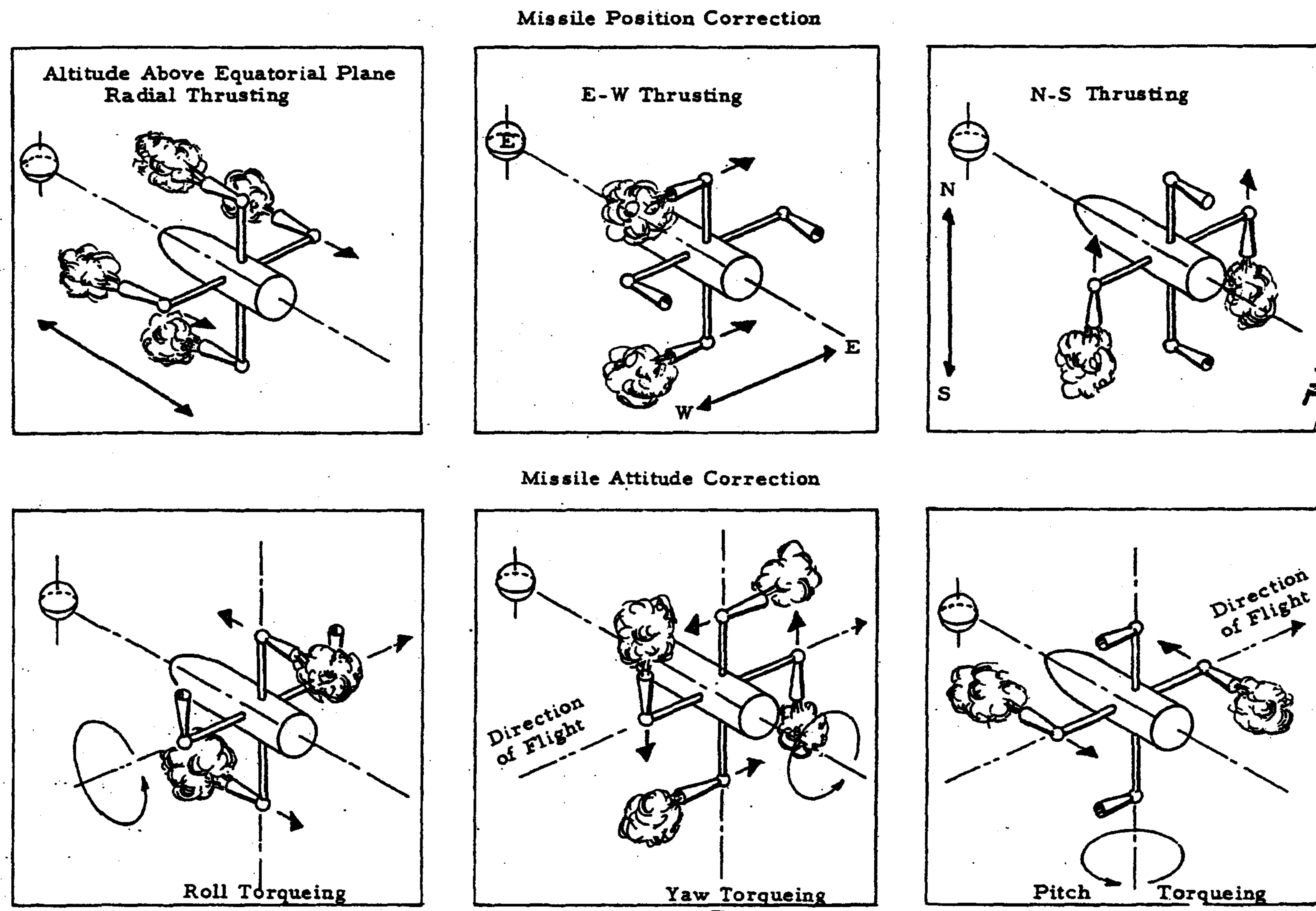

Figure 3-4. Coarse Gas Jet System.

and that the sum of the velocity component increments is 100 feet per second, the mass of gas expended in orbital corrections must be 5 per cent of the vehicle mass, i.e., about 45 pounds for the Thor-boosted vehicle and about 95 pounds for the Titan- or Atlas-boosted vehicle.

The bottom three sketches in Figure 3-4 show the same "coarse" gas jets when oriented to produce torque. The vehicle is shown in the orientation it would have in the 24-hour orbit. Again by exploiting the single axis of rotation of the jets, torques about axes intermediate between the yaw axis (yaw in the 24-hour orbit) and either the roll or pitch axis can be achieved in a single operation using only one pair of jets. However, combinations of roll and pitch require the use of both pairs of jets.

Because the diameter of the vehicle is about 4 feet (see Volume IV, Section 2.4) it may be assumed that the jets are each about 2-1/2 feet from the center line of the vehicle. Thus a pair of jets on the Thor-boosted vehicle would produce about 25 foot pounds of torque (2 jets x 2-1/2 feet x 5 pounds) or about 50 foot pounds (2 jets x 2-1/2 feet x 10 pounds) on the Titan- or Atlas-boosted vehicle.

At the time of this writing the final stage vehicle layout is not sufficiently solidified to compute exact values for the moments of inertia, but even very approximate values will suffice to illustrate the general behavior of the vehicle when acted upon by the torques of the gas jet system. Table 3-1 gives illustrative numbers for a nominal 90 degree rotation about an axis perpendicular to the long axis of the final stage of a Thor-boosted vehicle. The rotational characteristics are shown for the vehicle in the low-altitude orbit when it is completely loaded with fuel, in ascent coasting when the fuel is partly used up, and in the 24-hour orbit with only payload and structure. The assumed scheme of reorientation is to use the gas jets until an angular rate of 4 degrees per second is attained, then "coast" in rotation angle and finally apply the opposite torque impulse to arrest the angular rate. It will be noted that the total rotation time (including angular acceleration, coast and deceleration) is in all cases less than a half minute and is only slightly dependent on the assumed value for the moment of inertia.

[redacted]

CONFIDENTIAL

Table 3-1. Estimated Characteristics of Final Stage of Thor-Boosted Vehicle Rotating Through Nominal 90°.

Trajectory Phase	Moment of Inertia* (slug ft^2)	Angular Acceleration** (deg/sec^2)	Time to Gain or Lose 4 deg/sec (sec)	Angular Coast (deg)	Total Time of Rotation * (sec)	Residual Angular Rate*** (deg/sec)
Low-Altitude Coasting	1600	0.9	4.4	72.4	26.9	0.045
Ascent Coasting	800	1.8	2.2	81.6	24.8	0.09
In 24-Hour Orbit	500	2.9	1.4	84.4	23.9	0.145

*About axis perpendicular to center line of vehicle
**Assuming 25 foot pounds of torque
***Assuming 0.05 second require to cut off jets

[redacted] CONFIDENTIAL

Although the table applies to a Thor-boosted vehicle, the values for angles, times, angular rates and angular accelerations would be very similar for the final stage of a Titan- or Atlas-boosted vehicle since both the moments of inertia and the torques would be approximately doubled.

The total weight of gas used in reorientations may be estimated from the angular acceleration (and deceleration) times given in Table 3-1. During the low-altitude coast the reorientation to align the vehicle for perigee burning requires about 8.8 seconds of torqueing (4.4 for angular acceleration and 4.4 for deceleration). Assuming that two approximately 90-degree reorientations are required during ascent coasting (one to direct the transponder beacon antenna toward the ground and the second to align the vehicle for apogee burning), an additional 8.8 seconds of torqueing is required. To align the long axis of the vehicle along the vertical just after apogee burning requires another 2.8 seconds of torqueing. Altogether some 20.4 seconds of torqueing are required.

In the above computation we have neglected the initial torqueing time required to arrest the accidental angular rates imparted to the vehicle at the end of each burning period. As stated at the end of Section 3.2.1, these rates will not exceed 3 degrees per second. Consequently, arresting this angular rate can increase the torqueing period by 3.3 seconds during the low-altitude coast, 1.7 seconds during ascent coasting, and 1.0 seconds after reaching the 24-hour orbit. (The change in angle during these periods will have only a slight effect on the total time to perform the subsequent programmed reorientations.) When these additional 6.0 seconds are added to the 20.4 seconds required for the programmed turns, the total torqueing time is 26.4 seconds.

Since 5 pounds of thrust has been assumed for each nozzle and assuming that only two nozzles are used in the rotation, the total impulse is 264 pound seconds. This requires about 4.3 pounds of gas according to our prior assumption that the specific impulse of the gas jet system is 62 seconds. When the axis of rotation is such that the four nozzles must be used equally, then this figure must be increased bg$\sqrt{2}$, i.e., about 6.0 pounds of gas are required.

On the assumption that the gas jets can be cut off accurately to within 0.05 second, the last column of Table 3-1 gives the residual angular rates.

It is not difficult to measure angular rates more accurately than the numbers listed, either by using rate gyros (e.g. those in the perigee-apogee autopilot) or by appropriately differentiating and smoothing the gimbal angles of the inertial platform.

The most severe requirement for long-term attitude control occurs during the last 2 or 3 hours of ascent, because the transponder's antenna coverage requires holding attitude to 2 or 3 degrees. The residual angular rate of 0.09 degree per second would result in the attitude changing by 3 degrees in only 33 seconds. Consequently, unless throttling is used, a short impulsive torque would be required every half minute to keep the attitude within bounds Assuming that each impulse lasts 0.1 second which is just adequate to reverse the angular rate, the four jets would expend about 8 pounds of gas over the 3-hour period.

However, an alternative is to employ the fine gas jet system which is necessary in any event to meet the very strict attitude control requirements of the 24-hour orbit. The fine gas jets can take on a similar configuration to that shown for the coarse gas jets in Figure 3-4, i.e., there can be four jets each free to rotate about a single axis of rotation. An alternative configuration would use 12 fixed jets mounted in approximately the same positions as the jets of Figure 3-4, consisting of six pairs, one pair for positive pitch, one for negative pitch, etc. The fine gas jets would each produce only one thousandth the thrust of the coarse jets, i.e., each would produce 0.005 pound of thrust for the Thor-boosted vehicle, or 0.010 pound for a Titan- or Atlas-boosted vehicle. The corresponding torques would be 0.025 foot pound, or 0.050 foot pound.

The fine gas jets would be controlled by the steering and shutoff digital computer, operating on gimbal angle measurements from the gimbal angle resolves of the inertial platform. Each gimbal angle will provide information for controlling a single torque component.

Table 3-2 summarizes the characteristics of the fine gas jet system in arresting the residual angular rates left by the cutoff error in the coarse gas jet system. Fifty seconds are required to arrest these residual rates. During the arresting period an angular change of up to 3.6 degrees (after the

[redacted]

CONFIDENTIAL

Table 3-2. Characteristics of Fine Gas Jet System in Correcting Angular Rates of the Final Stage of a Thor-Boosted Vehicle.

Trajectory Phase	Moment of Inertia* (slug ft^2)	Angular Acceleration** (deg/sec^2)	Time to Arrest Residual Angular Rate of Coarse Gas Jet System (seconds)	Angular Error at End of Arresting Period (degrees)
Low-Altitude Coasting	1600	0.0009	50	1.125
Ascent Coasting	800	0.0018	50	2.25
In 24-Hour Orbit	500	0.0029	50	3.625

*About axis perpendicular to center line of vehicle
**Assuming 0.025 foot pound of torque

CONFIDENTIAL

[redacted]

reorientation in the 24-hour orbit) can occur. As the residual rate is reduced it can be measured by sequential observations of the gimbal angles of the gyro-stabilized platform (monopulse measurements may be used instead of gimbal angles in the 24-hour orbit, see Section 3.3). The slope of the resolver error in measuring these angles is likely to be the limiting factor affecting angular rate accuracy. Constant errors will not affect rate measurements. Assuming uncorrelated resolver errors as high as 0.05 degree, and assuming that an average angular rate is measured by noting the change in angle each 20 seconds, one should be able to determine the average angular rate over the past 20 seconds to 0.0035 degree per second. This average rate is in effect the angular rate which existed some 10 seconds (the delay due to smoothing) earlier. To find the current angular rate it is necessary to add on the change which has occurred during the last 10 seconds. This can be estimated by knowing the calibrated torque of the fine gas jets. For the case of stabilizing after the satellite is in the 24-hour orbit, the angular acceleration (see Table 3-2) will be about 0.003 degree per second^2. In 10 seconds this will change the angular rate by about 0.03 degree per second. Assuming that the calibration is good to 10 per cent, the change in angular rate can be predicted to about 0.003 degree per second. The rms current angular rate error due to the combination of resolver error and jet calibration error is about 0.005 degree per second. Fine gas jet cutoff errors are negligible when compared to this figure.

When the residual rate, as measured by the above method, is cancelled out an additional 10 seconds of torqueing is applied to give a nominal angular rate of 0.03 degree per second (for the case of the 24-hour orbit) in the direction to cancel the angular error which has accrued. About two minutes of angular coasting are then required to correct out the angular error of 3.6 degrees (see Table 3-2). During this angular coast period the constant angular rate can be measured to about 0.0006 degree per second (again assuming resolver errors of 0.05 degree). Consequently, as the correct attitude is established, the required change in angular velocity is known more accurately than it can be controlled at this time. In braking the approximately 0.03 degree per second angular rate, the calibration error of 10 per cent will lead to the limiting rate error of 0.003 degree per second. In 250 seconds more an angular error of

[redacted] CONFIDENTIAL

0.75 degree may have developed, but the angular rate can be measured to 0.0003 degree per second and with a similar error introduced by jet calibration, the new angular rate can be controlled to about 0.0005 degree per second. To correct this angular position an angular rate of about 0.0010 degree per second (controlled to 0.0005 degree per second) can be used to eliminate the angular error in 750 seconds. This constant angular rate can be measured to about 0.0001 degree per second and the 10 per cent calibration error in braking the 0.0010 degree per second is also about 0.0001 degree per second. However, assuming a jet cutoff uncertainty of 0.05 second, the cutoff error would be 0.00015 and is already the dominant error. The total angular rate error would have an rms value of 0.0002 degree per second or about 0.7 degree per hour.

The above detailed analysis for the satellite in the 24-hour orbit shows that attitude can be established to within 0.05 degree of the correct angle as read from the stable platform (which can have drifted 0.3 degree by this time) and with a null angular rate to within about 0.7 degree per hour in a matter of at most 20 minutes -- 30 seconds of coarse jet reorientation, 50 seconds for five jets to kill coarse jet residual rate, 120 seconds to eliminate accrued angular error due to coarse jet residual rate, 250 seconds drift away to measure angular rate, 750 seconds to return and measure angular rate with accuracy better than fine jet cutoff error.

Of course, these numbers are only meant to illustrate the rapid convergence of the attitude control procedure, even when conservative assumptions are made concerning angular measurements, jet calibration, and jet cutoff uncertainty. The 24-hour orbit stabilization problem was chosen for the above numerical example because the angles and angular rates to be corrected by the fine gas jet system were greater than those encountered during low-altitude coasting or during ascent coasting. Since the angular accelerations during ascent coasting are only 60 per cent of those of the vehicle when in the 24-hour orbit, the cutoff errors will be somewhat less and after no more than 20 minutes of attitude stabilization the vehicle will probably drift less than 1.5 degrees during the 3 hours or so in which the transponder must illuminate the ground tracker. Therefore, no further attitude corrections are needed.

[redacted] CONFIDENTIAL

[redacted]

CONFIDENTIAL

The total duration of fine gas jet torqueing for a typical reorientation will not exceed 100 seconds. With two jets each having a thrust of 0.005 pound, this only requires 1 pound second of impulse. Assuming this impulse is required for each of the three axes of rotation and multiplying by four, the total number of 12 pound seconds is required for the five gas jet system. Only 0.2 pound of gas are thus consumed.

Figure 3-5 illustrates a possible arrangement for generating gas for both the coarse and fine jet systems. A liquid monopropellant is stored in a flexible sack which is sealed to the outlet of the tank. Since the sack is kept under a constant pressure from a high-pressure gas storage tank, only the liquid in the sack (and not the pressurizing gas) can escape from the tank, even in free fall. In decomposition chambers, the monopropellant is catalytically decomposed into its gaseous components and stored in gas storage tanks. The monopropellant will be fed to the decomposition chamber only when the computer commands that pressure be maintained and the sensors on the gas storage tanks also indicate that the pressure is low.

3.3 ATTITUDE CONTROL IN 24-HOUR ORBIT

3.3.1 Requirements

Attitude control requirements, once the vehicle is in the 24-hour orbit, are set by the beamwidth of the airborne antenna. Of course, this assumes the vehicle is in the correct orbit. If the eccentricity of the orbit is such that the difference between perigee and apogee is as large as 250 miles, and if the attitude of the vehicle remains constant, maximum cyclical loss of coverage on the ground at the equator would be about 220 miles, and the loss would be, of course, substantially larger at higher latitudes where, in fact, the actual coverage is. Moreover, to attempt to continually compensate for the change in speed of the vehicle during its elliptical orbit by a constant change of attitude in the pitch plane would add considerably to complexity and increase the power required. Again, if the orbit of the vehicle is inclined to the nominal 24-hour orbit in the equatorial plane by, say, 250 miles, the change in north-south coverage would be 250 miles. In addition, constantly changing attitude

CONFIDENTIAL

[redacted]

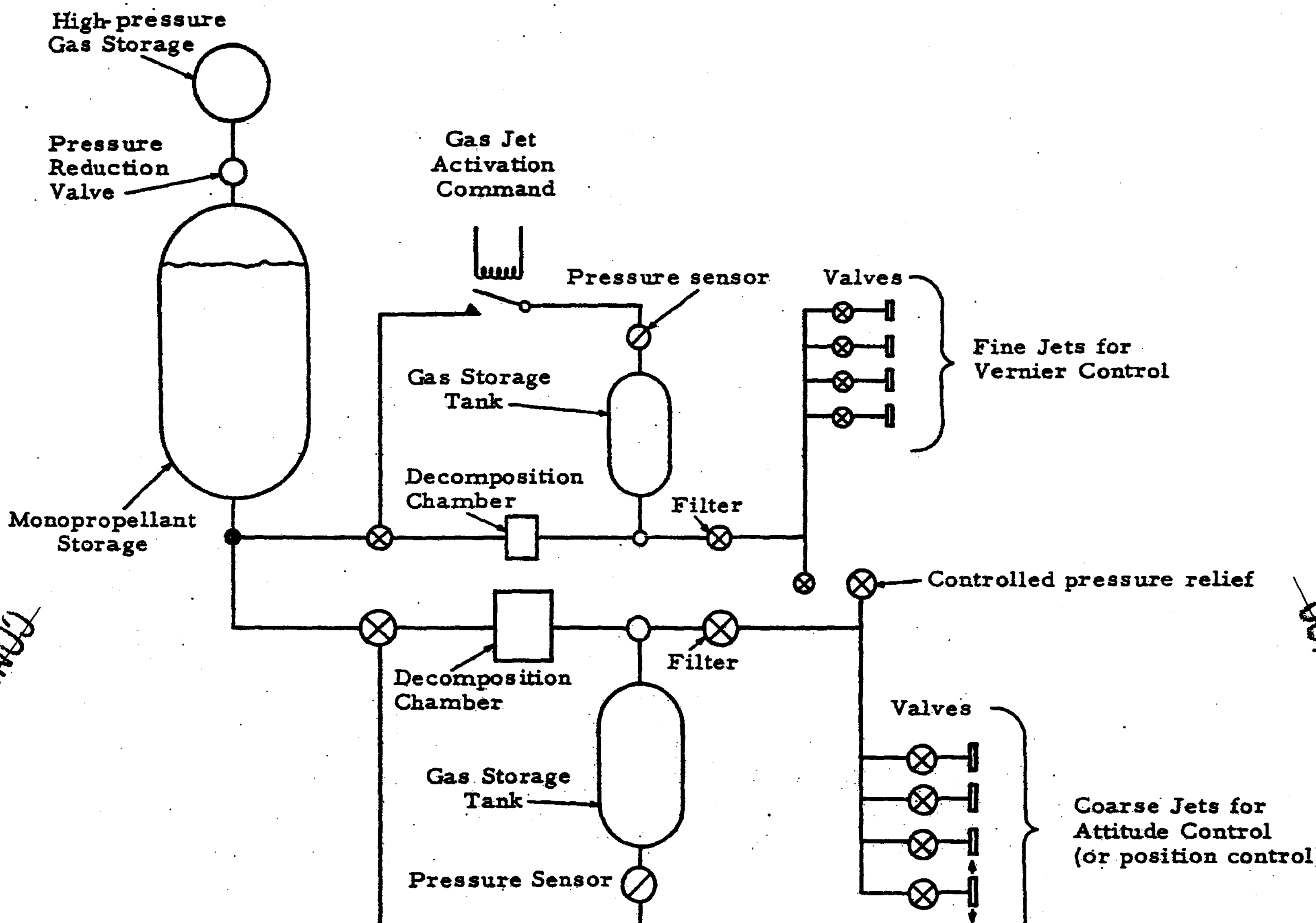

Note:
1. All valves have electric control
2. Jets rotate about one axis

Figure 3-5. Gas Jet System for Attitude Control and Velocity Correction in 24-Hour Orbit.

to compensate for this out-of-plane error would not only make for additional complexity, etc, but it would also require that the stabilizing force of the large flywheel would be constatnly overcome. Therefore, it is important that the final 24-hour orbit be established as accurately as possible.

As has been shown in Chapter 2, Section 2.6 it is possible to reduce both eccentricity to 10^{-3} and inclination to about 0.1 of a degree, which would give a daily change in coverage in north-south and east-west directions of about 50 miles. Such a loss is quite small and can be easily compensated for by adjusting the airborne beamwidth to fit the location of the particular ground stations covered by a given antenna.

The attitude should be established initially so accurately that the only possible change will be in the pitch plane, which is necessary since the vehicle must rotate in the pitch plane one revolution per day. If attitude deviation angles in roll and yaw are less than 2×10^{-3} and the angular rates less than 10^{-4} radians per second which the large flywheel must provide, no further corrections in roll and yaw will be required.

3.3.2 Stabilizing Machinery

The discussion in Sections 3.1 and 3.2 of this chapter show that the fine gas jet system using the platform as a reference and the steering and cutoff digital computer can supply the appropriate torques to achieve the required stability.

The system used to provide a reference for maintaining attitude control in the 24-hour orbit is illustrated in Figure 3-6. The analytic study, Appendix C, of rigid body motion of a vehicle at 22,000 miles above the surface of the earth shows that it is desirable to accomplish the attitude control in two periods. In the first period, immediately following apogee burnout and after the vehicle has been turned to the generally correct attitude from information given by the platform, the nonlinear terms in the equation of motion are quite important because of the initial conditions assumed, that is, an angular error (θ) of 2 degrees and an angular rate error $(\dot{\theta})$ of 5×10^{-2} radians per second, which are those estimated for ICBM nose cones. Fine gas jets can reduce the angular error to one milliradian and the angular rate error to 10^{-5} radian per second within minutes.

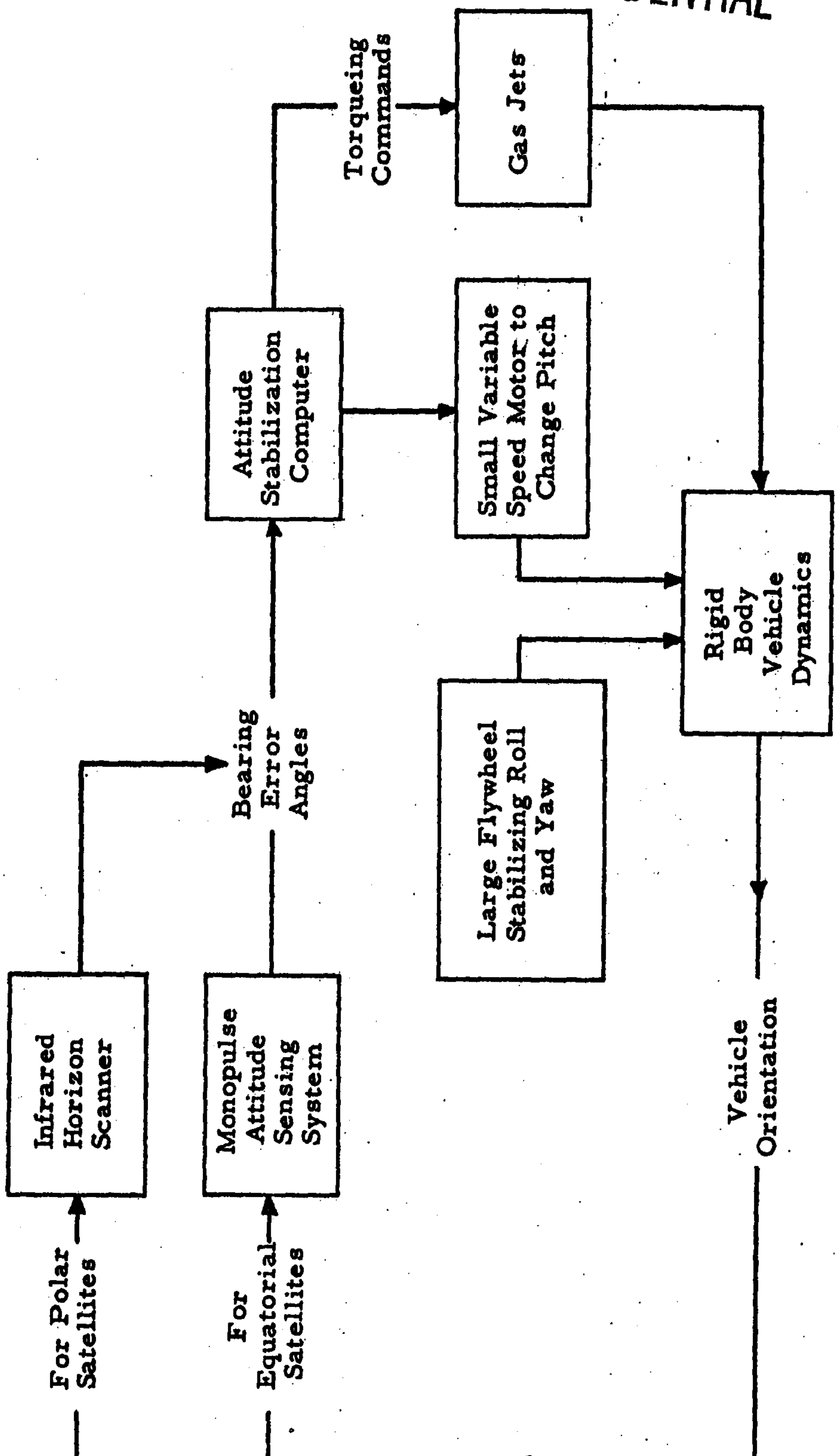

Figure 3-6. Guidance Scheme Proposed for Vernier Attitude Control.

When the gas jets are turned off, the yaw and roll motions will remain small ($\theta < 6$ mils and $\dot{\theta} \sim 10^{-4}$ radians per second) if an internal angular momentum of 80 slug feet^2 radians per second, fixed relative to the body, is oriented along the pitch axis. But as shown in Appendix C, components of angular momentum along other axes produce constant driving forces which tend to disturb yaw and roll stabilization. Therefore, it is normal to the orbital plane, since this supplies both yaw and roll stabilization. Pitch motion about the reference vertical is not stabilized and intermittent pitch control is required for the life of the vehicle. Since only very small forces are required for this long-term correction, a small variable speed motor rotating in the pitch plane can supply all the necessary correcting torques in pitch. However, if the yaw and roll rates could be reduced below 10^{-5} radians per second and the pitch motion error to 10^{-7} radians per second, the very weak torque exercised by the gravitational gradient about the pitch axis may be exploited. In this event, no control forces will be needed thereafter. However, it appears that errors in the alignment of the large flywheel or external forces such as meteorites will make this impossible, and additional forces can be supplied by the fine gas jets and the small flywheel.

3.3.2.1 Radio Monopulse Attitude-Sensing System for Equatorial Satellites

Once the vehicle is stabilized using the platform and fine gas jets with respect to a fixed set of points on the earth, it is proposed that the vehicle attitude be maintained using a radio direction-finding technique as a reference. Two ground transmitters will be observed by monopulse receivers in the vehicle and thereby determine the angle between the antenna axes and the line-of-sight to the transmitter. These error signals are transformed in the attitude stabilization computer to give true vehicle orientation about each of its three axes - roll, pitch, and yaw. The ground stations would be located as far apart as possible, since the yaw measurement (about the reference vertical) is quite sensitive to the projection difference angle. These ground stations could readily be combined with the communication transmitters. The airborne antennas would be fixed on the vehicle such that they would find the communication ground transmitters (see Figures 3-7 and 3-8) after reorientation in the final orbit.

[redacted]

CONFIDENTIAL

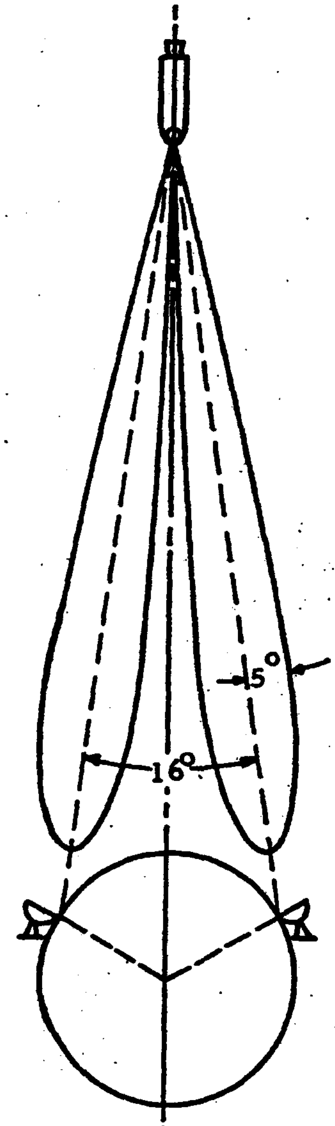

Figure 3-7. Orientation of Fixed Monopulse Attitude Receiving Beams.

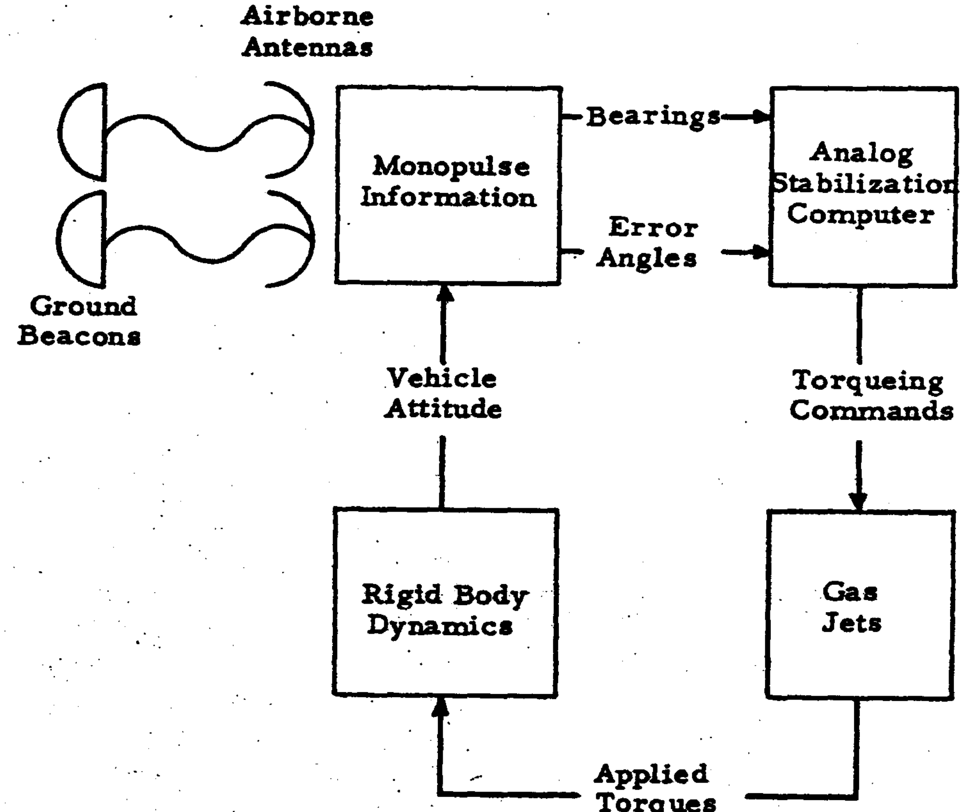

Figure 3-8. Block Diagram of Monopulse Attitude Control System.

CONFIDENTIAL

[redacted]

The rigid-body equations of motion for the vehicle are given in Appendix C, Equation 10. It is necessary to supply both a restoring and damping term for each angle. It is proposed that the restoring term be computed from the (resolved) angle measurements of the monopulse channels directly. The angular rate terms for damping could be obtained by differentiating the angular measurements.

A block diagram of the attitude-sensing arrangement for an antenna in one plane is shown in Figure 3-9. The signal at the point e is proportional to the error in tracking in one plane. The control system in one plane can be represented approximately as:

$$I \ddot{\epsilon} = \text{torque} = -g_1 \epsilon - \rho \dot{\epsilon} , \qquad (3.1)$$

where I is the moment of inertia of the satellite body, g_1 is a gain factor, and ρ is the magnitude of the damping term. ϵ is the angular position of the tracking antenna, taking zero as the direction to the ground station. The rate term is necessary for stability against noise-induced drifts. (See Figure 3-10.) The slope of the error output as a function of tracking error can be written as S/B, where S is the amplitude of the signal in the sum channel at the entrance to the phase detector and B is the beamwidth of the attitude-control antenna. Equation (2. 20) then becomes

$$I \ddot{\epsilon} + \rho \dot{\epsilon} + g_1 \frac{S}{B} \epsilon = -g_1 n ,$$

where n is the noise term at the output of the phase detector.

Propagation irregularities in the troposphere impose a wrinkling effect on the wavefront received at the vehicle. This produces a zero baseline tracking error of only 0.1 milliradian, according to the Maui propagation experiments, and shot noise in the receiver is probably the limitation on a system which seeks only 1 mil accuracy. There is no stiction noise in the antenna, since the antennas themselves do not track. On the assumption that the signal-to-noise ratio in the sum channel is high, the noise has a power spectral density of $2k\,T\,F\,(S^2/S_i^{\,2})$, where k is Boltzmann's constant, T is temperature in degrees Kelvin, F is the receiver noise figure, and S_i is the input signal amplitude in the sum channel. The factor 2 accounts for

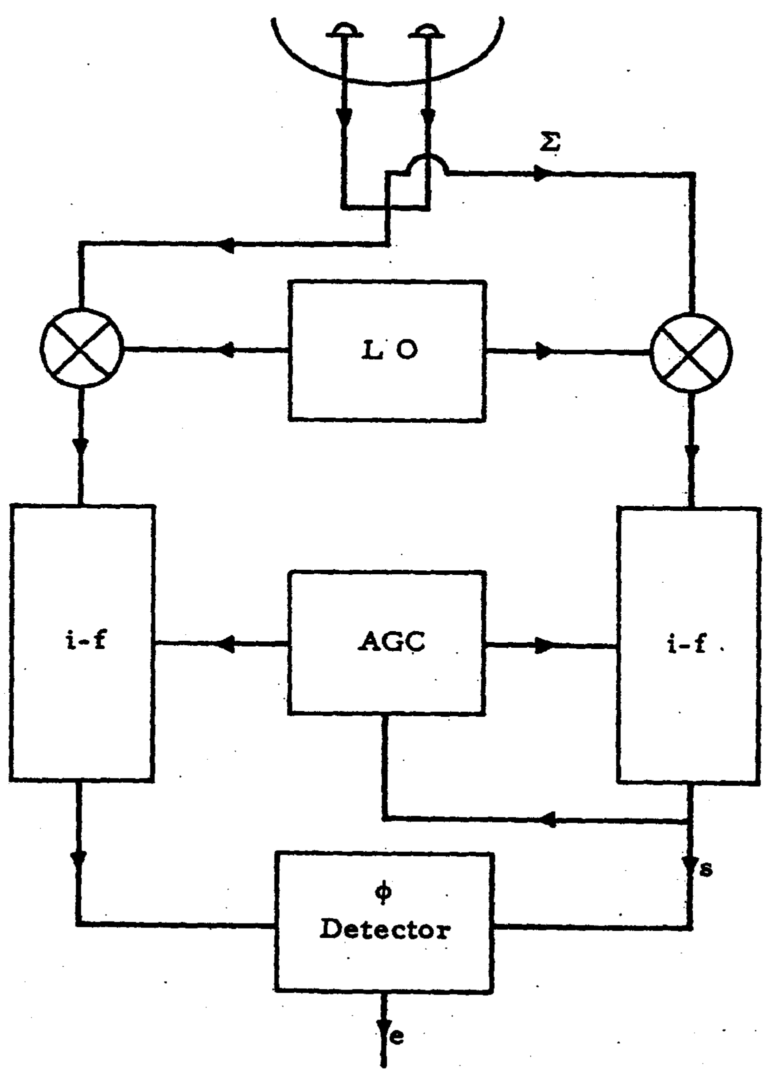

Figure 3-9. Block Diagram of One-Channel Monopulse System.

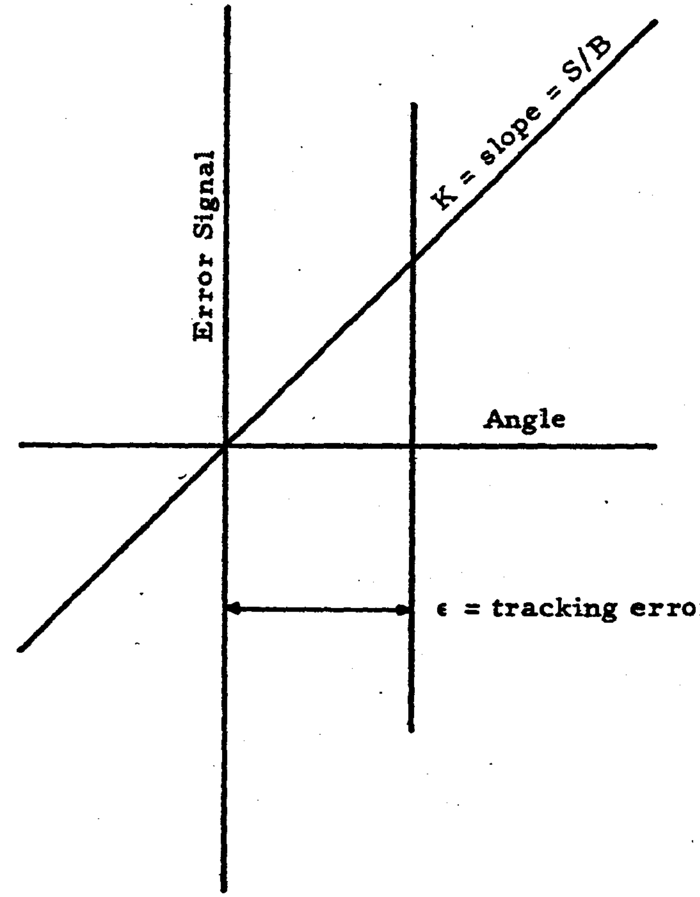

Figure 3-10. Error Characteristic of Monopulse Tracker.

the frequency folding effect of the phase detector in translating the signal at the IF frequency to zero frequency, and the term S^2/S_i^2 gives the effect of the average gain control.

Now, if one assumes that the servosystem is critically damped and writes β for its bandwidth, the mean-square error due to noise perturbation can be written approximately as

$$\overline{\epsilon}^2 = \frac{2k\,T\,F\,\beta\,B^2}{S_i^2} = \frac{B^2}{r}, \qquad (2.21)$$

where r is the power signal-to-noise ratio at the antenna input calculation on the basis of a bandwidth equal to the servobandwidth β. One can calculate what signal-to-noise ratio and beamwidth are required to obtain a given attitude accuracy from this equation. Taking a 1-foot diameter antenna in the satellite at X-band and using 2-foot diameter antennas on the ground with 10 watts radiated and a noise figure for the receiver of 10, it is found that at a distance of 22,752 nautical miles the signal-to-noise ratio is approximately $10^6/4$. If one assumes further that 1-mil tracking is desired, β must be $\leq$ 35 cycles. The equipment to perform the above functions would consist of receivers and would be similar to that diagrammed in Figure 3-9, but with the addition of two error channels, one for right-left and one for up-down, for each antenna. The antenna itself could be a dimple in the side of the satellite body and thus would weigh essentially nothing. The receivers themselves would probably weigh about 20 pounds and would use 75-watt dc power.

These elementary calculations show that it should be quite possible to design a tracking system for the attitude control which will hold the attitude to within one milliradian. Since the complete tracking system is a three-dimensional problem, it is felt that a complete analysis of this system will require a numerical simulation program.

3.3.2.2. Attitude Control for Polar Satellites

The attitude control system proposed for polar satellites is identical to those used for establishing equatorial satellites up through apogee burning, (i.e., using the platform as reference). The attitude corrections which are required to stabilize the vehicle in a synchronized orbit cannot be accomplished with the monopulse attitude control system, since the vehicle is continually changing positions with respect to any pair of ground stations. On the other hand, for polar orbits only a single communication beam is required to cover the entire earth with no yaw stabilization above the local vertical through the earth's center.

Any attitude sensing system which gives only pitch and roll stability can be provided by sensing radiation from the earth's surface. Infrared radiation is given off by the heated earth in sufficient quantities to make an infrared horizon scanner practical for a 24-hour orbital radius. A preliminary system study* of such a device shows that the bearing angle to the earth's center can be considered accurate to approximately one mil for an airborne weight of 7 pounds and 30 watts of dc power.** This simple device could provide sufficiently accurate data to the computer and roll sets to stabilize the communication aerials above the local vertical adequately.

3.3.3.3 Fine Constant Stabilization

As discussed in Appendix C, the angular rate of the vehicle in pitch must be 0.7292116×10^{-4} radians per second if it is to rotate once in a sidereal day. Furthermore, the actual rate must be adjusted to have an error less than 10^{-7} radians per second, if the attitude is to freely drift about the equilibrium position without exceeding the required tolerances. Although the fine gas jets can produce angular rates having the required accuracy, the cross coupling terms and minor disturbing torques become important, as shown in Appendix C, when such fine control is required. These difficulties can, in large part, be avoided if a stabilizing flywheel pictured in Figure 3-11 is used. The large flywheel is operated at constant angular momentum. The large constant-speed flywheel normally operates at about 10,000 rpm, has an angular

---

* "Proposal for Development of a Horizon Scanner," RFQ LMSD/36009, 18 October 1957, The Ramo-Wooldridge Corporation.

** Since the monopulse system will not be used on polar orbits, 17 pounds will be gained which can be used to offset the additional power required for the infrared scanner.

[redacted]

CONFIDENTIAL

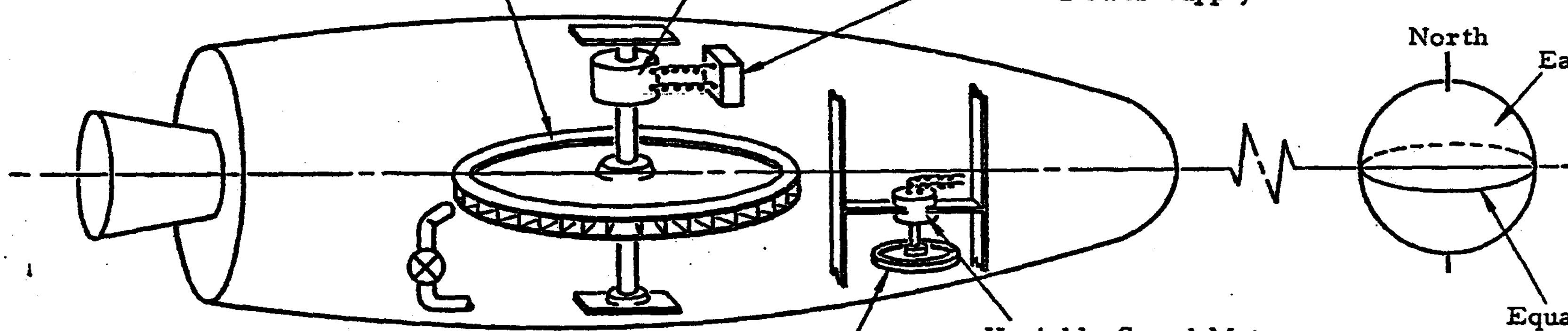

Figure 3-11. Schematic of Stabilizing Flywheel (Axis Perpendicular to Plane of Orbit).

CONFIDENTIAL

[redacted]

momentum of more than 80 slug $feet^2$ radians per second, and will weigh about 10 pounds. During the ascent trajectory, the flywheel is caged. At the end of apogee burning, the wheel is brought up to speed by means of a small gas jet. (Less than one-tenth pound of propellant is required for this purpose. The angular momentum incurred will be compensated by appropriate use of the coarse gas jet system.) Once in operation, the angular momentum of this flywheel is maintained to better than one part in 10^5 by means of temperature-compensated crystal-controlled electric power furnished to the driving synchronous motor. The angular momentum of this wheel is so large that the vehicle may be considered to be "pinned" in roll and yaw by the flywheel axis; the vehicle is free only in pitch. This flywheel could, in fact, be used as the inverter.

Fine adjustments in angular speed in pitch may be obtained by varying the speed of the small control motor and flywheel shown in Figure 3-11. This small flywheel has a maximum angular momentum of only 5×10^{-3} slug $feet^2$. Together with its actuating motor, it will weigh less than one pound and will be about 3 inches in diameter. The controls are so arranged that whenever the angular momentum of the control flywheel reaches the maximum design value, corrective torques are applied by the fine gas jets as shown in Figure 3-4. The control flywheel is then brought to rest and is thus again free to compensate for any small angular momentum which may develop in the vehicle. For example, the residual angular rate from the fine gas jet system is 0.7 degree per hour. To absorb this, the wheel would have to be turned at 0.7×10^6 degrees per hour, or 33 rpm.

Using information from Appendix F, Volume IV, Table 3-3, shows that any velocity changes due to meteoric impact are negligible. For the largest meteor considered likely to strike the vehicle (and then only once in ten years) the momentum transfer to the vehicle is 1.69×10^{-4} slug feet per second which can give at most a velocity change of 5.5×10^{-6} feet per second to the 1000-pound vehicle. The same meteor will produce an angular change in roll or yaw which is

$$\frac{10 \text{ ft} \times 1.69 \times 10^{-9} \text{ slugs} \times 10^{5} \text{ ft/sec}}{80 \text{ slug ft}^2 \text{ rad/sec}} = 0.8 \times 10^{4} \text{ rad}$$

[redacted]

CONFIDENTIAL

Table 3-3. Momentum Effects of Meteoric Impact.

Visual Magnitude	Mass (microslugs)	Number Striking Vehicle Each 24 Hours	Weight (pounds)	Diameter (inches)	Momentum Each Particle (slug ft/sec)
10	1.69×10^{-3}	2.5×10^{-4}	5.4×10^{-8}	.0095	1.69×10^{-4}
20	1.69×10^{-7}	2.5	5.4×10^{-12}	.00042	1.69×10^{-8}
30	1.69×10^{-11}	2.5×10^{4}	5.4×10^{-16}	.0000204	1.69×10^{-12}

CONFIDENTIAL

[redacted]

Since control to 0.1 degree or 0.01 degree is all that is necessary, this effect is also negligible.

In pitch the change in angular rate imparted by a similar meteorite is 1.69×10^{-6} radians per second. With such a rate it will take 10^{3} seconds to drift off by 0.1 degree. The angular momentum imparted to the vehicle by the meteor is at most 1.69×10^{-3} slug feet^{2} radians per second, which can easily be absorbed by the small wheel and motor rotating at 120 rpm.

There are a great many other possible sources of small disturbing torques in addition to meteorites which may affect the attitude of the vehicle. For example, the rotation of the heliocentric photovoltaic cells in the pitch plane will have an effect, since any changes in the moment of inertia will result in corresponding changes in the angular rate of the vehicle. However, this effect is small as compared with the effect of the large flywheel and can easily be controlled by the system here described.

Table 3-4 gives the weight and power required for the attitude-control system. The dominant factor is the gas required for the velocity control. Of course, more less gas will be required depending upon the accuracy of the guidance system used. It should be pointed out that the amount of power required by the monopulse system is dependent upon the number of measurements required. Probably the misalignment of the large flywheel will be sufficiently large to require frequent measurements. Other factors, such as meteorites, will also make frequent observations desirable.

Table 3-4. Attitude Control System

	Weight (pounds)	Power (watts)
Coarse Gas Jets (plumbing and main tank)	15	20*
Gas for Velocity Correction (Thor)	45	
(Titan)	90	
Gas for Reorientation	6	
Fine Gas Jets (plumbing)	5	
Gas for Fine Reorientation	0.6	
Gas for Continuous Attitude Correction in 24-Hour Orbit for Lifetime of One Year	5	
Monopulse System	20	75*
Attitude Stabilization Computer (analog)	15	20
Large Flywheel	12	20
Small Flywheel	2	10
Totals (Thor)	125.6	145
(Titan)	170.6	

*Used very intermittently

APPENDIX A

ERROR ANALYSIS FOR HIGH-ALTITUDE CIRCULAR SATELLITE ORBIT

1. Introduction

The flight plane under consideration is designed to place a vehicle in a specified high-altitude circular satellite orbit. The study is carried out in a nonrotating coordinate system with the origin at the center of the earth and the plane of the desired orbit as one of the principal coordinate planes. With suitable regard to the rotation of the earth and the inclination of the final orbit plane to the plane of the equator, these results can be used in the analysis of either an equatorial orbit or a polar orbit.

The nominal flight consists of four phases:

(a) The powered flight from launch yields burnout conditions suitable for a low-altitude circular orbit. The vehicle is permitted to coast in this orbit for a given elapsed time. This coast period may extend through several revolutions of the vehicle about the earth, and nominally terminates at some particular crossing of the desired final plane. In a nonrotating coordinate system, the repeated crossings of the desired final plane occur at the same (two) points, but for a rotating earth the longitudes corresponding to these crossings vary with time and the duration of the coast period through multiple crossings provides a means of adjusting the longitude.

(b) After the coast period, a short burning period causes the vehicle to enter a Hohmann transfer ellipse at perigee. In general, the plane of this ellipse may be inclined to the plane of the low-altitude circular satellite.

(c) The vehicle is permitted to coast from perigee to apogee. Since the burning period at perigee occurred at a crossing of the desired final plane and was assumed to be short, the apogee position of the vehicle also occurs at a crossing of the desired final plane.

(d) At apogee, a final short burning period supplies the additional velocity required to maintain the vehicle in a high-altitude circular orbit and simultaneously orients the plane of this orbit in the desired final plane.

The purpose of this appendix is to obtain first order estimates of the position and velocity errors at the end of each phase. After summarizing the notation there is a discussion of the equations of motion of the orbit. This is followed by an analysis of the perturbations of the orbit due to various error sources. The results are then applied to the four phases of the flight.

2. Notation

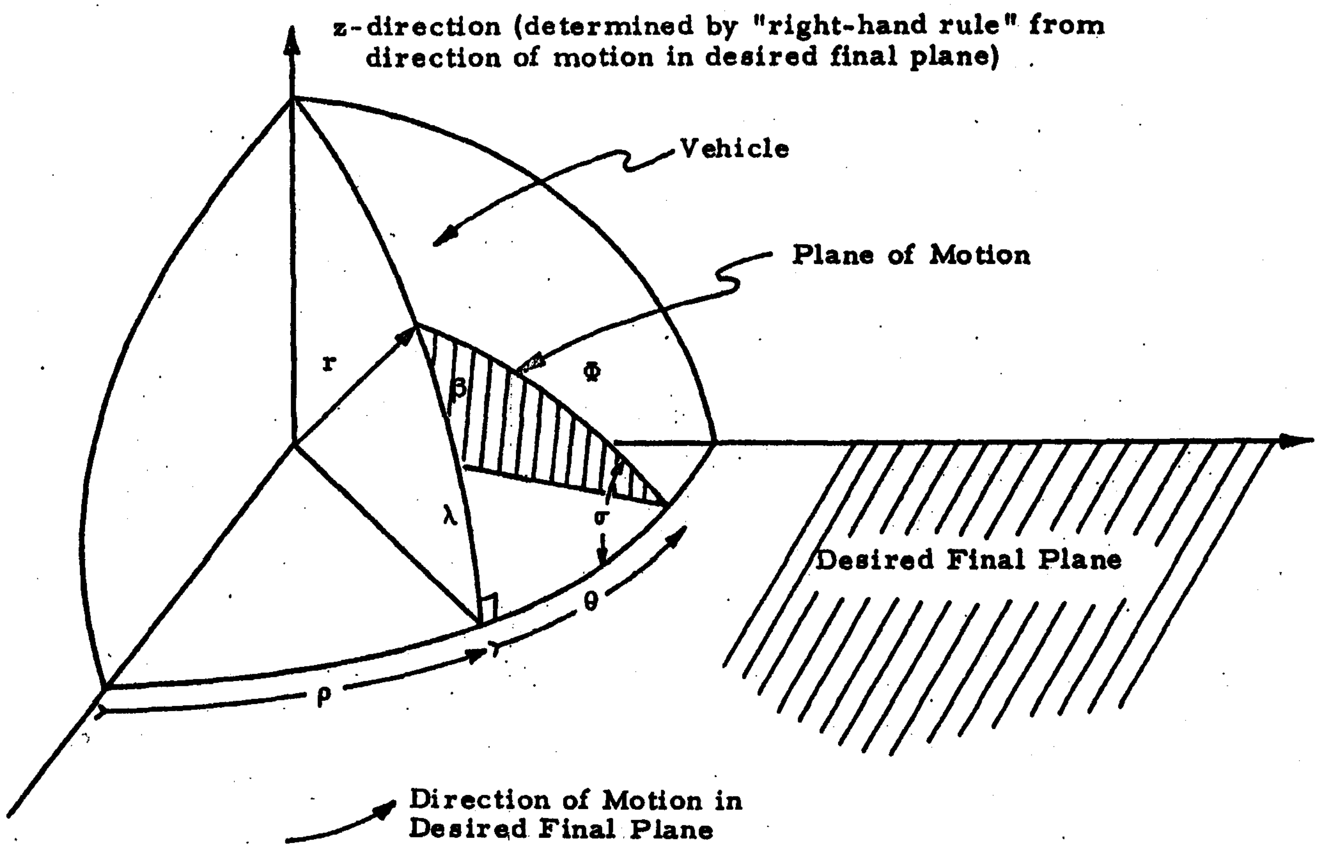

Figure A-1.

λ = Angular position of vehicle <u>above</u> desired final plane

ρ = Angular position in desired plane measured from arbitrary fixed reference (positive sense determined from desired direction of motion in final plane)

r = Radial distance from center of earth

λ = angular position of vehicle above desired final plane

ρ = angular position in desired plane measured from arbitrary fixed reference (positive sense determined from desired direction of motion in final plane)

r = radial distance from center of earth

ϕ = transit angle in plane of motion measured from burnout

V = total velocity

α = elevation angle of velocity vector measured from local horizontal

U = circumferential velocity, $r\dot{\phi}$ or $V \cos \alpha$

W = radial velocity, $\dot{r}$ or $V \sin \alpha$

β = azimuth of velocity vector measured from $(-z)$ direction with range, $0 - \pi$

σ = dihedral angle between plane of motion and desired final plane

Φ = transit angle from initial burnout to first crossing

θ = angular difference between burnout value of ρ and value of ρ at first crossing

μ = GM where G is the universal gravitational constant and M is the mass of earth

τ^* = nominal coast time during first phase

N = number of complete half-revolutions during first phase

τ^{**} = nominal coast time in Hohmann transfer

t = time measured from initial burnout

t_o = initial burnout time

t_1 = end of first coast period

t_2 = second burnout time

t_3 = end of Hohmann transfer

t_4 = final burnout time.

3. Equations of Motion

The orientation of the plane of motion is determined from the spherical triangle

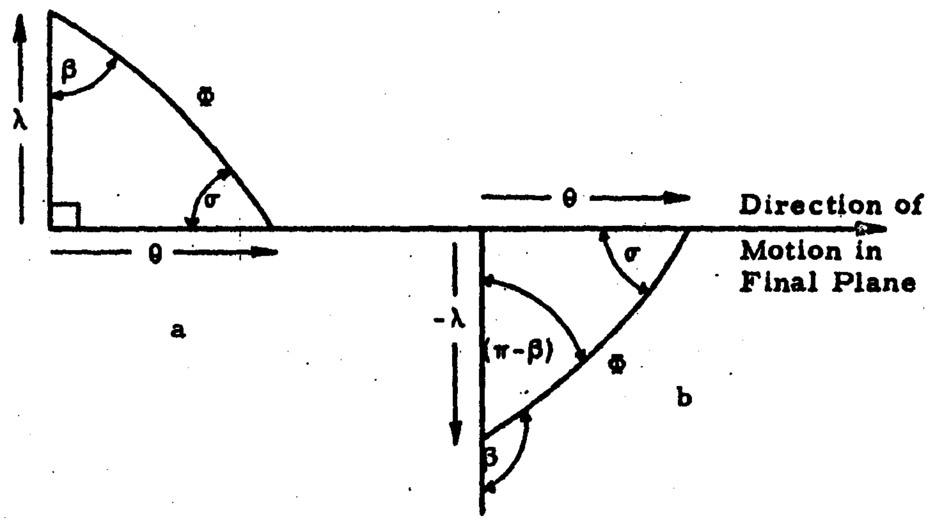

Figure A-2

The motion in the plane of the orbit must satisfy the equations

$$r^2 \dot{\phi} = c \ , \tag{A.1}$$

$$\ddot{r} = \frac{c^2}{r^3} - \frac{\mu}{r^2} \ , \tag{A.2}$$

and the initial conditions

$$(r)_o = r_o \ , \tag{A.3}$$

$$(r\dot{\phi})_o = V_o \cos \alpha_o \ , \tag{A.4}$$

$$(\dot{r})_o = V_o \sin \alpha_o \ . \tag{A.5}$$

The solution may be written in the form

$$r^2\dot{\phi} = r_o V_o \cos \alpha_o \ , \tag{A.6}$$

$$\frac{r_o}{r} = \frac{K}{\cos^2 \alpha_o} + \left(1 - \frac{K}{\cos^2 \alpha_o}\right) \cos \phi - \tan \alpha_o \sin \phi \ , \tag{A.7}$$

where

$$K = \frac{\mu}{r_o V_o^2} \tag{A.8}$$

We first verify that Equations (A.6) and (A.7) satisfy the initial conditions (A.3), (A.4), and (A.5). From (A.7) $r = r_o$ when $\phi = 0$. Hence (A.3) is satisfied. Condition (A.4) is satisfied by (A.6) and (A.3). From (A.7)

$$-\frac{r_o}{r^2}\dot{r} = -\left(1 - \frac{K}{\cos^2 \alpha_o}\right) \sin \phi \dot{\phi} - \tan \alpha_o \cos \phi \dot{\phi} \ ,$$

and using (A.6)

$$\dot{r} = \left(1 - \frac{K}{\cos^2 \alpha_o}\right) \sin \phi \ V_o \cos \alpha_o \tan \alpha_o \cos \phi V_o \cos \alpha_o \ . \tag{A.9}$$

Thus, when $\phi = 0$

$$(\dot{r})_o = V_o \sin \alpha_o \ ,$$

and (A.5) is satisfied. Thus, the initial conditions are all satisfied.

We now verify that (A.6) and (A.7) satisfy the differential Equations (A.1) and (A.2). Since $r_o V_o \cos \alpha_o$ is a constant, Equation (A.6) clearly satisfies (A.1). It only remains to verify that Equation (A.2) is satisfied with the same constant appearing for c in that equation. Differentiating Equation (A.9),

$$\ddot{r} = \left[\left(1 - \frac{K}{\cos^2 \alpha_o}\right) \cos \phi - \tan \alpha_o \sin \phi\right] \dot{\phi} V_o \cos \alpha_o \ .$$

Substituting from Equations (A.7) and (A.8)

$$\ddot{r} = \left(\frac{r_o}{r} - \frac{K}{\cos^2 a_o}\right) \frac{r_o V_o^2 \cos^2 a_o}{r^2} ,$$

$$\ddot{r} = \frac{(r_o V_o \cos a_o)^2}{r^3} - \frac{\mu}{r^2} .$$

Thus (A.2) is satisfied.

From Equations (A.6) the time may be expressed by

$$r_o V_o \cos a_o t = \int_o^{\phi} r^2 \, d\phi . \tag{A.10}$$

The cases to be studied in this appendix will involve small initial elevation angles, a_o. Writing this small elevation angle as δa_o and retaining only first order terms in Equations (A.6), (A.7), (A.9), and (A.10) yields

$$\frac{r_o}{r} = K + (1 - K) \cos \phi - \delta a_o \sin \phi , \tag{A.11}$$

$$r^2 \dot{\phi} = r_o V_o , \tag{A.12}$$

$$\frac{\dot{r}}{V_o} = (1 - K) \sin \phi + \delta a_o \cos \phi , \tag{A.13}$$

$$r_o V_o t = r_o^2 \int_o^{\phi} \left\{ \frac{1}{\left[K + (1 - K) \cos\phi\right]^2} + \frac{2 \delta a_o \sin \phi}{\left[K + (1 - K) \cos\phi\right]^3} \right\} d\phi . \tag{A.14}$$

4. Perturbed Equations of Motion

The perturbations of the nominal orbits are due to: (1) initial position variations, δr_o, $\delta \lambda_o$, $\delta \rho_o$; (2) initial velocity variations, δV_o, δa_o, $\delta \beta_o$; (3) variation of the nominal coast time, $\delta \tau$; and (4) uncertainty in the value of GM which will be expressed as $\delta \mu$. It is convenient to divide the study of these variations according to whether they affect the plane of the motion or cause perturbations of the orbit in the nominal plane of motion.

The in-plane perturbations of the orbit are found from Equations (A.11), (A.12), and (A.13) to be

$$\delta r = \frac{r\delta r_o}{r_o} - \frac{r^2}{r_o}\,\delta K(1-\cos\phi) + \frac{r^2}{r_o}\,\delta a_o \sin\phi + \frac{r^2}{r_o}(1-K)\sin\phi\,\delta\phi\,, \qquad (A.15)$$

$$\delta U = \delta(r\dot{\phi}) = \delta\left(\frac{r_o V_o}{r}\right) = \frac{V_o}{r}\,\delta r_o + \frac{r_o}{r}\,\delta V_o - \frac{r_o V_o}{r^2}\,\delta r\,, \qquad (A.16)$$

$$\delta W = \delta(\dot{r}) = \frac{\dot{r}\,\delta V_o}{V_o} - V_o\delta K\sin\phi + V_o(1-K)\cos\phi\,\delta\phi + V_o\cos\phi\,\delta a_o\,, \qquad (A.17)$$

where

$$\frac{\delta K}{K} = \frac{\delta\mu}{\mu} - \frac{\delta r_o}{r_o} - \frac{2\,\delta V_o}{V_o}\,. \qquad (A.18)$$

These perturbations are expressed in terms of initial variations, $\delta\mu$ and $\delta\phi$. The variation, $\delta\phi$, refers to a perturbation of the nominal transit angle. Since the orbit is an ellipse, a variation in the transit angle will cause a variation in both the position and velocity. The quantity, $\delta\phi$, can be found from (A.14).

$$\frac{V_o}{r_o}\,t = \int_o^{\phi}\frac{d\phi}{\left[K+(1-K)\cos\phi\right]^2} + 2\,\delta a_o\int_o^{\phi}\frac{\sin\phi\,d\phi}{\left[K+(1-K)\cos\phi\right]^3}\,, \qquad (A.19')$$

$$\frac{V_o}{r_o}\,t = \int_o^{\phi}\frac{d\phi}{\left[K+(1-K)\cos\phi\right]^2} - \frac{2\,\delta a_o}{1-K}\int_1^{\left[K+(1-K)\cos\phi\right]}\frac{dx}{x^3}\,,$$

$$\frac{V_o}{r_o}\,t = \int_o^{\phi}\frac{d\phi}{\left[K+(1-K)\cos\phi\right]^2} + \delta a_o\,\frac{\left[(1-K)(1-\cos^2\phi)+2K(1-\cos\phi)\right]}{\left[K+(1-K)\cos\phi\right]^2}\,, \qquad (A.19)$$

$$\delta\left(\frac{V_o t}{r_o}\right) = \frac{\delta\phi}{\left[K + (1 - K)\cos\phi\right]^2} - 2\,\delta K \int_o^{\phi} \frac{(1 - \cos\phi)\,d\phi}{\left[K + (1 - K)\cos\phi\right]^3}$$

$$+ \delta a_o \frac{\left[(1 - K)\sin^2\phi + 2K(1 - \cos\phi)\right]}{\left[K + (1 - K)\cos\phi\right]^2} \;. \qquad \text{(A.19 cont)}$$

The two orbits to be studied are the circular satellite and the Hohmann transfer. For a circular satellite

$$a_o = 0,\; W_o = 0,\; U_o = V_o = \sqrt{\frac{\mu}{r_o}} \;.$$

Hence, $W = 0$ and $r = r_o$ during the entire coast period. From Equation (A.8) $K = 1$, and from (A.18)

$$\delta K = \frac{\delta\mu}{\mu} - \frac{\delta r_o}{r_o} - \frac{2\,\delta V_o}{V_o} \;.$$

These results may be used to simplify Equations (A.15), (A.16), and (A.17), to yield the variations at the end of the circular coast period (nominally, at $t = \tau^*$).

$$\frac{\delta r_1}{r_o} = \frac{\delta r_o}{r_o}(2 - \cos\phi_1) + 2(1 - \cos\phi)\frac{\delta V_o}{V_o} - (1 - \cos\phi_1)\frac{\delta\mu}{\mu} + \sin\phi_1\,\delta a_o, \qquad \text{(A.20)}$$

$$\frac{\delta U_1}{V_o} = -\frac{\delta r_o}{r_o}(1 - \cos\phi_1) + (2\cos\phi_1 - 1)\frac{\delta V_o}{V_o} + (1 - \cos\phi_1)\frac{\delta\mu}{\mu} - \sin\phi_1\,\delta a_o\,, \qquad \text{(A.21)}$$

$$\frac{\delta W_1}{V_o} = \sin\phi_1\frac{\delta r_o}{r_o} + 2\sin\phi_1\frac{\delta V_o}{V_o} - \sin\phi_1\frac{\delta\mu}{\mu} + \cos\phi_1\,\delta a_o \;. \qquad \text{(A.22)}$$

Equation (A.19) also may be solved for $\delta\phi_1$ and the expression simplified by using $K = 1$, the above expression for δK, and the fact that the total transit angle $\phi_1 = V_o \tau^* / r_o$.

$$\delta \phi_1 = \delta \left(\frac{V_o \tau^*}{r_o} \right) + 2 \delta K \int_o^{\phi_1} (1 - \cos \phi) \, d\phi - 2 (1 - \cos \phi_1) \delta \alpha_o ,$$

$$\delta \phi_1 = \phi_1 \left(\frac{\delta V_o}{V_o} + \frac{\delta \tau^*}{\tau^*} - \frac{\delta r_o}{r_o} \right) + 2(\phi_1 - \sin \phi_1) \left(\frac{\delta \mu}{\mu} - \frac{\delta r_o}{r_o} - \frac{2 \delta V_o}{V_o} \right)$$
$$- 2 (1 - \cos \phi_1) \delta \alpha_o . \qquad \text{(A.23)}$$

For a Hohmann transfer starting at t_2 and terminating at $t_3 = t_2 + \tau^{**}$, the conditions are $\alpha_2 = 0$, $W_2 = 0$, $\phi_3 = \pi$. From (A.19)

$$\delta \left(\frac{V_2 \tau^{**}}{r_2} \right) = \frac{\delta \phi_3}{(2K - 1)^2} - 2 \delta K \int_o^{\pi} \frac{(1 - \cos \phi) d\phi}{\left[K + (1 - K) \cos \phi \right]^3} + \delta \alpha_2 \frac{4K}{(2K - 1)^2} , \qquad \text{(A.24)}$$

where now $K = \mu / r_2 V_2^2$. The integral appearing in Equation (A.24) can be readily evaluated. From any integral table

$$\int_o^{\phi} \frac{d\phi}{a + b \cos \phi} = \frac{1}{\sqrt{a^2 - b^2}} \tan^{-1} \left(\frac{\sqrt{a^2 - b^2} \sin \phi}{b + a \cos \phi} \right) \quad a > b > 0 ,$$

$$\int_o^{\pi} \frac{d\phi}{a + b \cos \phi} = \frac{\pi}{\sqrt{a^2 + b^2}} ,$$

$$\int_o^{\pi} \frac{d\phi}{\left[a + b \cos \phi \right]^2} = \frac{\partial}{\partial a} \int_o^{\pi} \frac{d\phi}{\left[a + b \cos \phi \right]} = \frac{\pi a}{(a^2 - b^2)^{3/2}} ,$$

For the particular case, $a = K$, $b = 1 - K$

$$\int_0^{\pi} \frac{d\,\phi}{\left[K + (1 - K)\cos\phi\right]^2} = \frac{\pi K}{(2K - 1)^{3/2}} \; .$$

Therefore, the integral of interest

$$\int_0^{\pi} \frac{(1 - \cos\phi)\, d\,\phi}{\left[K + (1 - K)\cos\phi\right]^3} = -\frac{1}{2}\,\frac{\partial}{\partial K} \int_0^{\pi} \frac{d\,\phi}{\left[K + (1 - K)\cos\phi\right]^2}$$

$$= -\frac{1}{2}\,\frac{\partial}{\partial K}\;\frac{\pi K}{(2K - 1)^{3/2}} = \frac{\pi(1 + K)}{2(2K - 1)^{5/2}} \; .$$

Substituting, and solving Equation (A.24) for $\delta\,\phi_3$ gives

$$\delta\,\phi_3 = (2K - 1)^2\,\delta\left(\frac{V_2\,\tau^{**}}{r_2}\right) + \frac{\delta K \pi (1 + K)}{\sqrt{2K - 1}} - 4\,K\,\delta\,a_2 \; .$$

This equation may be expressed more conveniently by noting from Equation (A.19') that the nominal value of $V_2\,\tau^{**}/r_2$ is given by

$$\frac{V_2\,\tau^{**}}{r_2} = \int_0^{\pi} \frac{d\,\phi}{\left[K + (1 - K)\cos\phi\right]^2} = \frac{\pi K}{(2K - 1)^{3/2}} \; ,$$

and from Equation (A.7) with $\phi = \pi$

$$(2K - 1) = \frac{r_2}{r_3} \; ,$$

$$K = \frac{r_2 + r_3}{2\,r_3} \; .$$

Thus, the expression for $\delta\phi_3$ becomes

$$\delta\phi_3 = (2K-1)^2 \frac{\pi K}{(2K-1)^{3/2}}\left(\frac{\delta V_2}{V_2} + \frac{\delta\tau^{**}}{\tau^{**}} - \frac{\delta r_2}{r_2}\right) + \frac{\pi(1+K)K}{(2K-1)^{1/2}}\left(\frac{\delta\mu}{\mu} - \frac{\delta r_2}{r_2} - \frac{2\,\delta V_2}{V_2}\right) - 4K\delta a_2 \ ,$$

$$\delta\phi_3 = \frac{\pi(r_2+r_3)}{4\sqrt{r_2 r_3}}\left[-3\,\frac{(r_2+r_3)}{r_3}\,\frac{\delta r_2}{r_2} - \frac{6\,\delta V_2}{V_2} + \frac{(r_2+3r_3)}{r_3}\,\frac{\delta\mu}{\mu} + \frac{2r_2}{r_3}\,\frac{\delta\tau^{**}}{\tau^{**}}\right] - 2\,\frac{r_2+r_3}{r_3}\,\delta a_2 \ . \tag{A.25}$$

Now, from Equations (A.15), (A.16), and (A.17), with $\phi_3 = \pi$ and $W_3 = 0$,

$$\frac{\delta r_3}{r_3} = \left(\frac{2r_2+r_3}{r_2}\right)\frac{\delta r_2}{r_2} + 2\left(\frac{r_2+r_3}{r_2}\right)\frac{\delta V_2}{V_2} - \left(\frac{r_2+r_3}{r_2}\right)\frac{\delta\mu}{\mu} \ , \tag{A.26}$$

$$\frac{\delta U_3}{V_3} = -\left(\frac{r_2+r_3}{r_2}\right)\frac{\delta r_2}{r_2} - \left(\frac{2r_3+r_2}{r_2}\right)\frac{\delta V_2}{V_2} + \left(\frac{r_2+r_3}{r_2}\right)\frac{\delta\mu}{\mu} \ , \tag{A.27}$$

$$\frac{\delta W_3}{V_3} = -\left(\frac{r_3-r_2}{2r_2}\right)\delta\phi_3 - \frac{r_3}{r_2}\,\delta a_2 \ . \tag{A.28}$$

In the above expressions, $W_3 = 0$ and Equation (A.12) have been used to replace V_2/V_3 by r_3/r_2.

The preceding results provide the in-plane perturbations for the cases of interest. The perturbations of the plane of motion are obtained from the spherical triangle (Figure A-2). From Figure A-2a

$$\cos\sigma = \cos\lambda\sin\beta,$$

$$\tan\theta = \sin\lambda\tan\beta,$$

$$\tan\Phi = \tan\lambda\sec\beta,$$

and from Figure A-2b

$$\cos\sigma = \cos\lambda\sin(\pi-\beta),$$

$$\tan\theta = -\sin\lambda\tan(\pi-\beta),$$

$$\tan\Phi = -\tan\lambda\sec(\pi-\beta).$$

The variations become

$$\delta\sigma = \frac{\sin\lambda\sin\beta}{\sin\sigma}\,\delta\lambda - \frac{\cos\lambda\cos\beta}{\sin\sigma}\,\delta\beta,$$

$$\delta\theta = \frac{\cos\lambda\tan\beta}{\sec^2\theta}\,\delta\lambda + \frac{\sin\lambda\sec^2\beta}{\sec^2\theta}\,\delta\beta,$$

$$\delta\Phi = \frac{\sec^2\lambda\sec\beta}{\sec^2\Phi}\,\delta\lambda + \frac{\tan\lambda\sec\beta\tan\beta}{\sec^2\Phi}\,\delta\beta\ .$$

or

$$\delta\sigma = \frac{-\sin(-\lambda)\sin(\pi-\beta)}{\sin\sigma}\,\delta\lambda + \frac{\cos\lambda\cos(\pi-\beta)}{\sin\sigma}\,\delta\beta\ ,$$

$$\delta\theta = \frac{\cos\lambda\tan(\pi-\beta)}{\sec^2\theta}\,\delta\lambda - \frac{\sin\lambda\sec^2(\pi-\beta)}{\sec^2\theta}\,\delta\beta,$$

$$\delta\Phi = -\frac{\sec^2\lambda\sec(\pi-\beta)}{\sec^2\Phi}\,\delta\lambda - \frac{\tan\lambda\sec(\pi-\beta)\tan(\pi-\beta)}{\sec^2\Phi}\,\delta\beta\ .$$

Using some identities of spherical trigonometry and the sign convention on λ established in Section 2, these results may be written

[redacted]

CONFIDENTIAL

$$\delta\sigma = \sin\theta\,(\operatorname{sgn}\lambda)\,\delta\lambda - \cos\Phi\,(\operatorname{sgn}\lambda)\,\delta\beta \quad , \tag{A.29}$$

$$\delta\theta = \cot\sigma\cos\theta(\operatorname{sgn}\lambda)\,\delta\lambda + \csc^2\sigma\sin\lambda\,\delta\beta \quad , \tag{A.30}$$

$$\delta\Phi = \csc\sigma\cos\theta\,(\operatorname{sgn}\lambda)\,\delta\lambda + \csc\sigma\cot\sigma\sin\lambda\,\delta\beta \quad . \tag{A.31}$$

These equations will be used later in the determination of variations in λ and ρ.

The analysis of the errors introduced during the short burning periods does not require the equations of motion. The short burning periods are assumed to produce finite increments in the velocity vector in negligible time. In the cases of interest, the elevation angle $\alpha = 0$ and the velocity increments take place in the horizontal plane. The subscripts i and j will be used to denote the states before and after the velocity change, respectively, and the symbol Δ will represent a finite increment. With these assumptions

$$\delta\lambda_j = \delta\lambda_i \quad , \tag{A.32}$$

$$\delta\rho_j = \delta\rho_i \quad , \tag{A.33}$$

$$\delta r_j = \delta r_i \quad . \tag{A.34}$$

Consider Figure A-3.

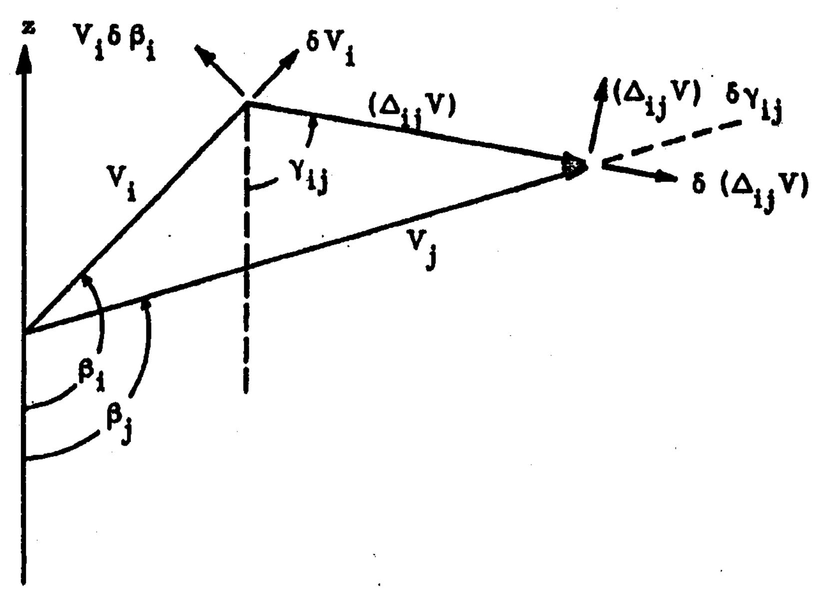

CONFIDENTIAL

Figure A-3

[redacted]

The initial velocity has magnitude, V_i, and azimuth, β_i, with errors, δV_i, and $V_i \delta\beta_i$. The applied increment has magnitude $(\Delta_{ij} V)$; azimuth, γ_{ij}; and elevation, ϵ_{ij}, with errors, $\delta(\Delta_{ij} V)$, $(\Delta_{ij} V)\, \delta\gamma_{ij}$, and $(\Delta V_{ij})\, \delta\epsilon_{ij}$. Nominally $\epsilon_{ij} = 0$ and the final velocity has magnitude, V_j, and azimuth, β_j. Thus

$$\delta W_j = \delta W_i + (\Delta_{ij} V)\, \delta\epsilon_{ij} \quad , \tag{A.35}$$

and from Figure A-3

$$\delta V_j = \delta V_i \cos(\beta_i - \beta_j) - V_i\, \delta\beta_i \sin(\beta_i - \beta_j) + \delta(\Delta_{ij} V) \cos(\beta_j - \gamma_{ij}) + (\Delta_{ij} V)\, \delta\gamma_{ij} \sin(\beta_j - \gamma_{ij}) \quad , \tag{A.36}$$

$$V_j \delta\beta_j = \delta V_i \sin(\beta_i - \beta_j) + V_i\, \delta\beta_i \cos(\beta_i - \beta_j) - \delta(\Delta_{ij} V) \sin(\beta_i - \gamma_{ij}) + (\Delta_{ij} V)\, \delta\gamma_{ij} \cos(\beta_j - \gamma_{ij}) \quad . \tag{A.37}$$

The results are valid for an arbitrary orientation of the figure. The errors in the velocity increment can be related to errors in the missile guidance system. For example, in the case of an all-inertial system, $\delta\gamma_{ij}$ and $\delta\epsilon_{ij}$ represent gyro drifts and $\delta(\Delta_{ij} V)$ the error due to an integrating accelerometer.

5. Flight Analysis

The nominal burnout conditions for the first phase are $W_o = 0$, $V_o = U_o = \sqrt{\mu/r_o}$, $\alpha_o = 0$. Hence at time $t_1 = \tau^*$: $r_1 = r_o$, $W_1 = 0$, $U_1 = U_o$, $\phi_1 = (\Phi + N\pi) = U_o \tau^*/r_o$. The variations δr_1, δU_1, δW_1, $\delta\phi_1$ are given by Equations (A.20), (A.21), (A.22), and (A.23), respectively, and are summarized in Table A-1a. The variation in orbit inclination, $\delta\sigma$, is given by (A.29) evaluated at t_o. In order to express the variations in λ and ρ, it is convenient to introduce

$\delta\Psi$ = angular deficit in transit angle measured to terminal crossing of desired plane,

$$\delta\Psi = \delta\Phi - \delta\phi_1 ,$$

where $\delta\Phi$ is given by Equation (A. 31) evaluated at t_o and $\delta\phi_1$ is given by Equation (A. 23). Then from Figure A-4,

$$\delta\lambda_1 = (-1)^N \sin\sigma\, \delta\Psi\, (\mathrm{sgn}\, \lambda_o), \tag{A.38}$$

$$\delta\rho_1 = \delta\rho_o + \delta\theta - \cos\sigma\, \delta\Psi , \tag{A. 39}$$

where $\delta\theta$ is obtained from (A. 30) evaluated at t_o and $\delta\rho_o$ represents the error in ρ at initial burnout. Examination of Figure A-4 shows

$$\beta_1 = \pi/2 - (-1)^N \sigma_1 (\mathrm{sgn}\, \lambda_o) = \pi/2 - (-1)^N \sigma_o (\mathrm{sgn}\, \lambda_o),$$

$$\delta\beta_1 = (-1)^{N+1} \delta\sigma_1 (\mathrm{sgn}\, \lambda_o). \tag{A. 40}$$

These results are summarized in Table A-lb.

At the end of the circular coast period a short burning period now supplies the additional velocity required to enter a Hohmann transfer ellipse. For a given perigee altitude, r_o, and a desired apogee altitude, r_4, the velocity required can be obtained from Equation (A. 7),

$$\frac{r_o}{r_4} = K + (1 - K)(-1),$$

$$2K = \frac{r_o + r_4}{r_4},$$

$$\frac{2\mu}{r_o V_2^2} = \frac{r_o + r_4}{r_4},$$

$$V_2 = \sqrt{\frac{\mu}{r_o}}\sqrt{\frac{2r_4}{r_o + r_4}} = V_o\sqrt{\frac{2r_4}{r_o + r_4}}$$

The variations at the end of this phase are given by Equations (A. 32) through (A. 37) with $i = 1$, $j = 2$. The values of $\Delta_{ij}V$ and γ_{ij} are predetermined for a given flight and the errors $\delta(\Delta_{ij}V)$, $\delta\gamma_{ij}$, and $\delta\epsilon_{ij}$ can be related to errors in the inertial guidance equipment. From (A. 34) it may be observed that $r_2 = r_1$. Nominally $r_1 = r_o$ and $V_1 = V_o$ since the first phase is a circular satellite. These relations and the further relation $r_4 = r_3$ which also follows from (A. 34) will be used to simplify the summarizing tables at the end of this appendix. The results are summarized in Table A-2.

Table A-1a

	$\frac{\delta r_o}{r_o}$	$\frac{\delta V_o}{V_o}$	δa_o	$\frac{\delta\mu}{\mu}$	$\frac{\delta\tau^*}{\tau^*}$
$\frac{\delta r_1}{r_o}$	$2 - \cos\phi_1$	$2(1 - \cos\phi_1)$	$\sin\phi_1$	$-(1 - \cos\phi_1)$	0
$\frac{\delta U_1}{V_o}$	$-(1 - \cos\phi_1)$	$2\cos\phi_1 - 1$	$-\sin\phi_1$	$1 - \cos\phi_1$	0
$\frac{\delta W_1}{V_o}$	$\sin\phi_1$	$2\sin\phi_1$	$\cos\phi_1$	$-\sin\phi_1$	0
$\delta\phi_1$	$2\sin\phi_1 - 3\phi_1$	$4\sin\phi_1 - 3\phi_1$	$2(\cos\phi_1 - 1)$	$2\phi_1 - 2\sin\phi_1$	ϕ_1

Table A-1b

	$\delta\beta_o$	$\delta\lambda_o$	$\delta\rho_o$	$\delta\phi_1$
$\delta\sigma_1 = \delta\sigma_o = (-1)^{N+1}(\text{sgn}\,\lambda_o)\delta\beta_1$	$-\cos\theta(\text{sgn}\,\lambda_o)$	$\sin\theta(\text{sgn}\,\lambda_o)$	0	0
$\delta\lambda_1$	$(-1)^N\cos\lambda_o\sin\theta$	0	0	$(-1)^{N+1}\sin\sigma_1(\text{sgn}\lambda_o)$
$\delta\rho_1$	$\sin\lambda_o$	0	1	$\cos\sigma_1$

Table A-2

	$\frac{\delta r_1}{r_o}$	$\frac{\delta U_1}{V_o}$	$\frac{\delta W_1}{V_o}$	$\delta\lambda_1$	$\delta\rho_1$	$\delta\beta_1$	$\frac{\delta(\Delta_{12} V)}{V_o}$	$\frac{\Delta_{12} V}{V_o}\delta(\epsilon_{12})$	$\frac{\Delta_{12} V}{V_o}\delta(\gamma_{12})$
$\frac{\delta r_2}{r_o}$	1	0	0	0	0	0	0	0	0
$\frac{\delta U_2}{V_2}$	0	$\cos(\beta_1-\beta_2)$	0	0	0	$-\sin(\beta_1-\beta_2)$	$\cos(\beta_1-\gamma_{12})$	0	$\sin(\beta_2-\gamma_{12})$
$\frac{\delta W_2}{V_o}$	0	0	1	0	0	0	0	1	0
$\delta\lambda_2$	0	0	0	1	0	0	0	0	0
$\delta\rho_2$	0	0	0	0	1	0	0	0	0
$\delta\beta_2 = (-1)^{N+1}\delta\sigma_2(\mathrm{sgn}\lambda_o)$	0	$\frac{V_o}{V_2}\sin(\beta_1-\beta_2)$	0	0	0	$\frac{V_o}{V_2}\cos(\beta_1-\beta_2)$	$-\frac{V_o}{V_2}\sin(\beta_2-\gamma_{12})$	0	$\frac{V_o}{V_2}\cos(\beta_2-\gamma_{12})$

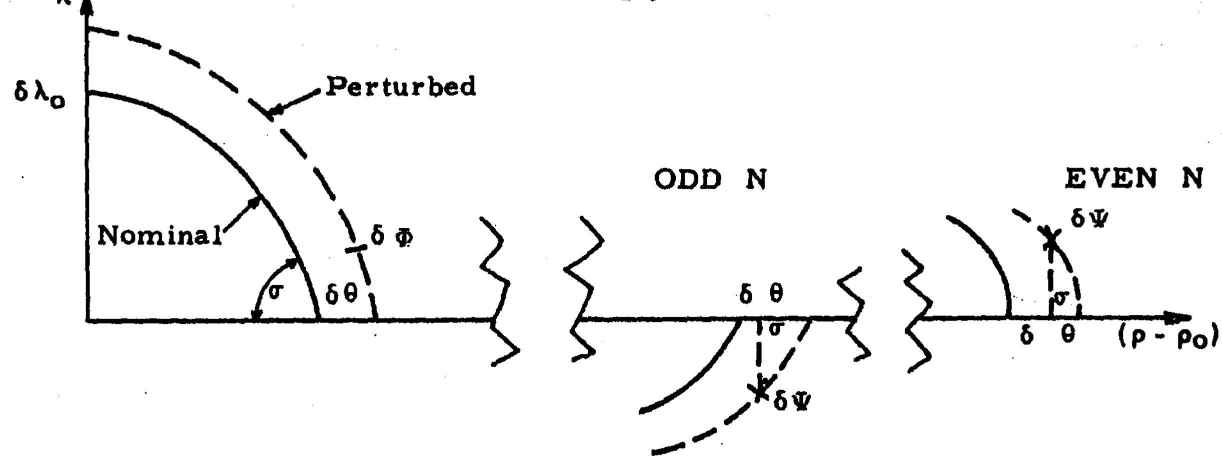

Figure A-4a

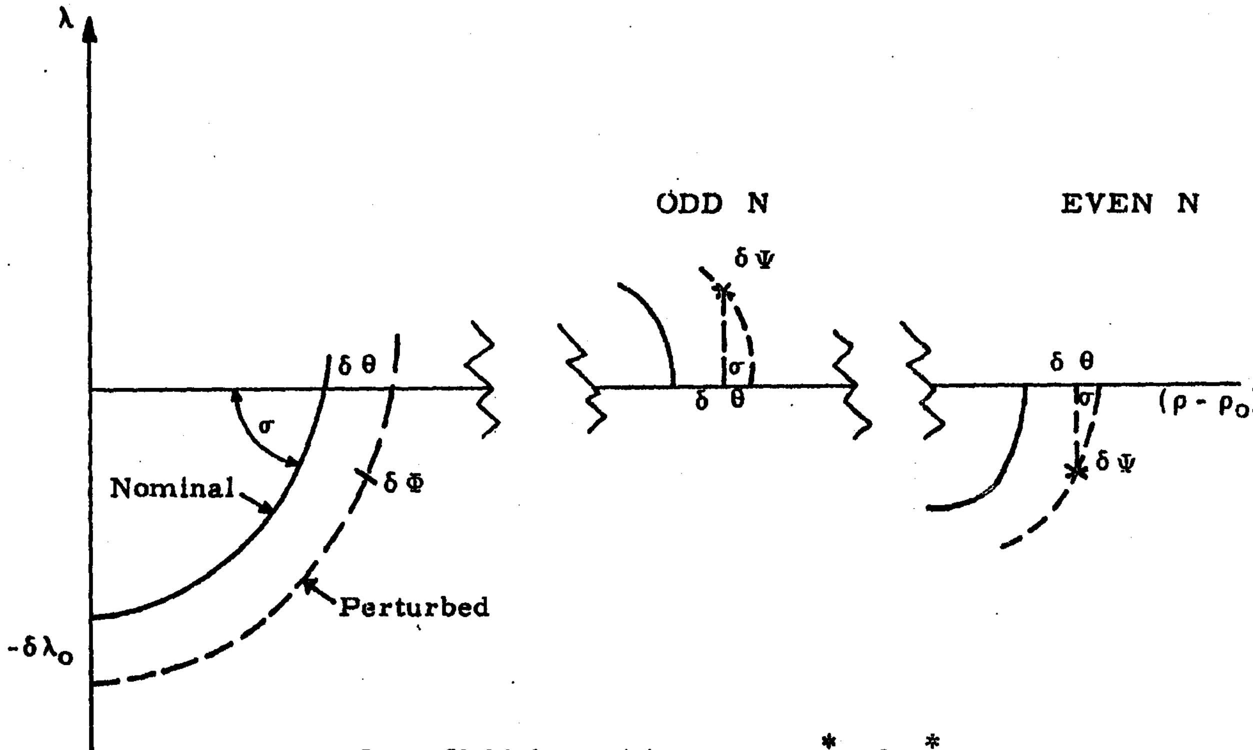

X = Vehicle position at $t = \tau^* + \delta \tau^*$

Figure A-4b

The vehicle now enters the transfer ellipse at perigee and coasts to apogee. The nominal conditions at t_2 are $\alpha_2 = 0$, $W_2 = 0$, and at $t_3 = t_2 + \tau^{**}$ they are $\alpha_3 = 0$, $W_3 = 0$, $\phi_3 = \pi$. From (A.6) the nominal velocity at perigee is

$$V_3 = \frac{r_o V_2}{r_4} .$$

Furthermore, since the perigee and the apogee positions are nominally on the desired final plane, $\lambda_2 = \lambda_3 = 0$. The variations δr_3, δU_3, δW_3, and $\delta\phi_3$ are given by Equations (A.25) through (A.28) and are summarized in Table A-3a. The variation in inclination angle is $\delta\sigma_3 = \delta\sigma_2$ where from (A.40) and (A.37) $\delta\sigma_2 = (-1)^{N+1}\,\delta\beta_2\,(\text{sgn}\,\lambda_o)$. Since the nominal perigee is at a crossing of the desired final plane and the nominal trajectory extends through one-half period, the variations in λ and ρ become

$$\delta\lambda_3 = -\delta\lambda_2 + (-1)^N (\text{sgn}\,\lambda_o) \sin\sigma_2\,\delta\phi_3 \quad , \qquad \text{(A.41)}$$

$$\delta\rho_3 = \delta\rho_2 + \cos\sigma_2\,\delta\phi_3 \quad . \qquad \text{(A.42)}$$

From (A.40) and the knowledge that N has increased by unity

$$\beta_3 = \pi/2 + (-1)^N (\text{sgn}\,\lambda_o)\,\sigma_3 = \pi/2 + (-1)^N (\text{sgn}\,\lambda_o)\,\sigma_2 \quad ,$$

and

$$\delta\beta_3 = (-1)^N (\text{sgn}\,\lambda_o)\,\delta\sigma_2 \quad . \qquad \text{(A.43)}$$

The results are summarized in Table A-3b.

At apogee a final short burning period is required to maintain the vehicle in a high-altitude circular orbit and to orient the plane of motion in the desired plane. The velocity required for the circular orbit is $U_4 = \sqrt{\mu/r_4}$. Equations (A.32) through (A.37) apply with $i = 3$, $j = 4$. The nominal value of β_4 is $\pi/2$. From the convention in Section 2 regarding β, a positive value for $\delta\beta_4$ represents a velocity component in the z-direction. The results are summarized in Table A-4.

Table A-3a

	$\frac{\delta r_2}{r_o}$	$\frac{\delta U_2}{V_2}$	$\frac{\delta W_2}{V_2}$	$\frac{\delta \mu}{\mu}$	$\frac{\delta \tau^{**}}{\tau^{**}}$
$\frac{\delta r_3}{r_4}$	$\left(2 + \frac{r_4}{r_o}\right)$	$2\left(1 + \frac{r_4}{r_o}\right)$	0	$-\left(1 + \frac{r_4}{r_o}\right)$	0
$\frac{\delta U_3}{V_3}$	$-\left(1 + \frac{r_4}{r_o}\right)$	$-\left(1 + \frac{2r_4}{r_o}\right)$	0	$\left(1 + \frac{r_4}{r_o}\right)$	0
$\frac{\delta W_3}{V_3}$	$\frac{3\pi(r_4 - r_o)(r_4 + r_o)^2}{8 r_o r_4 \sqrt{r_o r_4}}$	$\frac{3\pi(r_4^2 - r_o^2)}{4 r_o \sqrt{r_o r_4}}$	$-\frac{r_o}{r_4}$	$-\frac{\pi(r_4^2 - r_o^2)(r_o + 3r_4)}{8 r_o r_4 \sqrt{r_o r_4}}$	$-\frac{\pi(r_4^2 - r_o^2)}{4 r_4 \sqrt{r_o r_4}}$
$\delta \phi_3$	$-\frac{3\pi(r_o + r_4)^2}{4 r_4 \sqrt{r_o r_4}}$	$-\frac{3\pi(r_o + r_4)}{2\sqrt{r_o r_4}}$	$-2\left(\frac{r_o + r_4}{r_4}\right)$	$\frac{\pi(r_o + r_4)(r_o + 3r_4)}{4 r_4 \sqrt{r_o r_4}}$	$\frac{\pi r_o (r_o + r_4)}{2 r_4 \sqrt{r_o r_4}}$

Table A-3b

	$\delta\beta_2$	$\delta\lambda_2$	$\delta\rho_2$	$\delta\ \phi_3$
$\delta\sigma_3 = \delta\sigma_2 = (-1)^N (\text{sgn}\ \lambda_o)\delta\beta_3$	$(-1)^{N+1}(\text{sgn}\ \lambda_o)$	0	0	0
$\delta\lambda_3$	0	-1	0	$(-1)^N \sin\sigma_2\ (\text{sgn}\ \lambda_o)$
$\delta\rho_3$	0	0	1	$\cos\sigma_2$

Table A-4

	$\frac{\delta r_3}{r_4}$	$\frac{\delta U_3}{V_3}$	$\frac{\delta W_3}{V_3}$	$\delta\lambda_3$	$\delta\rho_3$	$\delta\beta_3$	$\frac{\delta(\Delta_{34} V)}{V_3}$	$\frac{\Delta_{34} V}{V_3} \delta\epsilon_{34}$	$\frac{\Delta_{34} V}{V_3} \delta\gamma_{34}$
$\frac{\delta r_4}{r_4}$	1	0	0	0	0	0	0	0	0
$\frac{\delta U_4}{V_3}$	0	$\sin\beta_3$	0	0	0	$\cos\beta_3$	$\sin\gamma_{34}$	0	$\cos\gamma_{34}$
$\frac{\delta W_4}{V_3}$	0	0	1	0	0	0	0	1	0
$\delta\lambda_4$	0	0	0	1	0	0	0	0	0
$\delta\rho_4$	0	0	0	0	1	0	0	0	0
$\delta\beta_4$	0	$-\frac{V_3}{V_4}\cos\beta_3$	0	0	0	$\frac{V_3}{V_4}\sin\beta_3$	$-\frac{V_3}{V_4}\cos\gamma_{34}$	0	$\frac{V_3}{V_4}\sin\gamma_{34}$

APPENDIX B

SATELLITE PERTURBATION RESULTING FROM LUNAR AND SOLAR EFFECTS

1. Introduction

The motion of an unpowered space vehicle is primarily determined by its initial motion and the gravitaional field through which it moves. Radiation pressure, magnetic field effects, collisions with foreign particles, etc., are neglected in the present analysis. For earth satellites computations based on the gravitational field of the earth alone provide the basic orbits. The purpose of this appendix is to investigate the perturbations of a 24-hour circular satellite orbit which are due to lunar and solar gravitational forces.

For simplicity, the effects of the sun and the moon are considered separately. In the solar case, it is assumed that the sun is fixed at the origin and the earth moves in a circle about the sun. In the lunar case the origin is taken at the center of mass of the earth-moon system and the earth and the moon are assumed to move in plane concentric circules about the origin.

After introducing suitable notation and a brief development of the general equations of motion for a modified three-body problem, the equations are specialized to the case of a 24-hour circular satellite orbit about the earth subject to the influence of either the sun or the moon. A general solution to these equations is then obtained and the particular effects of the sun and of the moon are considered separately. In either case the resulting perturbations are quite small, which provides post hoc justification for the separation of the two cases.

CONFIDENTIAL

r = distance from vehicle to earth

R = distance from vehicle to second body

D_1 = distance between earth and center of mass of the system

D_2 = distance between second body and center of mass of the system

ϕ = angular position of the earth

σ = dihedral angle between "plane of motion" and plane of gravitating bodies

ψ = transit angle of vehicle in "plane of motion"

γ = angular position of vehicle measured in plane of gravitating bodies

α = elevation angle of vehicle above plane of gravitating bodies

G = universal gravitational constant

M_s = mass of sun

M_e = mass of earth

M_m = mass of moon

μ_s = GM_s

μ_e = GM_e

μ_m = GM_m

A = nominal (constant) value of ψ

B = nominal (constant) value of ϕ

D = $D_1 + D_2$.

CONFIDENTIAL

2. Notation

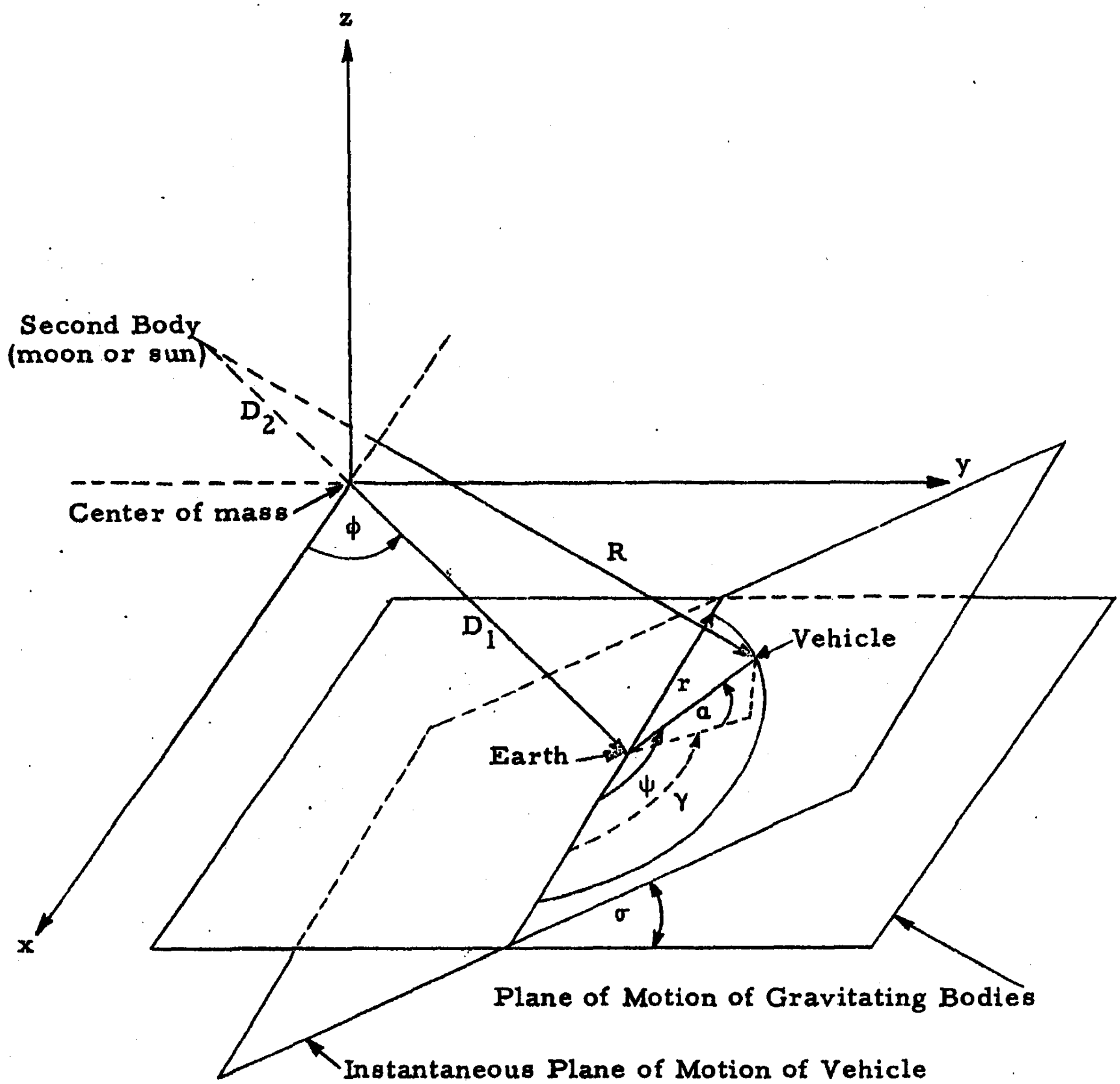

Figure B-1. Geometry and Notation for Vehicle and Moon-Sun Interaction.

CONFIDENTIAL

[redacted]

3. Equations of Motion

The motion will be determined from the Lagrange equations. The potential energy is given by

$$V = -\frac{\mu_e}{r} - \frac{\mu_2}{R}, \qquad \text{(B.1)}$$

where μ_2 equals μ_s or μ_m. The kinetic energy is

$$T = \frac{1}{2}(\dot{X}^2 + \dot{Y}^2 + \dot{Z}^2). \qquad \text{(B.2)}$$

It is convenient to convert these equations to earth coordinates:

$$X = D_1 \cos\phi + r\cos\alpha\cos\gamma,$$
$$Y = D_1 \sin\phi + r\cos\alpha\sin\gamma, \qquad \text{(B.3)}$$
$$Z = r\sin\alpha.$$

Consider the spherical triangle

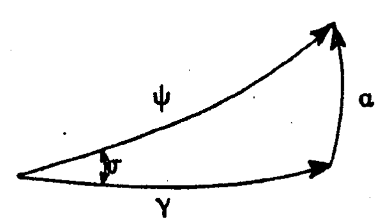

which yields the relations

$$\cos\alpha\cos\gamma = \cos\psi, \qquad \text{(B.4)}$$

$$\cos \alpha \sin \gamma = \cos \alpha \tan \alpha \cot \sigma$$

$$= \sin \sigma \sin \psi \cot \sigma \qquad \text{(B. 5)}$$

$$= \cos \sigma \sin \psi \, ,$$

$$\sin \alpha = \sin \sigma \sin \psi . \qquad \text{(B. 6)}$$

From the definitions of ψ and σ (Figure B-1) these relations are strictly true only when the motion is confined to a plane. The motion is known to consist of small perturbations from a plane and consequently these relations may be used in seeking the perturbations. A more rigorous point of view is to define an "instantaneous plane of motion" determined by the velocity vector and the center of the earth and then to measure ψ as the great-circle angular distance in this plane. With this convention, Equations (B. 4), (B. 5), and (B. 6) hold for arbitrary motion. These equations may be used in (B. 3) to obtain

$$X = D_1 \cos \phi + r \cos \psi ,$$

$$Y = D_1 \sin \phi + r \cos \sigma \sin \psi , \qquad \text{(B. 7)}$$

$$Z = r \sin \sigma \sin \psi .$$

The distance, R, is given by

$$R^2 = X + D_2 (\cos \phi)^2 + (Y + D_2 \sin \phi)^2 + Z^2 ,$$

or

$$R^2 = D^2 + r^2 + 2 Dr (\cos \phi \cos \psi + \cos \sigma \sin \phi \sin \psi) , \qquad \text{(B. 8)}$$

where $D = D_1 + D_2$. The kinetic energy is obtained by differentiating Equation (B. 7) and is found to be

$$
\begin{aligned}
2\,T = {} & \dot{r}^2 + r^2\dot{\psi}^2 + r^2 \sin^2\psi\, \dot{\sigma}^2 + D_1^2 B^2 \\
& + 2\, D_1 B \dot{r} (\cos\phi \cos\sigma \sin\psi - \sin\psi \cos\psi) \\
& + 2\, D_1 B r \dot{\psi} (\cos\phi \cos\sigma \cos\psi + \sin\phi \sin\psi) \\
& - 2\, D_1 B r \sin\psi\, \dot{\sigma} \sin\sigma \cos\phi, \qquad \text{(B. 9)}
\end{aligned}
$$

where $B = \dot{\phi} = \text{constant}$.

Consider first the Lagrange equation for ψ. Take $L = T - V$. Then

$$
\frac{\partial L}{\partial \dot{\psi}} = r^2 \dot{\psi} + D_1 B r (\cos\phi \cos\sigma \cos\psi + \sin\phi \sin\psi) ,
$$

$$
\begin{aligned}
\frac{d}{dt}\left(\frac{\partial L}{\partial \dot{\psi}}\right) = {} & \frac{d}{dt} (r^2 \dot{\psi}) + D_1 B \dot{r} (\cos\phi \cos\sigma \cos\psi + \sin\phi \sin\psi) \\
& - D_1 B r \dot{\sigma} (\cos\phi \sin\sigma \cos\psi) \\
& + D_1 B r \dot{\psi} (\sin\phi \cos\psi - \cos\phi \cos\sigma \sin\psi) \\
& + D_1 B^2 \dot{r} (\cos\phi \sin\psi - \sin\phi \cos\sigma \cos\psi) ,
\end{aligned}
$$

$$
\begin{aligned}
\frac{\partial L}{\partial \psi} = {} & r^2 \sin\psi \cos\psi\, \dot{\sigma}^2 + D_1 B \dot{r} (\cos\phi \cos\sigma \cos\psi + \sin\phi \sin\psi) \\
& - D_1 B r \dot{\sigma} \cos\psi \sin\sigma \cos\phi + D_1 B r \dot{\psi} (\sin\phi \cos\psi - \cos\sigma \sin\psi) \\
& - \frac{\mu_2}{R^3} R \frac{\partial R}{\partial \psi} ,
\end{aligned}
$$

$$
R \frac{\partial R}{\partial \psi} = D r (\sin\phi \cos\sigma \cos\psi - \cos\phi \sin\psi).
$$

Substitution of these quantities in the equation

$$\frac{d}{dt}\left(\frac{\partial L}{\partial \dot{\psi}}\right) - \frac{\partial L}{\partial \psi} = 0$$

gives

$$\frac{d}{dt}(r^2\dot{\psi}) - r^2 \sin\psi\cos\psi\,\dot{\sigma}^2 + (\cos\phi\sin\psi - \sin\phi\cos\psi\cos\sigma)\left(D_1 B^2 r - D r \frac{\mu_2}{R^3}\right) = 0 \qquad \text{(B.10)}$$

The Lagrange equation for r is obtained from

$$\frac{\partial L}{\partial \dot{r}} = \dot{r} + D_1 B (\cos\phi\cos\sigma\sin\psi - \sin\phi\cos\psi),$$

$$\frac{d}{dt}\left(\frac{\partial L}{\partial \dot{r}}\right) = \ddot{r} + D_1 B\dot{\psi}(\cos\phi\cos\sigma\cos\psi + \sin\phi\sin\psi)$$
$$- D_1 B\dot{\sigma}(\cos\phi\sin\sigma\sin\psi) - D_1 B^2(\sin\phi\cos\sigma\sin\psi + \cos\phi\cos\psi),$$

$$\frac{\partial L}{\partial r} = r\dot{\psi}^2 + r\sin^2\psi\,\dot{\sigma}^2 + D_1 B\dot{\psi}(\cos\phi\cos\sigma\cos\psi + \sin\phi\sin\psi)$$
$$- D_1 B\dot{\sigma}\cos\phi\sin\sigma\sin\psi - \frac{\mu_e}{r^2} - \frac{\mu_2}{R^3} R\frac{\partial R}{\partial r},$$

$$R\frac{\partial R}{\partial r} = r + D(\cos\phi\cos\psi + \cos\sigma\sin\phi\sin\psi).$$

Substitution of the above in

$$\frac{d}{dt}\left(\frac{\partial L}{\partial \dot{r}}\right) - \frac{\partial L}{\partial r} = 0$$

yields

$$\ddot{r} - r\,\dot{\psi}^2 - r\sin^2\psi\,\dot{\sigma}^2 + \frac{\mu_e}{r^2} + \frac{\mu_2 r}{R^3}$$

$$+ (\cos\phi\cos\psi + \sin\phi\sin\psi\cos\sigma)\left(\frac{\mu_2 D}{R^3} - D_1 B^2\right) = 0 . \qquad \text{(B.11)}$$

Similarly, in determining the Lagrange equation for σ it is necessary to compute

$$\frac{\partial L}{\partial \dot{\sigma}} = r^2 \sin^2\psi\,\dot{\sigma} - D_1 B r \sin\psi \sin\sigma \cos\phi,$$

$$\frac{d}{dt}\left(\frac{\partial L}{\partial \dot{\sigma}}\right) = \frac{d}{dt}\left(r^2\sin^2\psi\,\dot{\sigma}\right) - D_1 B \dot{r} \sin\psi\sin\sigma\cos\phi - D_1 B r \dot{\sigma} \sin\psi\cos\sigma\cos\phi$$

$$- D_1 B r\,\dot{\psi}\cos\psi\sin\sigma\cos\phi + D_1 B^2 r\sin\psi\sin\sigma\sin\phi,$$

$$\frac{\partial L}{\partial \sigma} = - D_1 B \dot{r}\cos\phi\sin\sigma\sin\psi - D_1 B r\,\dot{\psi}\cos\phi\sin\sigma\cos\psi$$

$$- D_1 B r\,\dot{\sigma}\sin\psi\cos\sigma\cos\phi - \frac{\mu_2}{R^3}\,R\frac{\partial R}{\partial \sigma},$$

$$R\frac{\partial R}{\partial \sigma} = - D r \sin\sigma\sin\phi\sin\psi .$$

From

$$\frac{d}{dt}\left(\frac{\partial L}{\partial \dot{\sigma}}\right) - \frac{\partial L}{\partial \sigma} = 0 ,$$

the equation for σ is found to be

$$\frac{d}{dt}\left(r^2\sin^2\psi\,\dot{\sigma}\right) + (r\sin\psi\sin\phi\sin\sigma)\left(D_1 B^2 - \frac{\mu_2 D}{R^3}\right) = 0 . \qquad \text{(B.12)}$$

The basic equations to be solved are Equations (B. 10), (B. 11), and (B. 12). The quantity $\left[D_1 B^2 - (D\mu_2/R^3)\right]$ occurs repeatedly. For circular motion of two gravitating bodies in a plane, $D_2 \dot{\phi}^2 = \mu_1/D^2$ and $D_1 \dot{\phi}^2 = \mu_2/D^2$. Consequently, $B^2 = \dot{\phi}^2 = \mu_1/D_2/D^2 = \mu_2/D_1 D^2$. With this observation,

$$D_1 B^2 - \frac{D\mu_2}{R^3} = D\mu_2 \left(\frac{1}{D^3} - \frac{1}{R^3}\right)$$

$$= \frac{D\mu_2}{D^3 R^3} (R - D) (R^2 + DR + D^2) = \frac{D\mu_2 (R^2 - D^2)(R^2 + DR + D^2)}{D^3 R^3 (R + D)}$$

$$= \frac{r B^2 \left(\frac{D_1}{D}\right) \left[1 + \frac{R}{D} + \left(\frac{R}{D}\right)^2\right]}{\left(\frac{R}{D}\right)^3 \left(1 + \frac{R}{D}\right)} \left[\left(\frac{r}{D}\right) + 2 (\cos\phi \cos\psi + \cos\sigma \sin\phi \sin\psi)\right]. \tag{B. 13}$$

For both the lunar and solar cases, the approximation $R \simeq D$ in Equation (B. 13) is sufficiently accurate for the study of first-order perturbations. In the lunar case,

$$1.18 < \frac{\left(1 + \frac{R}{D} + \frac{R^2}{D^2}\right)}{\left(\frac{R}{D}\right)^3 \left(1 + \frac{R}{D}\right)} < 1.96;$$

in the solar case,

$$\frac{\left(1 + \frac{R}{D} + \frac{R^2}{D^2}\right)}{\left(\frac{R}{D}\right)^3 \left(1 + \frac{R}{D}\right)} = 1.500 \pm 0.0005.$$

Clearly the approximation is adequate in the solar case; however, in the lunar case the magnitudes of the predicted first-order perturbations may be in error by as much as 30 per cent. With this approximation, Equations (B.10), (B.11), and (B.12) become

$$\frac{d}{dt}(r^2\dot{\psi}) = r^2 \sin\psi \cos\psi \, \dot{\sigma}^2 - \frac{3r^2}{2} B^2 \left(\frac{D_1}{D}\right)\left[\left(\frac{r}{D}\right) + 2(\cos\phi \cos\psi + \cos\sigma \sin\phi \sin\psi)\right]$$

$$(\cos\phi \sin\psi - \cos\psi \sin\phi \cos\sigma), \qquad \text{(B.14)}$$

$$\ddot{r} - r\dot{\psi}^2 + \frac{\mu_e}{r^2} + \frac{\mu_2 r}{D^3} = r \sin^2\psi \, \dot{\sigma}^2 + \frac{3}{2} r B^2 \left(\frac{D_1}{D}\right)\left[\left(\frac{r}{D}\right) + 2(\cos\phi \cos\psi + \cos\sigma \sin\phi \sin\psi)\right]$$

$$(\cos\phi \cos\psi + \sin\phi \sin\psi \cos\sigma), \qquad \text{(B.15)}$$

$$\frac{d}{dt}(r \sin\psi \, \dot{\sigma}) = -\dot{\sigma}(\dot{r} \sin\psi + r \cos\psi \, \dot{\psi}) - \frac{3}{2} r B^2 \left(\frac{D_1}{D}\right)$$

$$\left[\left(\frac{r}{D}\right) + 2(\cos\phi \cos\psi + \cos\sigma \sin\phi \sin\psi)\right] \sin\phi \sin\sigma. \qquad \text{(B.16)}$$

The unperturbed solution is known to be $\dot{r} = 0$, $\dot{\sigma} = 0$, $\dot{\psi} = A$, where A is a constant equal to 2π radians per sidereal day. In order to obtain the first-order perturbations, these unperturbed results are substituted in the right-hand sides of Equations (B.14), (B.15), and (B.16). Furthermore, $r/D << 1$ in both the lunar and solar cases and, consequently, this term is dropped in the expression $\left[(r/D) + 2(\cos\phi \cos\psi + \sin\phi \sin\psi \cos\sigma)\right]$. With these further approximations the equations for the perturned motion become

$$\frac{d}{dt}(r^2\dot{\psi}) = -3r^2 B^2 \left(\frac{D_1}{D}\right)(\cos\phi \cos\psi + \cos\sigma \sin\phi \sin\psi)$$

$$(\cos\phi \sin\psi - \cos\psi \sin\phi \cos\sigma), \qquad \text{(B.17)}$$

$$\ddot{r} - r\dot{\psi}^2 + \frac{\mu_e}{r^2} + \frac{\mu_2 r}{D^3} = 3\,r\,B^2\left(\frac{D_1}{D}\right)\ (\cos\phi\cos\psi + \cos\sigma\sin\phi\sin\psi)^2, \tag{B.18}$$

$$\frac{d}{dt}\ (r\sin\psi\,\dot{\sigma}) = -\,3\,r\,B^2\left(\frac{D_1}{D}\right)\ (\cos\phi\cos\psi + \cos\sigma\sin\phi\sin\psi)\ \sin\phi\sin\sigma. \tag{B.19}$$

4. <u>Solution of Perturbed Equations</u>

Using elementary trigonometric identities, Equation (B.17) becomes

$$\frac{d}{dt}\ (r^2\dot{\psi}) = -\frac{3\,r^2 B^2}{4}\left(\frac{D_1}{D}\right)\Big[\sin 2\psi\,(1 - \cos^2\sigma) + \sin 2\psi\,\cos 2\phi\,(1 + \cos^2\sigma) - 2\cos\sigma\,\sin 2\phi\,\cos 2\psi\Big]. \tag{B.20}$$

On the right-hand side, $\dot{\psi} = A$, $\dot{\phi} = B$, $\dot{\sigma} = 0$, and $\dot{r} = 0$. Consequently, Equation (B.20) may be integrated directly

$$r^2\dot{\psi} = r^2 A + \frac{3\,r^2 B^2}{8\,A}\left(\frac{D_1}{D}\right)\Bigg\{\cos\,(2\,At + 2\psi_o)\,(1 - \cos^2\sigma) + \frac{(1 + \cos^2\sigma)}{2}\left[\frac{\cos 2\,(At + Bt\psi_o + \phi_o)}{(1 + B/A)} + \frac{\cos 2\,(At - Bt + \psi_o - \phi_o)}{(1 - B/A)}\right] - \cos\sigma\left[\frac{\cos 2\,(At + Bt + \psi_o + \phi_o)}{(1 + B/A)} - \frac{\cos 2\,(At - Bt + \psi_o - \phi_o)}{(1 - B/A)}\right]\Bigg\}, \tag{B.21}$$

$$\psi = \psi_o + A_1 t + \frac{3}{16}\frac{B^2}{A^2}\left(\frac{D_1}{D}\right)\left\{(1 - \cos^2\sigma)\sin 2(At + \psi_o)\right.$$

$$+ \frac{(1+\cos^2\sigma)}{2}\left[\frac{\sin 2(At + Bt + \psi_o + \phi_o)}{(1 + B/A)^2} + \frac{\sin 2(At - Bt + \psi_o - \phi_o)}{(1 - B/A)^2}\right]$$

$$\left. - \cos\sigma\left[\frac{\sin 2(At + Bt + \psi_o + \phi_o)}{(1 + B/A)^2} - \frac{\sin 2(At - Bt + \psi_o - \phi_o)}{(1 - B/A)^2}\right]\right\}. \qquad (B.22)$$

In Equation (B.18), take $r = r_o + \delta$, where r_o is the solution of

$$- r_o A^2 + r_o \frac{\mu_2}{D^3} + \frac{\mu_e}{r_o^2} = 0. \qquad (B.23)$$

Equation (B.18) becomes

$$\ddot{\delta} - (r_o + \delta)\left(A^2 - \frac{\mu_2}{D^3}\right) + \frac{\mu_e}{(r_o+\delta)^3} = 3 r_o \left(1 + \frac{\delta}{r_o}\right) B^2 \left(\frac{D_1}{D}\right)(\cos\phi\cos\psi + \cos\sigma\sin\phi\sin\psi)^2. \qquad (B.24)$$

But from Equation (B.23)

$$- (r_o + \delta)\left(A^2 - \frac{\mu_2}{D^3}\right) + \frac{\mu_e}{(r_o+\delta)^3} = - (r_o+\delta)\frac{\mu_e}{r_o^3} + \frac{\mu_e}{(r_o+\delta)^2} = \frac{\mu_e}{r_o^3 (r_o+\delta)^2}\left[r_o^3 - (r_o+\delta)^3\right],$$

and retaining first-order terms in δ,

$$- (r_o + \delta)\left(A^2 - \frac{\mu_2}{D^3}\right) + \frac{\mu_2}{(r_o+\delta)^3} \simeq - \frac{3 r_o^2 \delta \mu_e}{r_o^5} = - \frac{3\mu_e}{r_o^3}\delta . \qquad (B.25)$$

[redacted]

But for the unperturbed circular satellite, $\frac{\mu_e}{r_o^3} = A^2$, and Equation (B.24) becomes

$$\ddot{\delta} - 3A^2\delta \simeq 3r_o B^2 \left(\frac{D_1}{D}\right)(\cos\phi\cos\psi + \cos\sigma\sin\phi\sin\psi)^2. \tag{B.26}$$

The solution of the homogeneous equation is $\delta = 0$, and consequently it is only necessary to find a particular integral. The equation may be rewritten in the form

$$\ddot{\delta} - 3A^2\delta = 3r_o B^2\left(\frac{D_1}{D}\right)\left[\frac{(1+\cos\sigma)^2}{4}\cos^2(\psi-\phi) + \frac{(1-\cos\sigma)^2}{4}\cos^2(\psi+\phi) + \frac{(1-\cos^2\sigma)}{2}\cos(\psi+\phi)\cos(\psi-\phi)\right],$$

or

$$\ddot{\delta} - 3A^2\delta = 3r_o B^2\left(\frac{D_1}{D}\right)\left\{\frac{(1+\cos\sigma)^2}{8}\left[1+\cos 2(\psi-\phi)\right] + \frac{(1-\cos\sigma)^2}{8}\left[1+\cos 2(\psi+\phi)\right] + \frac{(1-\cos^2\sigma)}{4}(\cos 2\psi + \cos 2\phi)\right\}. \tag{B.27}$$

Hence,

$$\delta = \delta_o + C_1\cos 2(\psi-\phi) + C_2\cos 2(\psi+\phi) + C_3\cos 2\psi + C_4\cos 2\phi. \tag{B.28}$$

Substitution of (B.28) in (B.27) determines the unknown coefficients, C_i.

[redacted]

The result is

$$\delta = -\frac{r_o}{2}\frac{B^2}{A^2}\left(\frac{D_1}{D}\right) - \frac{3 r_o B^2}{8 A^2}\left(\frac{D_1}{D}\right)\frac{(1+\cos\sigma)^2}{\left[4(1-B/A)^2+3\right]}\cos 2(\psi-\phi)$$

$$-\frac{3 r_o B^2}{8 A^2}\left(\frac{D_1}{D}\right)\frac{(1-\cos\sigma)^2}{\left[4(1+B/A)^2+3\right]}\cos 2(\psi+\phi) - \frac{3 r_o}{28}\frac{B^2}{A^2}\left(\frac{D_1}{D}\right)(1-\cos^2\sigma)\cos 2\psi$$

$$-\frac{3 r_o}{4}\left(\frac{B^2}{A^2}\right)\left(\frac{D_1}{D}\right)(1-\cos^2\sigma)\frac{\cos 2\phi}{(3+4B^2/A^2)} \quad . \qquad \text{(B. 29)}$$

Equation (B. 19) for $\dot{\sigma}$ is written in terms of $(r \sin\psi\,\dot{\sigma})$. This quantity represents the velocity normal to the nominal plane of motion. Let $\dot{W} = r\sin\psi\dot{\sigma}$. From Equation (B. 19)

$$\ddot{W} = -\frac{3 r \sin\sigma}{4} B^2\left(\frac{D_1}{D}\right)\left[(1-\cos\sigma)\sin(\psi+2\phi) - (1+\cos\sigma)\sin(\psi\ 2\phi) + 2\cos\sigma\sin\psi\right],$$

$$\dot{W} = \frac{3 r \sin\sigma}{4}\left(\frac{B^2}{A}\right)\left(\frac{D_1}{D}\right)\left[\frac{(1-\cos\sigma)\cos(\psi+2\phi)}{(1+2B/A)} - \frac{(1+\cos\sigma)\cos(\psi-2\phi)}{(1-2B/A)} + 2\cos\sigma\cos\psi\right], \qquad \text{(B. 30)}$$

$$W = \frac{3 r \sin\sigma}{4}\left(\frac{B^2}{A^2}\right)\left(\frac{D_1}{D}\right)\left[\frac{(1-\cos\sigma)\sin(\psi+2\phi)}{(1+2B/A)^2} - \frac{(1+\cos\sigma)\cos(\psi-2\phi)}{(1-2B/A)^2} + 2\cos\sigma\sin\psi\right]. \qquad \text{(B. 31)}$$

5. Lunar Perturbations

When the moon is the second body, B = 2 radians per month, $\mu_2/\mu_e \simeq 1/80$, and $(D_1/D) \simeq 1/80$. Take $r = 26 \times 10^3$ miles and $B/A = 1/28$. The magnitudes of the various perturbations are then easily estimated.

From Equations (B.21) and (B.22),

$$\dot{\psi} \simeq A + 3.75 \times 10^{-5} \text{ (periodic terms) rad/day,}$$

$$\psi = \psi_o + At + 3\ 10^{-6} \text{ (periodic terms) rad (t in days).}$$

The periodic terms do not add up to more than 5. With this observation and recalling that the approximation used in Equation (B.13) might be 30 per cent low, the maximum estimated perturbations due to the moon are

$$\delta(\dot{\psi})_{max} < 1.02 \times 10^{-5} \text{ rad/hr} = 1.7 \times 10^{-7} \text{ rad/min} = 2.8 \times 10^{-9} \text{ rad/sec,}$$

$$\delta(r\dot{\psi})_{max} < 0.265 \text{ mile/hr} = 0.39 \text{ ft/sec,}$$

$$\delta(\psi)_{max} < 1.95 \times 10^{-5} \text{ rad} = 0.001 \text{ deg,}$$

$$\delta(r\psi)_{max} < 0.51 \text{ mile.}$$

From Equation (B.29),

$$\delta(\dot{r})_{max} < 0.13 \text{ mile/hr,}$$

$$\delta(r)_{max} < 0.26 \text{ mile.}$$

The mean value of r is not quite the same as the unperturbed value. From Equation (B.23),

$$r_o^3 = \frac{\mu_e}{A^2\left(1 - \frac{B^2}{A^2}\frac{D_1}{D}\right)},$$

$$r_o = r_o^*\left(1 + \frac{1}{3}\frac{B^2}{A^2}\frac{D_1}{D}\right),$$

where $r_o^* = \sqrt[3]{\frac{\mu_e}{A^2}}$ is the unperturbed value of r. The mean value of r is given by

$$r_o + \delta_o = r_o^* - \frac{1}{6}\frac{B^2}{A^2}\frac{D_1}{D}\; r_o \simeq r_o^* - 0.09 \text{ mile.}$$

From Equations (B.30) and (B.31),

$$\delta\,(\dot{W})_{max} < 0.6 \text{ mile/hr} = 0.9 \text{ ft/sec,}$$

$$\delta\,(W)_{max} < 2.4 \text{ miles.}$$

6. <u>Solar Perturbations</u>

When the sun is the second body, $B = 2\pi$ radians per year and $\left(\frac{D_1}{D}\right) \simeq 1$. With $r = 26 \times 10^3$ miles and $B/A = \frac{1}{365}$, the magnitudes of the perturbations are again easily estimated.

From Equations (B.21) and (B.22),

$$\delta\,(\dot{\psi})_{max} < 4 \times 10^{-6} \text{ rad/hr} = 1.1 \times 10^{-9} \text{ rad/sec,}$$

$$\delta\,(r\dot{\psi})_{max} < 0.104 \text{ mile/hr} = 0.15 \text{ ft/sec,}$$

$$\delta\,(\psi)_{max} < 7.5 \times 10^{-6} \text{ rad} = 4 \times 10^{-4} \text{ deg,}$$

$$\delta\,(r\psi)_{max} < 0.20 \text{ mile.}$$

From Equation (B.29)

$$\delta\,(\dot{r})_{max} < 0.05 \text{ mile/hr,}$$

$$\delta\,(r)_{max} < 0.1 \text{ mile.}$$

The mean radial distance is

$$r_o = r_o^* - 0.034 \text{ mile.}$$

From Equations (B.30) and (B.31)

$$\delta\,(\dot{W})_{max} < 0.23 \text{ mile/hr}$$

$$\delta\,(W)_{max} < 0.9 \text{ mile.}$$

APPENDIX C

ATTITUDE CONTROL

The first step in setting up the equations of attitude motion is the choice of a suitable attitude reference system. We shall choose the geocentric reference axes xyz with origin at the center of mass of the vehicle. The z axis is directed along the outward-pointing geocentric radius through the vehicle. The x axis is normal to the z axis and lies in the instantaneous orbital plane. It has the same sense as the vehicle's orbital velocity. The y axis is chosen normal to the xz plane so as to form a right-handed coordinate system. The angular velocity of this xyz system in inertial space is

$$\vec{\omega} = \omega_x \vec{e}_x + \omega_y \vec{e}_y + \omega_z \vec{e}_z ,$$

resolved along the xyz system.

There are other more complicated attitude reference systems which are discussed in detail by R. E. Roberson,* a leading authority on attitude motions of satellite vehicles. We shall use his notation in the following analysis.

Let XYZ form a right-handed orthogonal system of axes imbedded in the body of the vehicle, such that XYZ coincides with xyz for the correct attitude. Let us choose the XYZ system along the principal axes of inertia of the vehicle which has principal moments of inertia I_X, I_Y, and I_Z. The angular velocity of XYZ in inertial space resolved along the XYZ system is

$$\vec{\omega}^* = \omega_X \vec{e}_X + \omega_Y \vec{e}_Y + \omega_Z \vec{e}_Z .$$

---

*Roberson, Robert E., (a) Attitude Control of a Satellite Vehicle--An Outline of the Problems. Presented at the Eighth International Astronautical Congress, Barcelona, Spain, October 6 to 12, 1957. (b) Orbital Behavior of Earth Satellites; (c) Torques on a Satellite Vehicle From Internal Moving Parts; (d) Gravitational Torque on a Satellite Vehicle; (e) Principles of Inertial Control of Satellite Attitude.

These papers may be obtained from Autonetics, North American Aviation, Inc., Downey, California.

If L_X, L_Y, and L_Z are the torques applied about the X, Y, and Z axes of the body, then Euler's equations, which describe the general motion of the body about its center of mass, take the form

$$I_X\dot{\omega}_X + (I_Z - I_Y)\,\omega_Z\omega_Y = L_X \tag{C.1a}$$

$$I_Y\dot{\omega}_Y + (I_X - I_Z)\,\omega_X\omega_Z = L_Y \tag{C.1b}$$

$$I_Z\dot{\omega}_Z + (I_Y - I_X)\,\omega_Y\omega_X = L_Z\,. \tag{C.1c}$$

Now we must express these equations in terms of attitude deviation angles. Let the angles θ_1, θ_2, and θ_3 specify the orientation of XYZ relative to xyz. These angles are measured in the way shown in Figure C-1. θ_1 is a rotation about the x axis. θ_2 is a rotation about the y' axis which lies in the yz plane and makes the angle θ_1 with the y axis. θ_3 is a rotation about the z" axis which lies in the z'x' plane and makes an angle θ_2 with the z' axis. The unit vectors in the XYZ and xyz systems are related by

$$\vec{e}_X = \cos\theta_2\cos\theta_3\vec{e}_x + (\sin\theta_1\sin\theta_2\cos\theta_3 + \sin\theta_3\cos\theta_1)\,\vec{e}_y + (\sin\theta_1\sin\theta_3 - \sin\theta_2\cos\theta_1\cos\theta_3)\,\vec{e}_z \tag{C.2a}$$

$$\vec{e}_Y = -\sin\theta_3\cos\theta_2\vec{e}_x + (\cos\theta_1\cos\theta_3 - \sin\theta_1\sin\theta_2\sin\theta_3)\,\vec{e}_y + (\cos\theta_3\sin\theta_1 + \sin\theta_2\sin\theta_3\cos\theta_1)\,\vec{e}_z \tag{C.2b}$$

$$\vec{e}_Z = \sin\theta_2\vec{e}_x - \sin\theta_1\cos\theta_2\vec{e}_y + \cos\theta_1\cos\theta_2\vec{e}_z\,. \tag{C.2c}$$

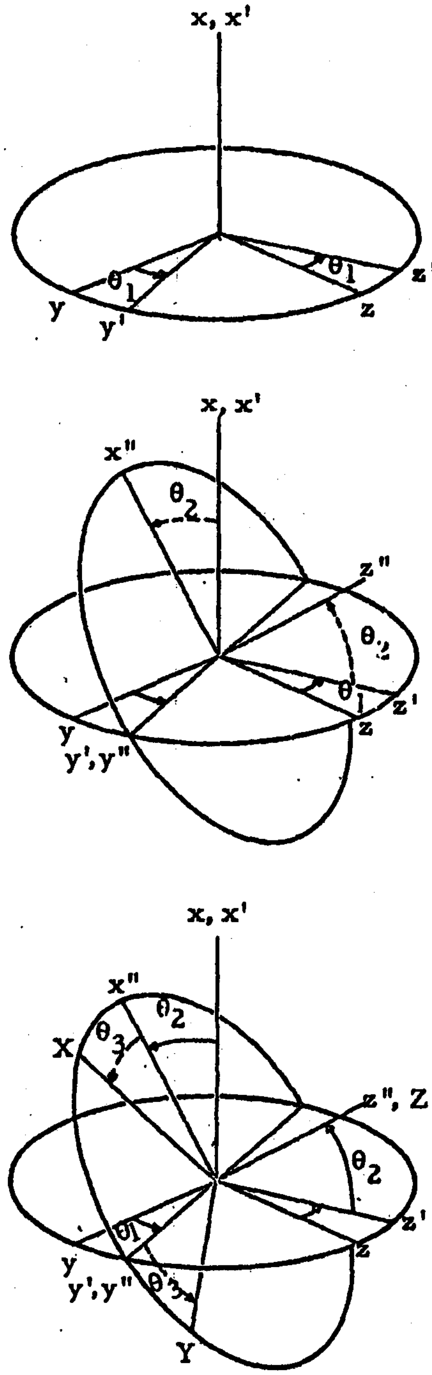

Figure C-1. Relationship of Body Axes to Reference Axes.

Any infinitesimal rotation may be expressed as a vector $\overrightarrow{d\theta}$ which is

$$\overrightarrow{d\theta} = d\theta_1 \vec{e}_x + d\theta_2 \vec{e}_{y'} + d\theta_3 \vec{e}_{z''}$$

$$= (d\theta_1 + d\theta_3 \sin\theta_2)\vec{e}_x + (d\theta_2 \cos\theta_1 - d\theta_3 \cos\theta_2 \sin\theta_1)\vec{e}_y$$

$$+ (d\theta_2 \sin\theta_1 + d\theta_3 \cos\theta_2 \cos\theta_1)\vec{e}_z \, . \qquad (C.3)$$

The angular velocity $\vec{\omega}'$ of the body axes relative to the reference axes is therefore

$$\vec{\omega}' = (\dot{\theta}_1 + \dot{\theta}_3 \sin\theta_2)\vec{e}_x + (\dot{\theta}_2 \cos\theta_1 - \dot{\theta}_3 \sin\theta_1 \cos\theta_2)\vec{e}_y$$

$$+ (\dot{\theta}_2 \sin\theta_1 + \dot{\theta}_3 \cos\theta_1 \cos\theta_2)\vec{e}_z \, . \qquad (C.4)$$

The relationship between the angular velocities is

$$\vec{\omega}^* = \vec{\omega} + \vec{\omega}' \, . \qquad (C.5)$$

$\vec{\omega}$ and $\vec{\omega}'$ may be expressed in terms of $\vec{e}_X$, $\vec{e}_Y$, and $\vec{e}_Z$ by Equations (C.2). Then it follows immediately from Equation (C.5) that, for small attitude deviations,

$$\omega_X = \omega_x + \dot{\theta}_1 + \omega_y\theta_3 - \omega_z\theta_2 + \dot{\theta}_2\theta_3 \qquad (C.6a)$$

$$\omega_Y = \omega_y + \dot{\theta}_2 + \omega_z\theta_1 - \omega_x\theta_3 - \dot{\theta}_1\theta_3 \qquad (C.6b)$$

$$\omega_Z = \omega_z + \dot{\theta}_3 + \omega_x\theta_2 - \omega_y\theta_1 + \dot{\theta}_1\theta_2 \, . \qquad (C.6c)$$

When these expressions are placed in Equations (C.1), the equations of attitude motion for small values of θ_1, θ_2, and θ_3 (less than 10°) take a useful form:

$$I_X \frac{d}{dt} \left(\underline{\omega_x} + \dot{\theta}_1 + \omega_y \theta_3 - \underline{\omega_z \theta_2} + \dot{\theta}_2 \theta_3 \right)$$

$$+ (I_Z - I_Y) \left(\omega_y + \dot{\theta}_2 + \underline{\omega_z \theta_1} - \underline{\omega_x \theta_3} - \dot{\theta}_1 \theta_3 \right) \left(\underline{\omega_z} + \dot{\theta}_3 + \underline{\omega_x \theta_2} - \omega_y \theta_1 + \dot{\theta}_1 \theta_2 \right)$$

$$= L_X \qquad \text{(C.7a)}$$

$$I_Y \frac{d}{dt} \left(\omega_y + \dot{\theta}_2 + \underline{\omega_z \theta_1} - \underline{\omega_x \theta_3} - \dot{\theta}_1 \theta_3 \right)$$

$$+ (I_X - I_Z) \left(\underline{\omega_x} + \dot{\theta}_1 + \omega_y \theta_3 - \underline{\omega_z \theta_2} + \dot{\theta}_2 \theta_3 \right) \left(\underline{\omega_z} + \dot{\theta}_3 + \underline{\omega_x \theta_2} - \omega_y \theta_1 + \dot{\theta}_1 \theta_2 \right)$$

$$= L_Y \qquad \text{(C.7b)}$$

$$I_Z \frac{d}{dt} \left(\underline{\omega_z} + \dot{\theta}_3 + \underline{\omega_x \theta_2} - \omega_y \theta_1 + \dot{\theta}_1 \theta_2 \right)$$

$$+ (I_Y - I_X) \left(\omega_y + \dot{\theta}_2 + \underline{\omega_z \theta_1} - \underline{\omega_x \theta_3} - \dot{\theta}_1 \theta_3 \right) \left(\underline{\omega_x} + \dot{\theta}_1 + \omega_y \theta_3 - \underline{\omega_z \theta_2} + \dot{\theta}_2 \theta_3 \right)$$

$$= LZ \qquad \text{(C.7c)}$$

Now in our application the terms containing ω_x and ω_z in Equations (C.7) are extremely small compared to other terms and so may be neglected. If $\dot{\Lambda}_\Omega$ is the rate of regression of the nodes, γ is the angle the orbital plane makes with the equator, and β is the angle from the ascending node to the satellite, as shown in Figure C-2, then

$$\omega_x = \dot{\Lambda}_\Omega \sin\gamma \cos\beta$$

$$\omega_y = \dot{\beta} + \dot{\Lambda}_\Omega \cos\gamma$$

$$\omega_z = \dot{\Lambda}_\Omega \sin\gamma \sin\beta \, .$$

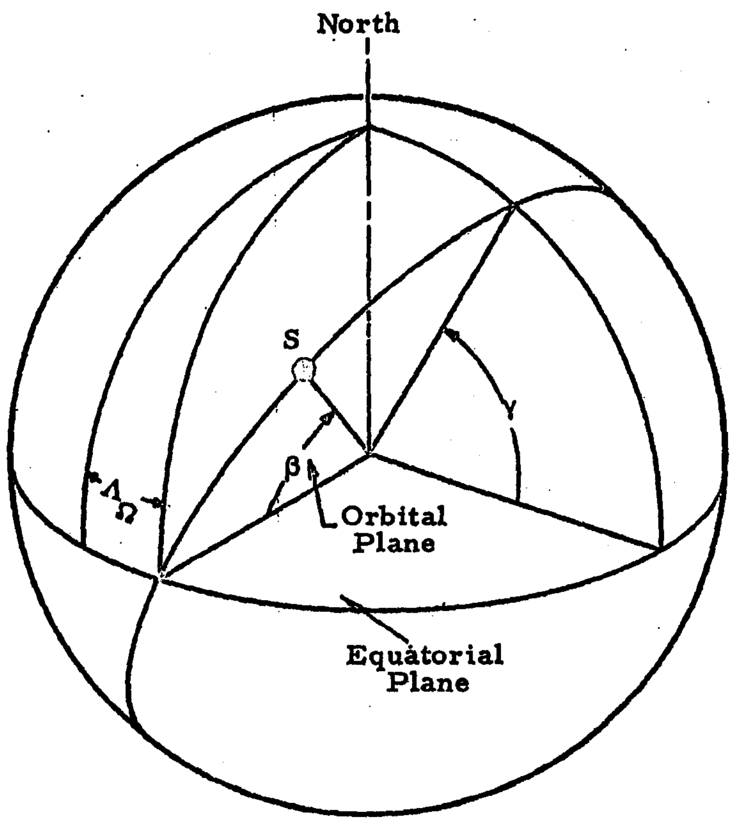

S = Satellite

Figure C-2. Geometry of the Coordinate System for the Satellite in Orbit.

If the orbit were kept exactly circular and at either $\gamma = 0$ or $\pi/2$, ω_x and ω_z would be zero. If the orbit is such at $\gamma \leq 2^o$ or $\geq 88^o$, the forces required to overcome the oblateness perturbations are about a gram in size (assuming a 1000-pound satellite). If these correction forces are not applied, the values of ω_x and ω_y may be found from the rate of regression of the nodes given by Blitzer and Wheelon.*

$$\text{For } \gamma \leq 2^o \begin{cases} \dot{\Lambda}_\Omega \leq 3 \times 10^{-9} \text{ rad/sec} \\ \therefore \quad \omega_x, \omega_z < 10^{-10} \end{cases}$$

$$\text{For } \gamma \geq 88^o \begin{cases} \dot{\Lambda}_\Omega \leq 10^{-10} \\ \therefore \quad \omega_x, \omega_z < 10^{-10} \end{cases}$$

Thus, it is clear that, in any case, ω_x and ω_z are so small that the terms underlined in Equations (C.7) may be neglected. The terms containing ω_y may also be neglected and wherever ω_y appears it may be replaced by ω_o, the angular orbital velocity of the satellite. ω_o is approximately 10^{-4} rad/sec.

The torque L on the satellite is produced by the gravitational gradient, by rotating internal parts, by electric and magnetic forces, by radiation pressure, by a control system, and by many other forces. We shall consider here only those torques arising from the gravitational field, the control system, and a rotating part having a constant angular mementum, H, fixed relative to the body. The other torques are mostly small enough to neglect, though it is conceivable that in certain satellite designs they could play an important part. The components of $\vec{L}$ are

---

*(a) Blitzer, Leon, Morris Weisfeld, and Albert D. Wheelon, "Perturbations of a Satellite's Orbit Due to the Earth's Oblateness," J. Appl. Phys., 27, 1141, October 1956.
(b) Blitzer, Leon and Albert D. Wheelon, "Oblateness Perturbation of Elliptical Satellite Orbits," J. Appl. Phys., 28, 279, February 1957.
(c) Blitzer, Leon, "Apsidal Motion of an ICY Satellite," J. Appl. Phys., 28, 1362, November 1957.

$$L_X = -3\omega_o^2 (I_Y - I_Z)\,\theta_1 + H_Y(\dot{\theta}_3 + \dot{\theta}_1\theta_2 - \theta_1\omega_y) - H_Z(\omega_y - \dot{\theta}_1\theta_3 + \dot{\theta}_2) + L_{Xa} \qquad \text{(C.8a)}$$

$$L_Y = -3\omega_o^2 (I_X - I_Z)\,\theta_2 + H_Z(\dot{\theta}_1 + \dot{\theta}_2\theta_3 + \omega_y\theta_3) - H_X(\dot{\theta}_3 + \dot{\theta}_1\theta_2 - \omega_y\theta_1) + L_{Ya} \qquad \text{(C.8b)}$$

$$L_Z = H_X(\dot{\theta}_2 - \dot{\theta}_1\theta_3 + \omega_y) - H_Y(\dot{\theta}_1 + \dot{\theta}_2\theta_3 + \omega_y\theta_3) + L_{Za}, \qquad \text{(C.8c)}$$

where $\vec{L}_a$ is the torque applied by the control system and

$$\vec{H} = H_X\vec{e}_X + H_Y\vec{e}_Y + H_Z\vec{e}_Z$$

is an angular mementum fixed in the body of the satellite. Apparently we should choose $H_X = H_Z = 0$ in order to eliminate the constant driving torques in Equations (C.8a) and (C.8c). Placing the expressions for L_X, L_Y, and L_Z in Equations (C.7), replacing ω_y by ω_o, and dropping small terms, we obtain

$$I_X\ddot{\theta}_1 + (I_X + I_Z - I_Y)(\dot{\theta}_2\dot{\theta}_3 + \underline{\omega_o\dot{\theta}_3}) = -\underline{4\omega_o^2(I_Y - I_Z)}\,\theta_1 + H_Y(\dot{\theta}_3 - \underline{\theta_1\omega_o}) + L_{Xa} \qquad \text{(C.9a)}$$

$$I_Y\ddot{\theta}_2 + (I_X - I_Z - I_Y)\,\dot{\theta}_1\dot{\theta}_3 = \underline{-3\omega_o^2(I_X - I_Z)\,\theta_2} + L_{Ya} \qquad \text{(C.9b)}$$

$$I_Z\ddot{\theta}_3 + (I_Y - I_X + I_Z)\,\dot{\theta}_1\dot{\theta}_2 + \underline{(I_Y - I_X - I_Z)}\,\omega_o\dot{\theta}_1 = -H_Y(\dot{\theta}_1 + \underline{\omega_o\theta_3}) + L_{Za} + (I_Y - I_X)\,\omega_o^2\,\theta_3 \qquad \text{(C.9c)}$$

Let us now consider the initial motion of the satellite, when it has been placed in the desired orbit. To be conservative, let us assume the initial angles and rates to be around 2° and 1/2 rpm (3.5×10^{-2} radian and 5×10^{-2} radian per second). These are typical separation angles and tumbling rates for present nose cones. Suppose that it is desired to reduce θ and $\dot{\theta}$ down to 10^{-3} radians and 10^{-4} radians per second, respectively. For this range of angles and rates, the terms underlined in Equations (C.9) may be neglected. Let us assume that H_Y is of the order of 10 slug ft^2 radians per second and that I_X, I_Y, and I_Z are of the order of a few hundred slug ft^2. Keeping only the important terms in Equations (C.9) we obtain

$$I_X \ddot{\theta}_1 = H_Y \dot{\theta}_3 - (I_X + I_Z - I_Y) \dot{\theta}_2 \dot{\theta}_3 + L_{Xa} \qquad \text{(C.10a)}$$

$$I_Y \ddot{\theta}_2 = -(I_X - I_Z - I_Y) \dot{\theta}_1 \dot{\theta}_3 + L_{Ya} \qquad \text{(C.10b)}$$

$$I_Z \ddot{\theta}_3 = -H_Y \dot{\theta}_1 - (I_Y - I_X + I_Z) \dot{\theta}_1 \dot{\theta}_2 + L_{Za} . \qquad \text{(C.10c)}$$

In order to make the solution of these equations as simple as possible, choose control torques

$$L_{Xa} = -k_1 \theta_1 - \lambda_1 \dot{\theta}_1 + (I_X + I_Z - I_Y) \dot{\theta}_2 \dot{\theta}_3 - H_Y \dot{\theta}_3 \qquad \text{(C.11a)}$$

$$L_{Ya} = -k_2 \theta_2 - \lambda_2 \dot{\theta}_2 + (I_X - I_Z - I_Y) \dot{\theta}_1 \dot{\theta}_3 \qquad \text{(C.11b)}$$

$$L_{Za} = -k_3 \theta_3 - \lambda_3 \dot{\theta}_3 + (I_Y - I_X - I_Z) \dot{\theta}_1 \dot{\theta}_2 + H_Y \dot{\theta}_1 . \qquad \text{(C.11c)}$$

Then Equations (C.10) become

$$I_X \ddot{\theta}_i + \lambda_i \dot{\theta}_i + k_i \theta_i = 0 , \qquad i = 1, 2, 3 , \qquad \text{(C.12)}$$

which have the simple solutions

$$\theta_i(t) = \theta_i(0) \exp \left(-\frac{\lambda_i}{2I_i} t\right)\left[\cos \Omega_i t + \frac{1}{\Omega_i}\left(\frac{\dot{\theta}_i(0)}{\theta_i(0)} + \frac{\lambda_i}{2I_i}\right) \sin \Omega_i t\right], \quad i = 1, 2, 3 \tag{C.13}$$

where

$$\Omega_i = \frac{1}{2}\left[4\frac{k_i}{I_i} - \left(\frac{\lambda_i}{I_i}\right)^2\right]^{1/2} \tag{C.14}$$

This solution can be rewritten

$$\theta_i(t) = C_i^* \exp\left(\frac{\lambda_i}{2I_i} t\right) \cos (\Omega_i t + \epsilon_i^*) , \tag{C.15}$$

where

$$C_i^* = \frac{\theta_i(0)}{\cos \epsilon_i^*} \tag{C.16}$$

and

$$\epsilon_i^* = \tan^{-1}\left[-\frac{\dot{\theta}_i(0) + \frac{\lambda_i}{2I_i}\theta_i(0)}{\Omega_i \theta_i(0)}\right] . \tag{C.17}$$

If we choose $\lambda_i \simeq 80$ foot pound seconds per radian and $k_i \simeq 90$ foot pounds per radian, Ω_i will have the value 1/3 radian per second and the oscillations will not exceed 10 degrees in magnitude. The forces needed to apply the torques $\lambda\theta$ and $k\theta$ do not exceed two pounds. The forces required to cancel the terms containing H_Y and $\dot{\theta}_i \dot{\theta}_j$ do not exceed one pound. Within two or three minutes the oscillations should be reduced to the desired values and the control system turned off. If we choose simpler torques:

$$L_{Xa} = -k_1\theta_1 - \lambda_1\theta_1 ,$$

$$L_{Ya} = -k_2\theta_2 - \lambda_2\dot{\theta}_2 ,$$

$$L_{Za} = -k_3\theta_3 - \lambda_3\dot{\theta}_3 ,$$

and solve Equations (C. 10) numerically, we find that the oscillations behave qualitatively in the same way. The angles still remain less than 10 degrees and in a few minutes they are reduced to the samll values desired.

Now suppose that the oscillations have been reduced so that $\theta < 10^{-3}$ radian and $\theta < 10^{-4}$ radian per second. Is a control system necessary, or will the oscillations remain small? The largest terms in Equations (C. 9a) and (C. 9c) are the H_Y terms. The dominant motion of θ_1 and θ_3 is then given by the equations

$$I_X\ddot{\theta}_1 = H_Y\theta_3 \qquad \text{(C. 18)}$$

$$I_Z\ddot{\theta}_3 = -H_Y\theta_1 \qquad \text{(C. 19)}$$

The solutions are

$$\theta_1(t) = \theta_1(0) + \frac{1}{H_Y}\left(\dot{\theta}_3(0)\,I_Z + \theta_1(0)\sqrt{I_XI_Z}\,\sin\Omega\,t - \dot{\theta}_3(0)\,I_Z\cos\Omega\,t\right) \qquad \text{(C. 20)}$$

$$\theta_3(t) = \theta_3(0) + \frac{1}{H_Y}\left(-\dot{\theta}_1(0)\,I_X + \dot{\theta}_3(0)\sqrt{I_XI_Z}\,\sin\Omega t + \dot{\theta}_1(0)\,I_X\cos\Omega\,t\right) \qquad \text{(C. 21)}$$

where

$$\Omega = \frac{H_Y}{\sqrt{I_XI_Z}} . \qquad \text{(C. 22)}$$

Therefore, if $\theta(0) \simeq 10^{-3}$ and $\dot{\theta}(0) \simeq 10^{-4}$, $I_X \simeq 800$ slug ft^2 and $I_Z \simeq 150$ slug ft^2, then θ_1 and θ_3 will stay less than 1.5×10^{-3} radians if we choose $H_Y = 80$ slug ft^2 radians per second.

The θ_2 behavior is given by

$$I_Y \ddot{\theta}_2 + (I_X - I_Z - I_Y)\,\dot{\theta}_1 \dot{\theta}_3 = -3\omega_o^2 (I_X - I_Z)\,\theta_2 \qquad \text{(C. 23)}$$

The gravitational restoring torque on the right-hand side is not large enough to keep θ_2 small. To see this, let $I_X = I_Y + I_Z$ (to remove the nonlinear term). Then the solution of Equation (C. 23) is

$$\theta_2(t) = \frac{\dot{\theta}_2(0)}{\omega_g} \sin \omega_g t + \theta_2(0) \cos \omega_g t \, ,$$

where

$$\omega_g = \left[3\omega_o^2 \, \frac{(I_X - I_Z)}{I_Y} \right]^{1/2} \simeq 10^{-4} \, . \qquad \text{(C. 24)}$$

for $\theta(0) \simeq 10^{-3}$ and $\dot{\theta}(0) \simeq 10^{-4}$,

$$\theta_2(t) \simeq \sin 10^{-4} t + 10^{-3} \cos 10^{-4} t \, ,$$

from which it is clear that θ_2 will not remain small. The gravitational torgue will not be helpful unless $\dot{\theta}_2(0)$ is less than 10^{-6} radians per second.

Now let us consider the θ_2 motion when the nonlinear term of Equation (C. 23) is not zero (letting $I_X = 800$, $I_X = 650$, and $I_Z = 150$ slug ft^2).

$$I_Y \ddot{\theta}_2 + (I_X - I_Z - I_Y)\,\dot{\theta}_1 \dot{\theta}_3 = 0 \qquad \text{(C. 25)}$$

(Here we have neglected the gravitational torque because it is small compared to the nonlinear term.) Using the solutions for θ_1 and θ_3 given in Equations (C.20) and (C.21), we obtain

$$\theta_2(t) = \theta_2(0) + \dot{\theta}_2(0)\,t + \frac{(I_X - I_Z - I_Y)}{4\Omega^2 I_Y}\left\{ -\dot{\theta}_1(0)\,\dot{\theta}_3(0)\,(1 - \cos 2\Omega t) + \left[\dot{\theta}_3^2(0)\sqrt{\frac{I_Z}{I_X}} - \dot{\theta}_1^2(0)\sqrt{\frac{I_X}{I_Z}}\right]\left(\frac{1}{2}\sin 2\Omega t - \Omega t\right)\right\}.$$

Apparently θ_2 will not remain small. Therefore, it will be necessary to use an applied torque, L_{Ya}, to control the θ_2 motion. The control forces required are less than a gram in size. If $\dot{\theta}_2(0)$ can be reduced to 10^{-6} radians per second, corrections will be needed only about once a day. If H_Y were perfectly aligned along the Y principal axis of the body, it might be possible to reduce all three angular rates to 10^{-7} rad/sec, in which case it would follow from Equation (C.23) that control forces would no longer be needed.

ACTUAL DISTRIBUTION LIST

Copy Nos.	
1-40	R. A. Park